Supplementary information

Exploration of cobalt (II) modification in Phenanthroline-based conjugated organic polymer towards trifunctional electrocatalysis

Sugandha Singh[a], Manas K. Ghorai[b*], Kamal K. Kar[c*]

[a] *Advanced Nanoengineering Materials Laboratory, Materials Science Programme, Indian Institute of Technology Kanpur, Kanpur 208016, India*

[b] *Department of Chemistry, Indian Institute of Technology Kanpur, Kanpur 208016, India*

[c] *Advanced Nanoengineering Materials Laboratory, Materials Science Programme and Department of Mechanical Engineering, Indian Institute of Technology Kanpur, Kanpur 208016, India*

*Corresponding authors

E-mail address: mkghorai@iitk.ac.in (Manas K. Ghorai), kamalkk@iitk.ac.in (Kamal K. Kar)

Table of contents

Chemicals, Physicochemical measurements	S3
Electrochemical measurements	S4-S7
Synthesis	S8-S15
Structural characterizations of TBB-phen	S16-S23
Electrochemical characterizations of TBB-phen towards ORR and HER	S23-S26
Structural characterizations of Co@TBB-phen	S27-S33
Electrochemical characterizations of Co@TBB-phen towards ORR, OER, and HER	S33-S49
Benchmark materials comparison	S50-S54
DFT computations	S54-S96
References	S96-S98

Chemicals

All the solvents and chemicals were utilized as received without any further purification. 1,10-phenanthroline, ethynyltri(methyl)silane (TMSA), tetrahydrofuran (THF), *N,N*-dimethylformamide (DMF), acetonitrile and *N,N*-diethylethanamine (NEt_3) were purchased from Spectrochem Pvt. Ltd. 1, 3, 5-tribromobenzene was purchased from Alfa Aesar Co. Nitrobenzene, bromine, $Pd(PPh_3)_2Cl_2$, $Pd(PPh_3)_4$, and cuprous iodide were purchased from Sigma-Aldrich Chemical Co.

Physicochemical measurements

The ^1H and ^{13}C Nuclear magnetic resonance (NMR) spectroscopy were recorded on a JEOL 500 MHz spectrometer. Singlet and doublet split patterns in proton NMR were denoted as s and d. The Fourier transform-infrared (FTIR) spectroscopy was performed on Bruker-Tensor 27 in the range of 4000 to 400 cm^{-1} using KBr as a beam splitter. The CHN elemental analysis was done on PerkinElmer Series-II CHNS/O analyzer 2400. The ^{13}C solid-state- NMR has been recorded on Bruker Avance HD 500 MHz spectrometer in the range of 0 to 200 ppm without any solvent system. The electron paramagnetic resonance (EPR) spectroscopy was recorded on Bruker BioSpin GmbH in the magnetic field range of 0 to 8000 Gauss and microwave frequency of 9.456 GHz. The optical band gap was determined by performing solid-state Ultra-violet visible (UV-vis) spectroscopy on Cary 5000 UV-vis-NIR spectrophotometer at a scan rate of 1.67 nms^{-1} in the range of 200 to 800 nm. The powder X-ray diffraction (PXRD) was recorded on a Panalytical XPert X-ray diffractor (ACMS) in the 2-theta range of 3-50 degrees and a scan rate of 1 degree per minute with an X-ray source of Cu K_α ($\lambda = 1.54$ Å). The thermogravimetric analysis (TGA) was performed on a Perkin-Elmer Diamond TG/DTA analyzer in the range of 30 ^oC to 800 ^oC at the heating rate of 10 degrees per minute in an inert atmosphere (N_2 gas flow = 20 mL/min). Inductively coupled plasma-mass spectroscopy (ICP-MS) was performed on X- series thermos scientific instruments. Surface area and porosity studies were performed by N_2 adsorption at 77 K on a Quantachrome analyzer. 50 mg of samples were degassed at 100 ^oC for 6 h before measurements to remove the adsorbed water or other solvents. The X-ray photon spectroscopy (XPS) was performed on PHI 5000 Versa Prob II, FEI Inc. The morphological study was performed by imaging on Field emission-scanning electron microscopy (FE-SEM) instrument JSM-7100F, JEOL. The powder samples were thoroughly dispersed by ultrasonication in dichloromethane for 1 h followed by

drop-casting on aluminium foil. The as-prepared FESEM samples were dried under vacuum at 60^{o}C for 2 h and gold coated before imaging. Energy dispersive X-ray spectroscopy (EDS) and elemental mapping were performed on the very instrument. The high resolution-transmission electron microscopic (HR-TEM) imaging was performed on Titan G2 at an accelerating voltage of 300 KV. Thoroughly dispersed samples were drop cast on carbon-coated copper grids.

Electrochemical measurements

Electrode preparation

The electrochemical tests were initiated by preparing catalyst ink by adding 2 mg of active material in 980 µL of isopropanol and deionized (DI) water (1:1) and 20 µL Nafion (Alfa Aesar, 5%). The solution was sonicated for 30 minutes for thorough dispersion, followed by the addition of 2 mg carbon black and sonication for another 30 minutes. 5 µL of freshly prepared ink was drop-casted on a 4 mm diameter glassy carbon (GC) electrode with a mass loading of 80 µgcm^{-2} for ORR and HER. 10 µL was drop-casted for OER measurements. Before measurements, the GC working electrode was cleaned with 0.3 µm alumina paste on velvet cloth in the motion of eight by light hand weight and washed with acetone and deionized water for 1 h. All the measurements were performed at ambient conditions (~ 25^{o}C).

Testing parameters

The synthesized polymers were investigated for electrochemical performance using a home-built rotating disk electrode (RDE) system on Metrohm M204 multiAutolab potentiostat/galvanostat. The ORR and OER tests were conducted in alkaline media using 0.1 M KOH solution, and HER was conducted in acidic media using 0.5 M H_2SO_4. A typical 3-electrode cell was used where glassy carbon was used as the working electrode, Ag/AgCl (saturated KCl) as our reference electrode, and platinum as our counter electrode. The electrochemical performance of our synthesized catalysts was studied using cyclic voltammetry (CV), linear sweep voltammetry (LSV), and *i-t* chronoamperometry. The observed potential was calibrated to a reversible hydrogen electrode (RHE) potential using the Nernst equation, $E_{RHE} = E_{Ag/AgCl} + E^{0}_{Ag/AgCl} + 0.059\times pH$, and the obtained current was normalized to the geometric surface area of the electrode. Prior to ORR measurements, the electrolyte was saturated with O_2, and for OER and HER, the electrolyte was saturated with N_2 gas to avoid saturation of the electrolyte with evolving gases.

ORR tests

The electrocatalytic activity of polymer for O_2 reduction was studied by recording CV at a scan rate of 50 mVs^{-1} in O_2, and N_2 saturated 0.1 M KOH in the hydrostatic condition in the potential range of 1.2 to 0 V (vs. RHE). The LSV was recorded in hydrodynamic conditions at the rotation rates of 100, 400, 900, 1600, 2500, and 3600 rpm and a sweep rate of 5 mVs^{-1} in O_2 saturated 0.1 M KOH in the potential range of 1.2-0 V (vs. RHE). The possible number of electrons transferred during the O_2 reduction reaction was determined by Koutecky´–Levich (K-L) equation as follows

$$\frac{1}{j} = \frac{1}{j_L} + \frac{1}{j_K} = \frac{1}{B\omega^{\frac{1}{2}}} + \frac{1}{j_K} \qquad \text{Eq. (1)}$$

$$B = 0.62\, nFC_{\circ}\left(D_{\circ}\right)^{\frac{2}{3}} \nu^{-\frac{1}{6}} \qquad \text{Eq. (2)}$$

$$j_K = nFkC_{\circ} \qquad \text{Eq. (3)}$$

Where j is the determined current density, j_L, and j_K are the limiting diffusion and kinetic current density, respectively. ω is the angular rotation rate (rad/s), n is the no. of electrons transferred, F is Faraday's constant (96485 C/mol), C_o is the concentration of O_2 for 0.1 M KOH (1.9×10^{-5} mol/cm^3), D_o is diffusion coefficient of O_2 for 0.1 M KOH (1.2×10^{-6} mol/cm^3), ν is the kinematic viscosity of 0.1 M KOH (0.01 cm^2/s), and k is electron transfer rate.

Tafel slope was determined by recording LSV at a slow sweep rate of 1 mVs^{-1} at 1600 rpm in O_2 saturated electrolyte and was linearly fitted to a Tafel equation given below

$$\eta = b \log j + a \qquad \text{Eq. (4)}$$

where, η = overpotential (mV), j is the current density, and b is the Tafel slope.

Catalyst stability and robustness were further determined by *i-t* chronoamperometric measurements at a potential corresponding to approximately -1 $mAcm^{-2}$ (0.67V vs. RHE) and were utilized to investigate the stability for ORR for 12 h in 0.1 M KOH. A slow and continuous flow of O_2 gas was supplied throughout the test duration. Electrochemical impedance spectrum was recorded at 0.66 V vs. RHE in a frequency range of 0.1 to 10^5 Hz

OER tests

The water oxidation capability of prepared organic polymers was first investigated by CV at a fast scan rate of 50 mVs^{-1} in an N_2 environment in the scan range of 1 to 2 V (vs. RHE). LSV data was acquired by recording at 5 mVs^{-1} in N_2 saturated electrolyte at 0 and 1600 rpm. To determine the Tafel slope, LSV was recorded at a slow scan rate of 1 mVs^{-1} at 1600 rpm and is calculated as per equation (4). To explore the stability of the catalyst, LSV was recorded at a fast sweep rate of 50 mVs^{-1} at 1600 rpm for considerable 500 cycles in the potential range 1-2 V. For *i-t* chronoamperometric measurements, a potential corresponding to 10 $mAcm^{-2}$ (1.8 V vs. RHE) was utilized to investigate the stability for 6 h in 0.1 M KOH. The electrochemical impedance spectrum was recorded at 1.76 V vs. RHE in a frequency range of 0.1 to 10^5 Hz

Since all the atoms deposited on the electrode do not participate in the redox reaction, we have investigated how much the actual surface area contributes to the observed output (here, current density). Since OER is triggered by the addition of cobalt atoms in the organic system, we determine how much cobalt contributes to the oxygen evolution reaction. For electrocatalytic calculations of Co@TBB-phen towards OER, the electrochemically active surface area (EASA) is calculated by measuring the double-layer capacitance (Cdl) and specific capacitance (Cs), which is done by recording CV in the non-faradaic region at different scan rates on GC loaded with Co@TBB-phen and bare GC. The EASA is given as

$$EASA = \frac{C_{dl}}{C_s} \qquad \text{Eq. (5)}$$

The roughness factor is the ratio of EASA to the geometrical surface area

$$RF = \frac{EASA}{GSA} \qquad \text{Eq. (6)}$$

To determine the surface coverage (τ_o), which signifies the active number of cobalt atoms, the cyclic voltammetry program is recorded in the cobalt redox-active potential range at different sweep rates. The average of cathodic and anodic current is utilized to determine the surface coverage and, eventually, the active number of Co atoms by the equation given below

$$slope = \frac{n^2F^2\tau_{\circ}A}{4RT} \qquad \text{Eq. (7)}$$

where n= no. of electrons involved in a redox reaction

F= Faraday's constant (96485 C/mol)

A= Geometric surface of glassy carbon

τ_o = surface coverage

R= universal gas constant (VC/K/mol)

T= Temperature (K)

$$TOF = \frac{(Avogadro's\ no) \times j\ (1\ mA/cm^2)}{4 \times RF \times F \times \tau_o} \qquad \text{Eq. (8)}$$

HER measurements

The proton reduction and subsequent H_2 evolution activity of as-prepared polymers were studied by recording LSV at a scan rate of 5 mVs^{-1} in N_2 saturated 0.5 M H_2SO_4 in the potential range of 0 to -1 V (vs. RHE) in hydrostatic condition and hydrodynamic condition (1600 rpm). Tafel slope was determined by recorded LSV at a slow scan rate of 1 mVs^{-1} at 1600 rpm in N_2 saturated 0.5 M H_2SO_4 in the same potential range. The stability of the electrocatalyst is determined by recording LSV at 1600 rpm for 500 cycles at a scan rate of 50 mVs^{-1} in the potential range of 0 to -1 V (vs. RHE). The chronoamperometry test was performed to determine its stability with time at overpotential corresponding to obtaining a current density of 10 $mAcm^{-2}$ for 12 h. The electrochemical impedance spectrum was recorded at -0.48 V vs. RHE in a frequency range of 0.1 to 10^5 Hz

The EASA and RF were determined by following the same procedure as OER but in 0.5 M H_2SO_4 and equations (5) and (6) were utilized. The number of active sites was determined by recording CV at the current onset region at varying scan rates and taking current values at an overpotential of 250 mV. The TOF was determined at 10 $mAcm^{-2}$ by utilizing the given formula below

$$TOF = \frac{j \times SA}{n \times F \times N} \qquad \text{Eq. (9)}$$

Where j is the current density, SA is the surface area, n is the number of electrons (here, 2), F is Faraday's constant, and N is the number of active sites.

Synthesis

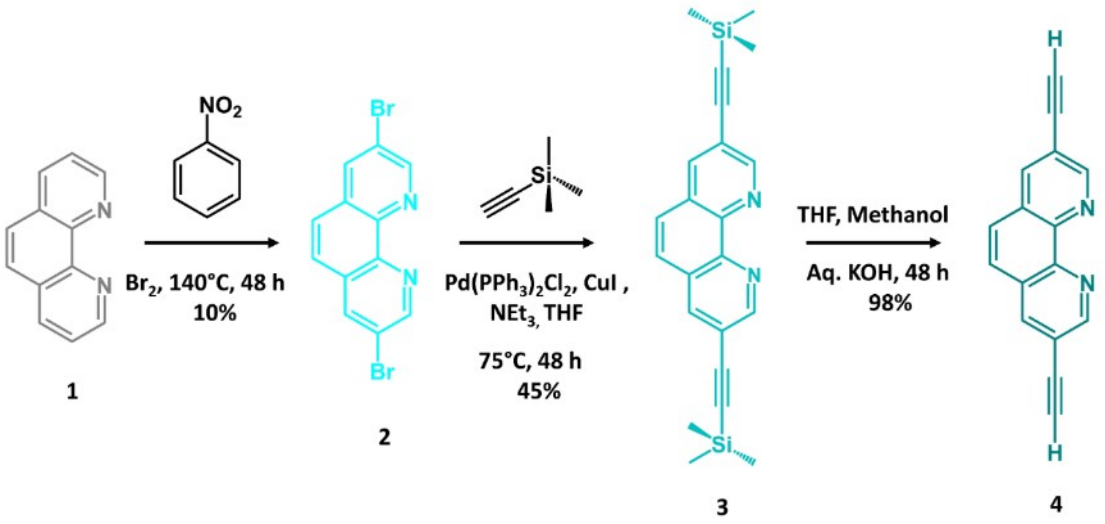

Fig S1. Synthesis scheme for acceptor phen **(4)**

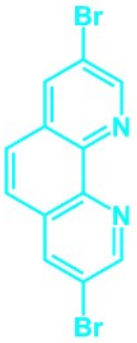

Synthesis of 3,8-dibromo-1,10-phenanthroline (2): A Schlenk flask is charged with 1,10- phenanthroline **(1)** (10.7 gm, 59.37 mmol) in nitrobenzene (20 mL). The reaction mixture is heated at 140°C under an argon atmosphere in an oil bath. Then bromine (4.1 mL, 79. 46 mmol) in nitrobenzene (10 mL) is loaded dropwise to the reaction mixture. The reaction mixture is stirred for 10 days at 140°C. Advancements in the reaction are tracked by thin-layer chromatography (TLC). After the successful completion of the reaction, excess residual bromine is neutralized with an aqueous thiosulfate solution, followed by extraction with dichloromethane. The resulting organic layer is separated and evaporated to dryness resulting in a crude compound, which is treated for flash column chromatography (silica gel, dichloromethane/methanol =96:4, Rf = 0.4) to obtain a white solid as a pure product. mp = 270-273°C, yield: 10% (2 gm, 5.92 mmol). IR (KBr, I/ν_{max}): 3438, 3097, 3025, 2922, 2852, 2362, 2342, 1850, 1821, 1675, 1615, 1585, 1573, 1478, 1413, 1371, 1340, 1288, 1252, 1208, 1104, 1061, 1035, 966, 939, 905, 892, 807, 732, 784,

775, 721, 712, 557, 526, 507 cm^{-1}; ^{1}H NMR (500 MHz, $CDCl_3$) δ = 7.74 (s, 2H, c, d), 8.38 (d, ^{3}J = 2.26 Hz, 2H, a, e), 9.16 (d, ^{3}J = 2 Hz, 2H, b, f); ^{13}C {^{1}H} NMR (125 MHz, $CDCl_3$) δ = 120.3, 127.0, 129.7, 137.7, 144.2, 151.7 ppm. Anal. Calcd for C12H6N2Br2: C, 42.64; H, 1.79; N, 8.29; Found: C, 40.72; H, 1.41; N, 7.54.

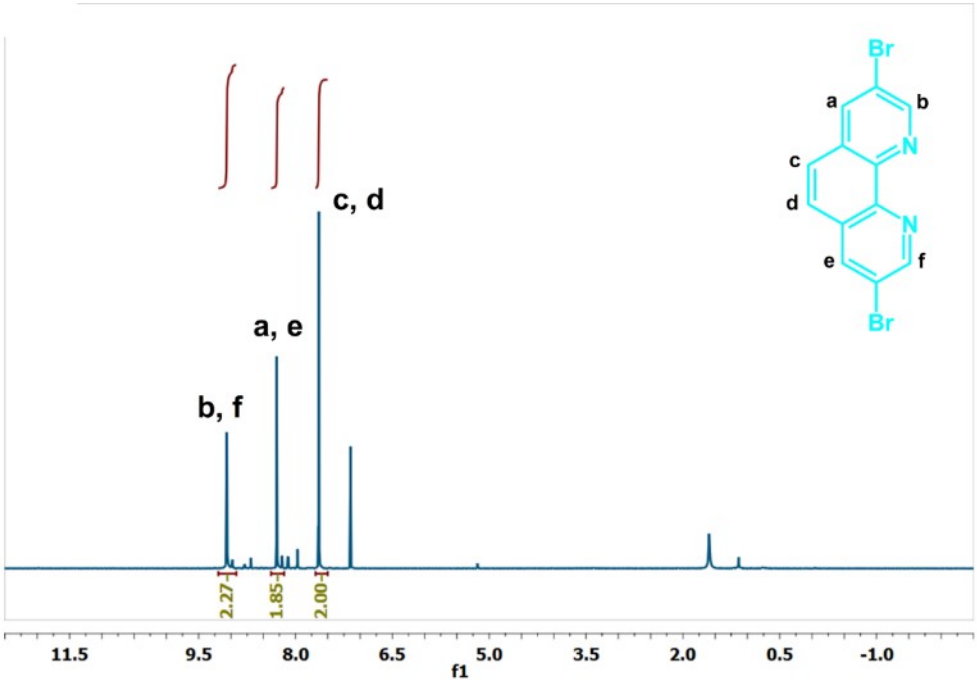

Fig S2(a). ^{1}H NMR spectrum ($CDCl_3$, 500 MHz) of compound **2**

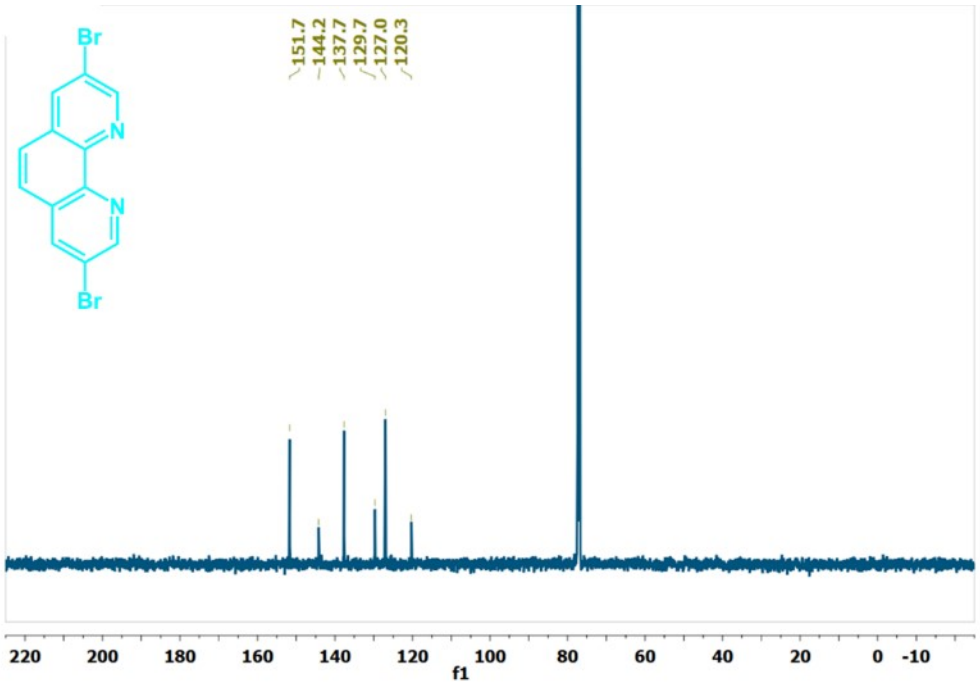

Fig S2(b). ^{13}C NMR spectrum ($CDCl_3$, 125 MHz) of compound **2**

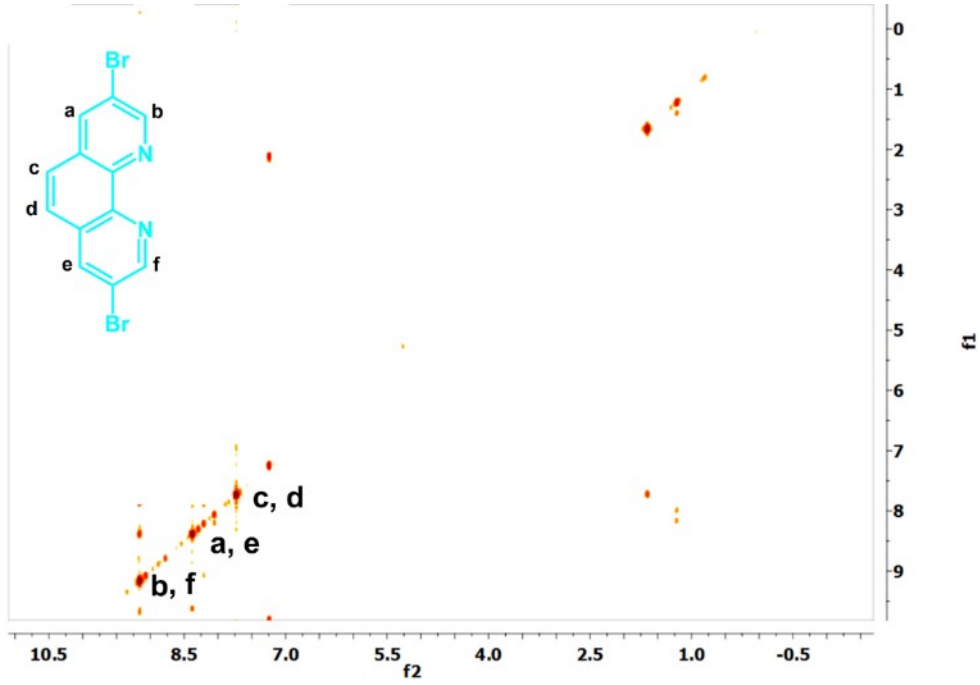

Fig S2(c). ^{1}H-^{1}H COSY NMR spectrum ($CDCl_3$, 500 MHz) of compound **2**

Synthesis of 3, 8-bis(trimethylsilylethynyl)-1, 10-phenanthroline (3): A single neck round bottom flask is loaded with 3,8-dibromo-1,10-phenanthroline (1.0 g, 2.958 mmol), copper iodide (336 mg, 1.764 mmol), bis (triphenylphosphine)

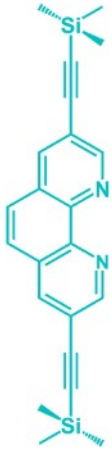

palladium chloride (620 mg, 0.884 mmol), triethylamine (4 mL), and tetrahydrofuran (6 mL). To the reaction mixture, trimethylsilylacetylene (8 mL, 56.21 mmol) is added in the end, and the reaction vessel is sealed immediately. The reaction mixture is allowed to heat at 75°C for 48 h in an oil bath. After the successful completion of the reaction, the reaction mixture is brought to room temperature and evaporated to dryness in a rotary evaporator. The solid residue is treated with aqueous sodium cyanide to remove copper from the organic layer. All the used glassware is quenched with aqueous ferric chloride solution immediately, and the solid residue is extracted by drying in a rotary evaporator followed by column chromatography (SiO_2, DCM/hexane = 50:50, R_f= 0.5) to afford dark brown color solid as the pure product. mp. = 180-183°C, yield = 45% (500 mg, 1.341 mmol). IR (KBr, I/ν_{max}): 3428, 3049, 3029, 3013, 2956, 2926, 2897, 2850, 2348, 2155, 1950, 1834, 1610, 1585, 1550, 1483, 1466, 1420, 1368, 1348, 1316, 1264, 1247, 1230, 1170, 1112, 968, 911, 861, 844, 758, 729, 701, 644, 596, 569, 544, 529 cm^{-1}. ^1H NMR (500 MH_z, $CDCl_3$) δ = 0.29 (s, 18H, a, h), 7.73 (s, 2H, d, e), 8.3 (d, ^3J = 2 H_z, 2H, c, f), 9.17 (d, ^3J = 2.3 H_z, 2H, b, g);^{13}C {^1H} NMR (125 MH_z, $CDCl_3$) δ = -0.1, 100.1, 101.7, 119.8, 126.9, 128.1, 138.8, 144.4, 152.7 ppm. Anal. Calcd for C22H24N2Si2: C, 70.91; H, 6.49; N, 7.52. Found: C, 69.37; H, 6.33; N, 7.21.

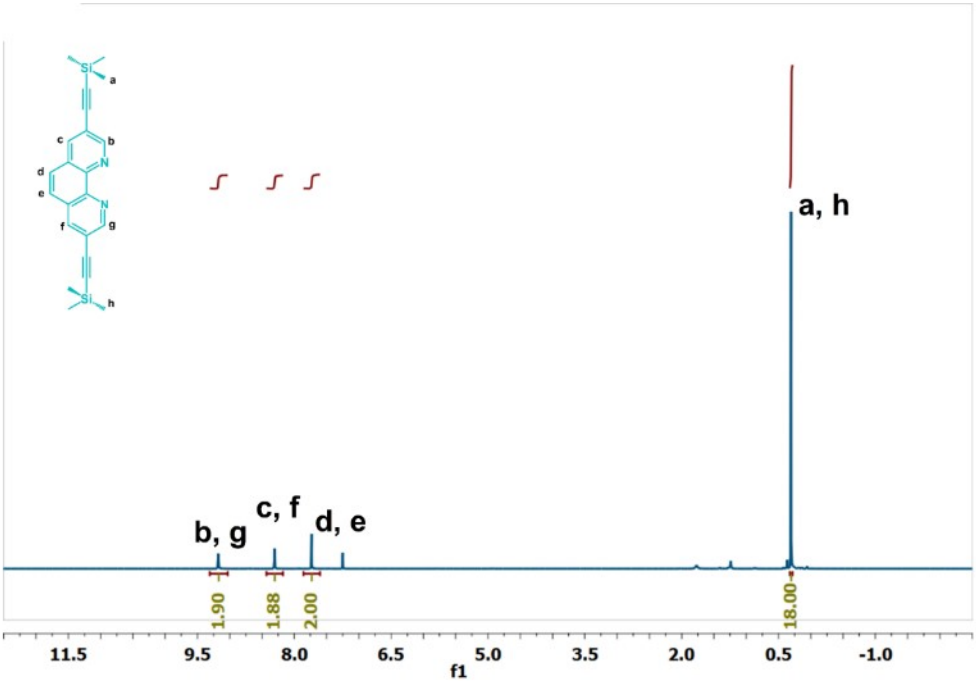

Fig S3(a). ^1H NMR spectrum ($CDCl_3$, 500 MHz) of compound **3**

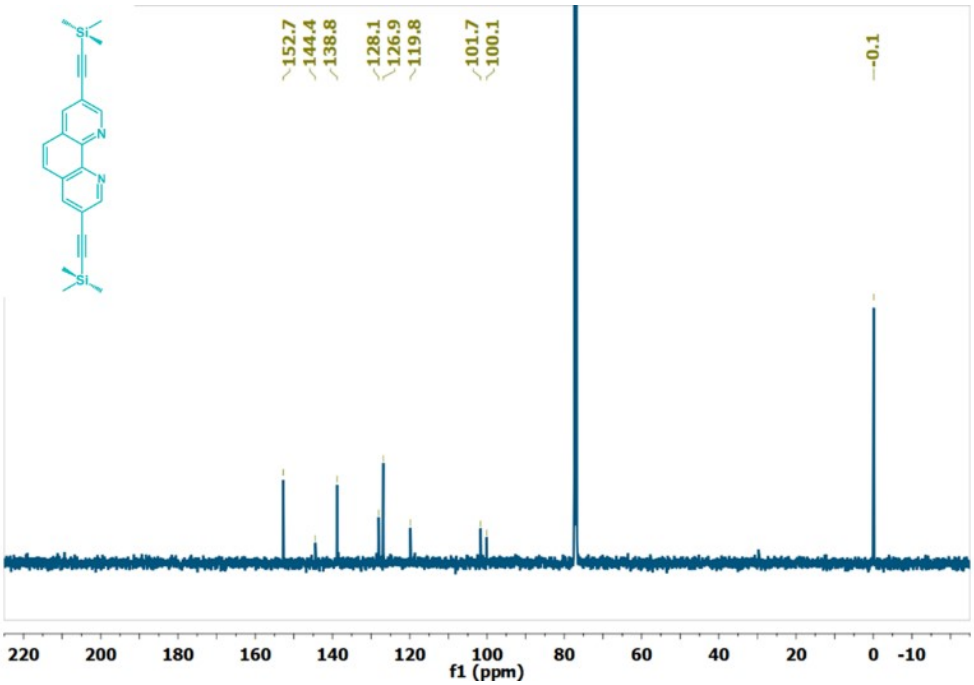

Fig S3(b). ^{13}C NMR spectrum ($CDCl_3$, 125 MHz) of compound **3**

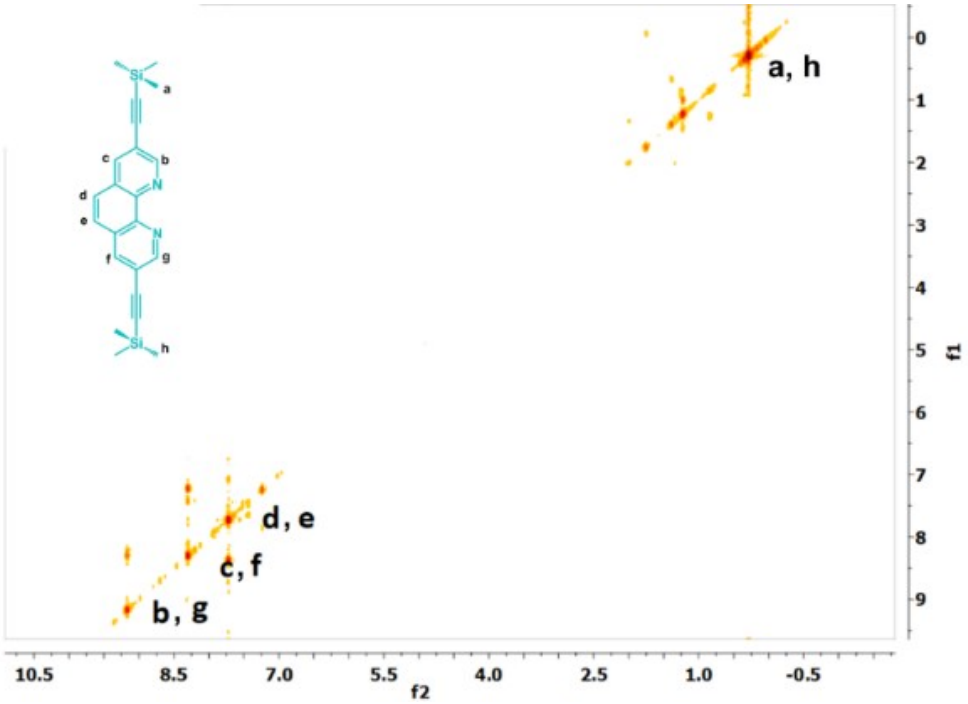

Fig S3(c). ^{1}H-^{1}H COSY NMR spectrum ($CDCl_3$, 500 MHz) of compound **3**

Synthesis of 3, 8-diethynyl-1, 10-phenanthroline (4): A single neck round bottom flask is charged with 3, 8-bis(trimethylsilylethynyl)-1, 10-phenanthroline (500 mg, 1.342 mmol) and 50 mL of 2N KOH is added to it along with methanol followed by addition of THF until a transparent solution is obtained. The reaction solution is kept for stirring at room temperature over a magnetic stirrer. After completion of the desilylation process, the reaction solution is evaporated to dryness in a rotary evaporator, and the organic part is extracted using dichloromethane. The obtained solution is evaporated to dryness in a rotary evaporator to afford a muddy brown color solid as a pure product. mp. = 295-300°C, yield = 98% (300 mg, 1.314 mmol). IR (KBr, I/ν_{max}): 3415, 3296, 3172, 2953, 2923, 2853, 2095, 1877, 1854, 1686, 1614, 1559, 1489, 1437, 1420, 1384, 1348, 1310, 1350, 1269, 1226, 1165, 1118, 968, 913, 762, 724, 688, 629, 566, 539, 513, 461 cm^{-1}. ^1H NMR (500 MH_z, $CDCl_3$) δ = 3.36 (s, 2H, a, h), 7.78 (s, 2H, d, e), 8.36 (d, ^3J = 1.85 H_z, 2H, c, f), 9.22 (d, ^3J = 2.18 H_z, 2H, b, g); ^{13}C {^1H} NMR (125 MH_z, $CDCl_3$) δ = 126.9, 139.2, 152.9 ppm. Anal. Calcd for $C_{16}H_8N_2$: C, 84.19; H, 3.53; N, 12.27. Found: C, 75.06; H, 3.70; N, 7.21.

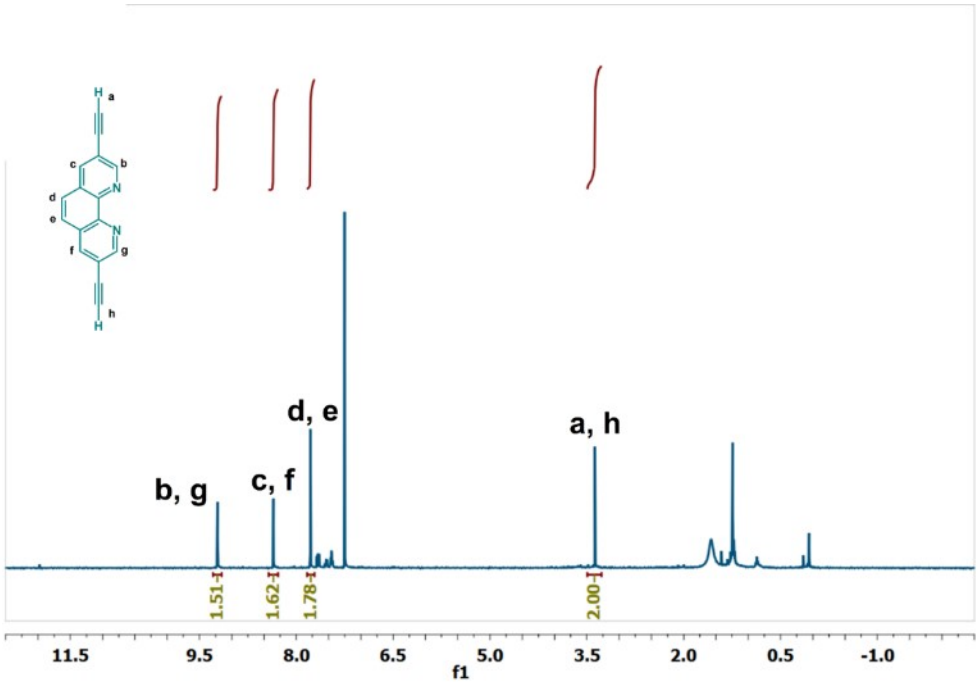

Fig S4(a). ^1H NMR spectrum ($CDCl_3$, 500 MHz) of compound **4**

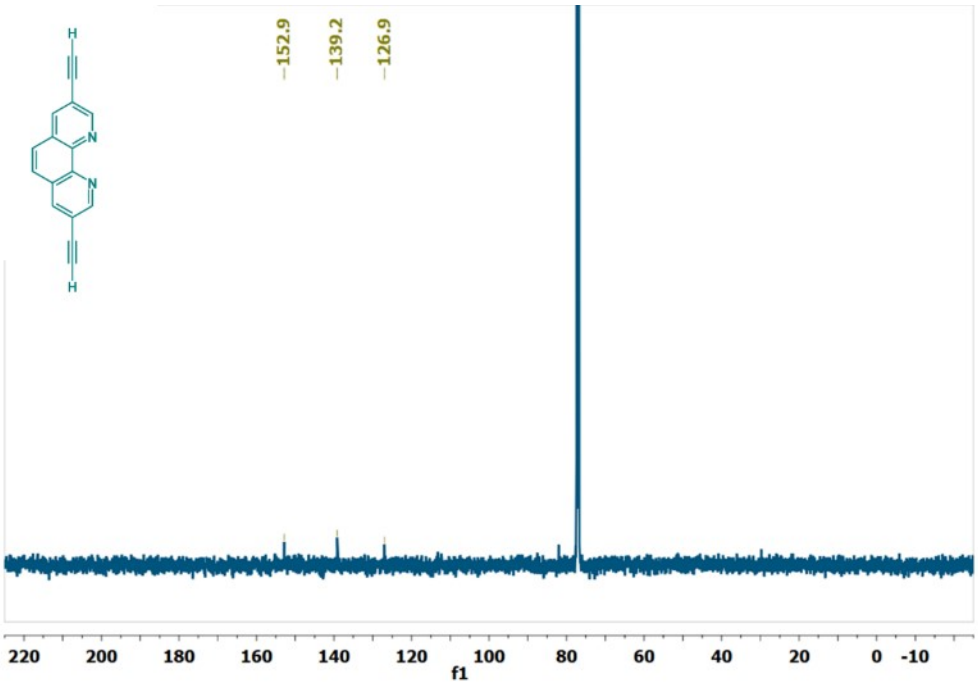

Fig S4(b). ^{13}C NMR spectrum ($CDCl_3$, 125 MHz) of compound **4**

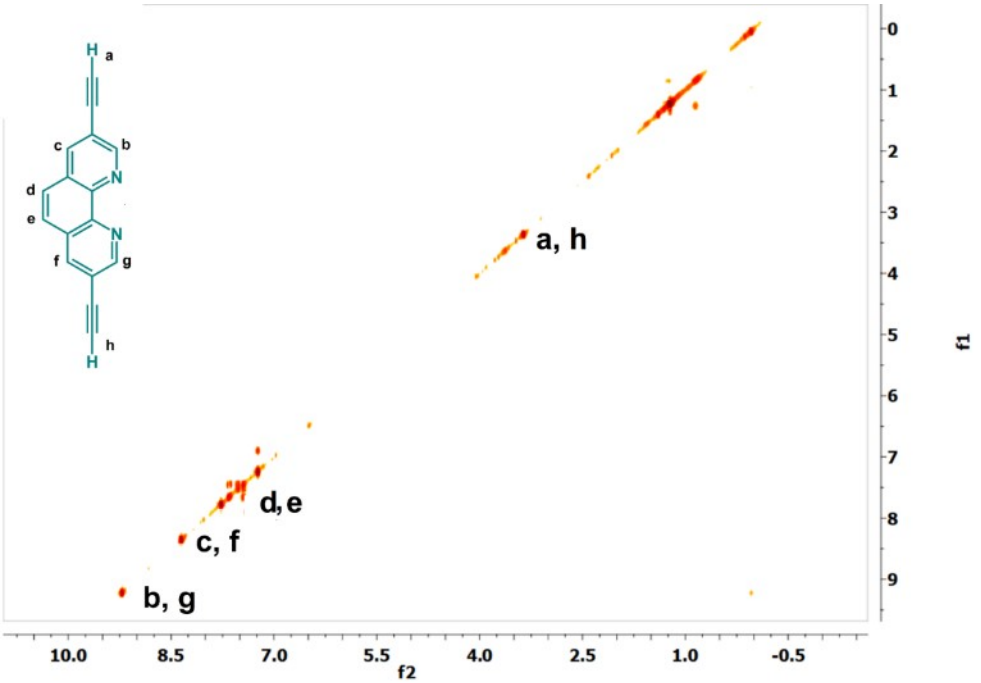

Fig S4(c). ^{1}H-^{1}H COSY NMR spectrum ($CDCl_3$, 500 MHz) of compound **4**

Synthesis of TBB-phen

The Schlenk flask is charged with compounds **4** (100mg, 0.438 mmol), 1, 3, 5-tribromobenzene (91.9 mg, 0.292 mmol), dimethylformamide (2 mL), and triethylamine (2 mL). The reaction mixture is degassed using the freeze-pump-thaw method with argon, followed by the addition of tetrakis(triphenylphosphine) palladium (101 mg, 0.0876 mmol). Again, the reaction mixture is degassed by the prior mentioned method. The reaction vessel is heated to 100°C for 12 h in a silicon oil bath for completion of the reaction. Then, the reaction vessel is brought to room temperature. The obtained dark yellow colored precipitate is ground and washed over Whatman 40 filter paper with tetrahydrofuran (THF) and boiling dimethylformamide (DMF). The residual polymer is further Soxhlated by tetrahydrofuran (THF) to extract residual palladium catalyst to obtain our organic polymer TBB-phen as a dark yellow solid powder. The obtained polymer is dried under vacuum for 4 h at 70°C. (Fig 6). Yield= 150 mg, IR (KBr, I/ν_{max}): 3439, 2206, 1651, 1637, 1578, 1548, 1479, 1425, 1366, 1251, 1105, 911, 864, 729, 675, 538 cm^{-1}. Anal. Calcd for $C_{20}H_{12}N_2$: C,62.11; H, 3.13; N, 7.24. Found: C, 64.27; H, 3.25; N, 6.92.

Synthesis of Co@TBB-phen conjugated organic polymer

For in-situ doping of cobalt in the pristine sample, a metal ion solution of 10^{-2} M concentration ($CoCl_2.6H_2O$ as cobalt source) in acetonitrile is prepared. 10 mg of TBB-phen is added to 3 mL of salt solution and is stirred for 4 h. The residual sample is centrifuged and dried in a vacuum for 4 h to afford dark yellow colored polymer as our Co@TBB-phen. IR (KBr, I/ν_{max}): 3356, 2210, 1601, 1550, 1502, 1430, 1373, 1271, 1111, 918, 868, 749, 723, 675, 538 cm^{-1}. Anal. Calcd for $C_{20}H_{12}N_2$: C,53.9; H, 2.71; N, 6.29. Found: C, 56.55; H, 3.21; N, 6.58.

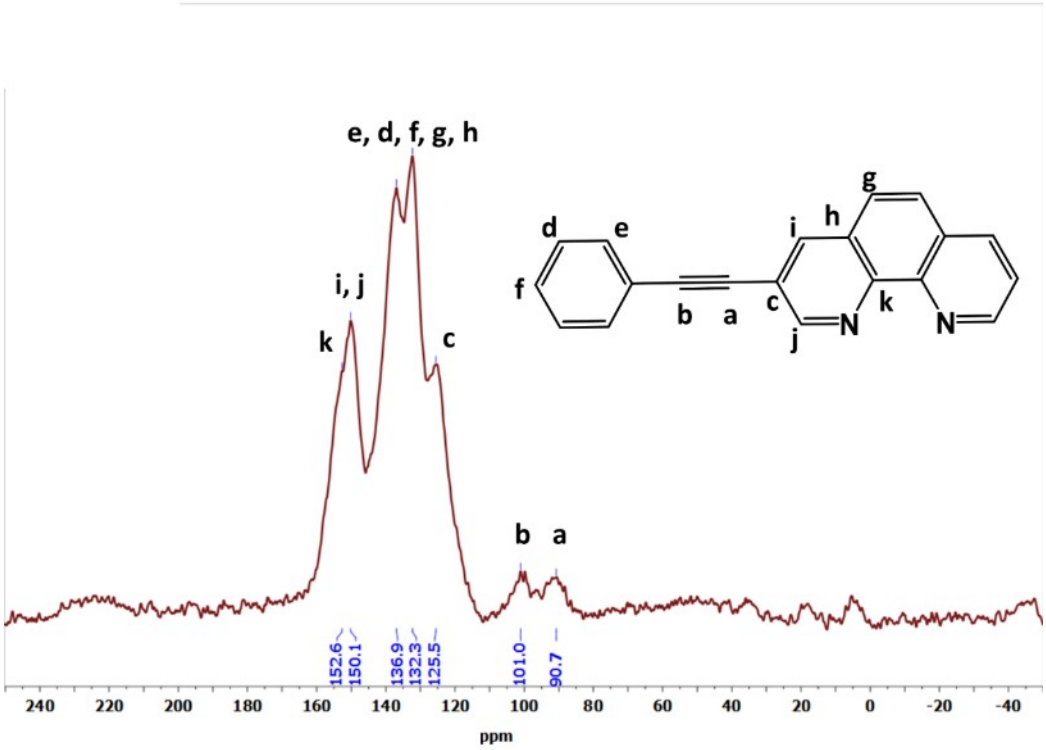

Fig S5. ^{13}C solid-state CP/MAS NMR spectrum of TBB-phen

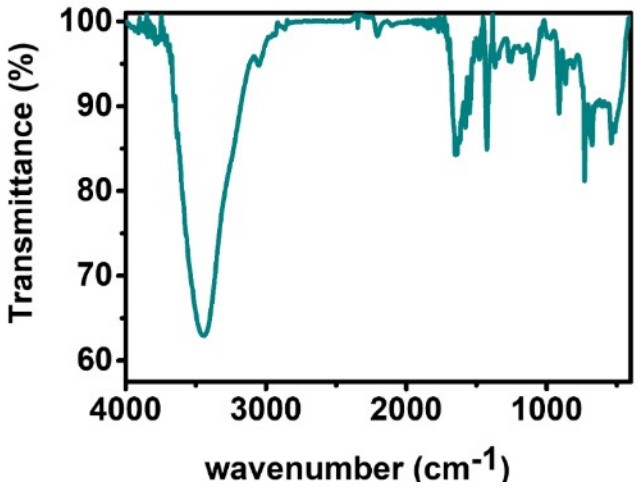

Fig S6. Fourier transform-infrared spectroscopy of TBB-phen

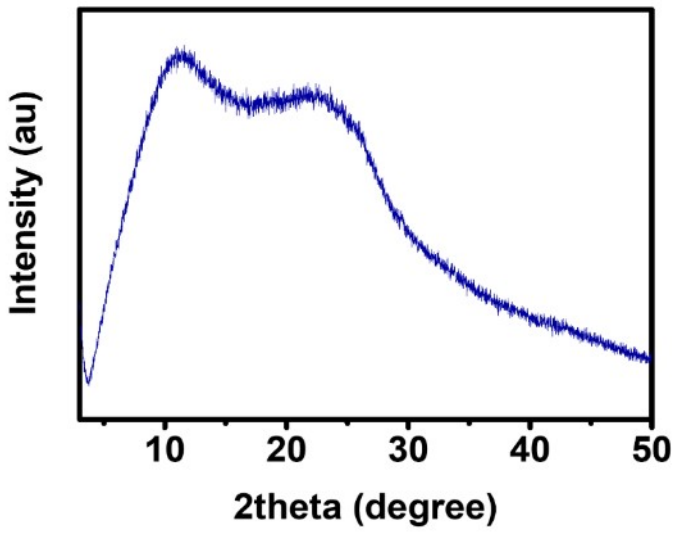

Fig S7. Powder X-ray diffraction pattern of TBB-phen

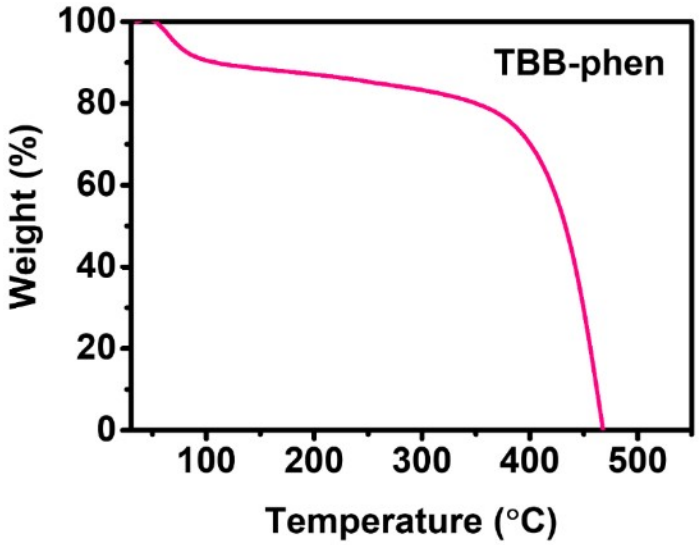

Fig S8. Thermogravimetric plot of TBB-phen

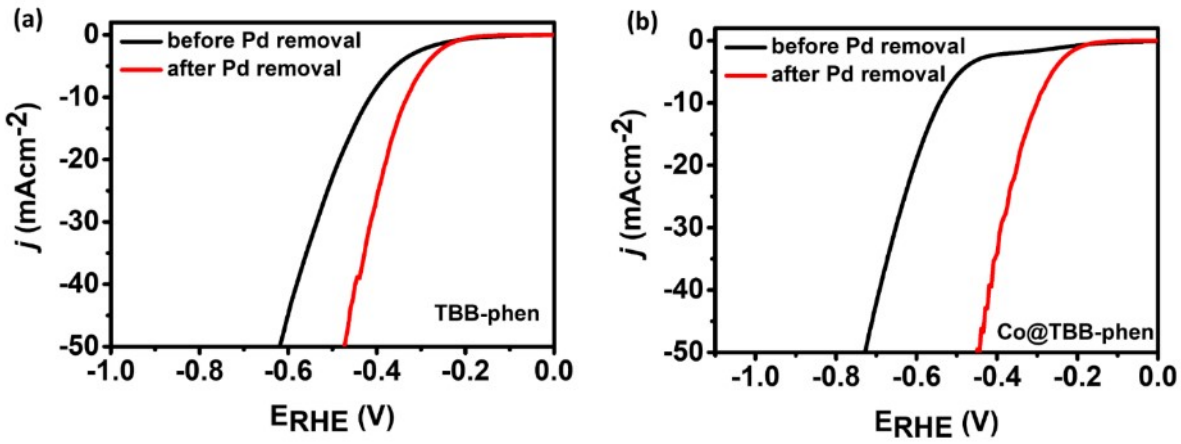

Fig S9. HER performance before and after residual Pd (a) TBB-phen, and (b)Co@TBB-phen

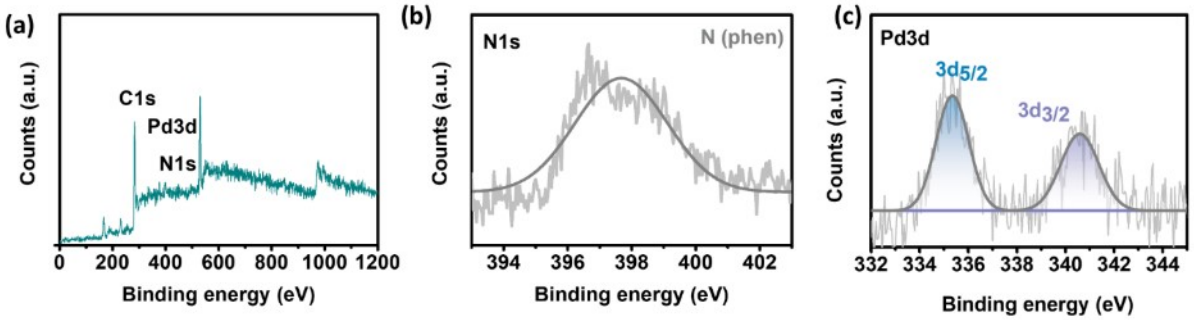

Fig S10 (a). Full X-ray photoelectron spectrum, (b) deconvoluted peak of N1s, and (c) deconvoluted Pd3d from TBB-phen

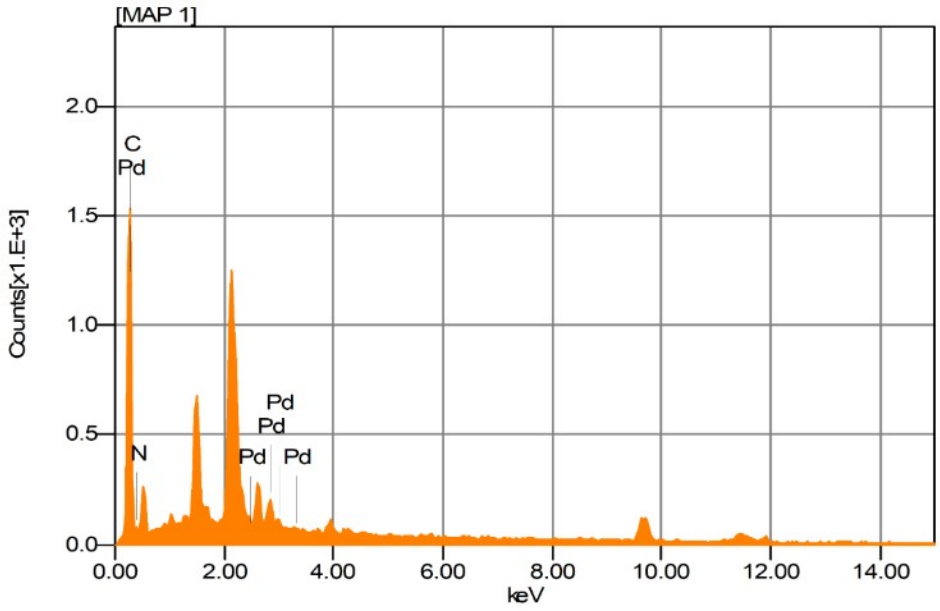

Fig S11. The energy dispersive spectrum of TBB-phen

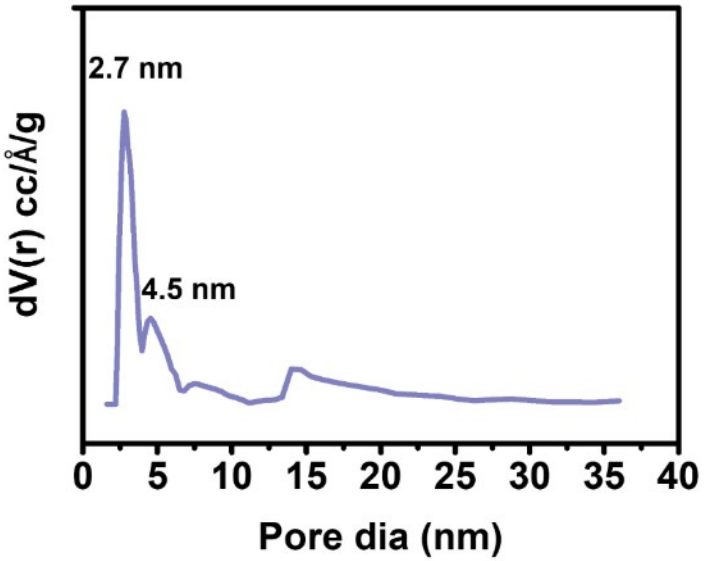

Fig S12. Non-local density functional theory (NLDFT) pore diameter of TBB-phen

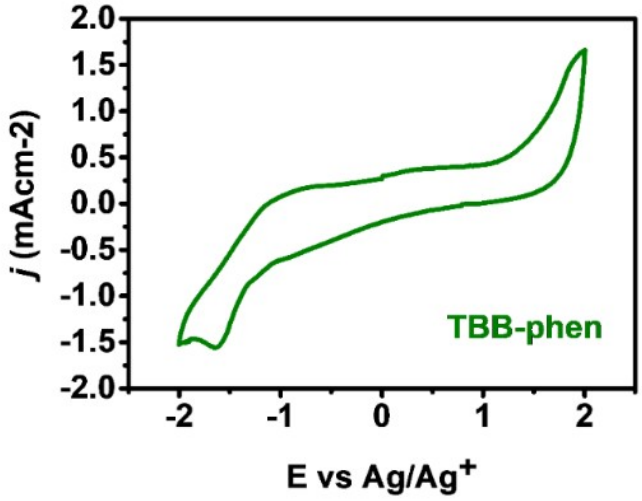

Fig S13. Cyclic voltammetry (CV) of TBB-phen recorded in 0.1 M tetrabutylammonium perchlorate (TBAP) solution in anhydrous acetonitrile with respect to $Ag/AgNO_3$

A typical 3-electrode cell is made where glassy carbon is the working electrode, platinum is the counter electrode, and Ag/Ag^+ is the reference electrode. The working electrode is prepared by drop-casting 5 µL of prepared ink and drying in ambient conditions, as previously mentioned. Non-aqueous Ag/Ag^+ reference electrode is filled with 0.01 M $AgNO_3$ and 0.1 M tetrabutylammonium perchlorate (TBAP) solution in anhydrous acetonitrile. The electrolyte utilized is 0.1 M TBAP solution in anhydrous acetonitrile. CV is recorded at a scan rate of 50 mVs^{-1} in the potential range of 2 to -2 V vs. Ag/Ag^+. The obtained redox potentials are converted into RHE prior bandgap calculations as given below:

$E_{RHE} = E_{Ag/Ag^+} + E^0_{Ag/Ag^+} + 0.059 \times pH$ Eq. (10)

where E_{RHE} is the corresponding potential in RHE, E_{Ag/Ag^+} is the standard electrode potential for Ag/Ag^+ couple, and E is the observed potential using Ag/Ag^+ couple

The onset oxidation and reduction potentials are found to be 2.28 V and 0.72 V, respectively.

$E^{onset}_{oxRHE} = 0.799 + (1.07) + 0.413 = 2.28$ V Eq. (11)

$E^{onset}_{redRHE} = 0.799 + (-0.49) + 0.413 = 0.72$ V (Eq. 12)

Equations (11) and (12) were utilized to determine the experimental electrochemical HOMO and LUMO levels in terms of eV

E (HOMO) = -e [E_{oxRHE}^{onset} + 4.44] Eq. (10)

E (LUMO) = -e [E_{redRHE}^{onset} + 4.44] Eq. (11)

The calculated HOMO and LUMO levels came out to be -6.30 eV and -3.29 eV respectively giving the gap of **3.01 eV**.

E (HOMO) = -e [2.28 - 0.42 + 4.44] = **-6.30 eV**

E (LUMO) = -e [-0.72 - 0.42 + 4.44] = **-3.29 eV**

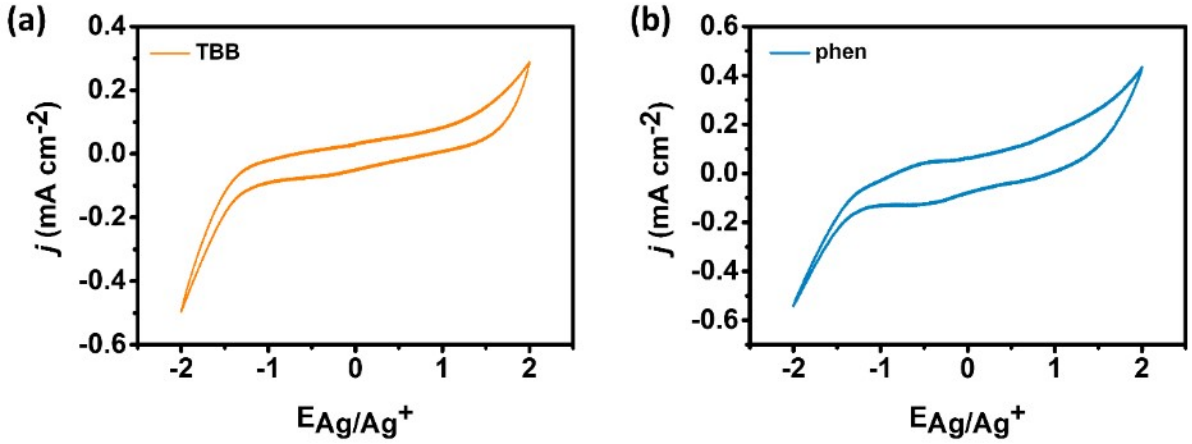

Fig S14. CV of (a) TBB and (b) phen recorded in 0.1 M TBAP solution in anhydrous acetonitrile with respect to Ag/$AgNO_3$

The HOMO-LUMO gap determination in TBB

The onset oxidation and reduction potentials are found to be 2.25 V and 0.17 V, respectively.

E_{oxRHE}^{onset} = 0.799 + (1.04) + 0.413 = 2.25 V

E_{redRHE}^{onset} = 0.799 + (-1.04) + 0.413 = 0.17 V

The calculated HOMO and LUMO levels came out to be -6.27 eV and -3.84 eV respectively giving the gap of 2.46 eV.

E (HOMO) = -e [2.25 - 0.42 + 4.44] = -6.27 eV

E (LUMO) = -e [-0.17 - 0.42 + 4.44] = -3.84 eV

The HOMO-LUMO gap determination in phen

The onset oxidation and reduction potentials are found to be 1.76 V and 0.10 V, respectively.

E_{oxRHE}^{onset} = 0.799 + (0.55) + 0.413 = 1.76 V

E_{redRHE}^{onset} = 0.799 + (-1.11) + 0.413 = 0.10 V

The calculated HOMO and LUMO levels came out to be -5.78 eV and -3.91 eV respectively giving the gap of 1.86 eV.

E (HOMO) = -e [1.76 - 0.42 + 4.44] = -5.78 eV

E (LUMO) = -e [-0.10 - 0.42 + 4.44] = -3.91 eV

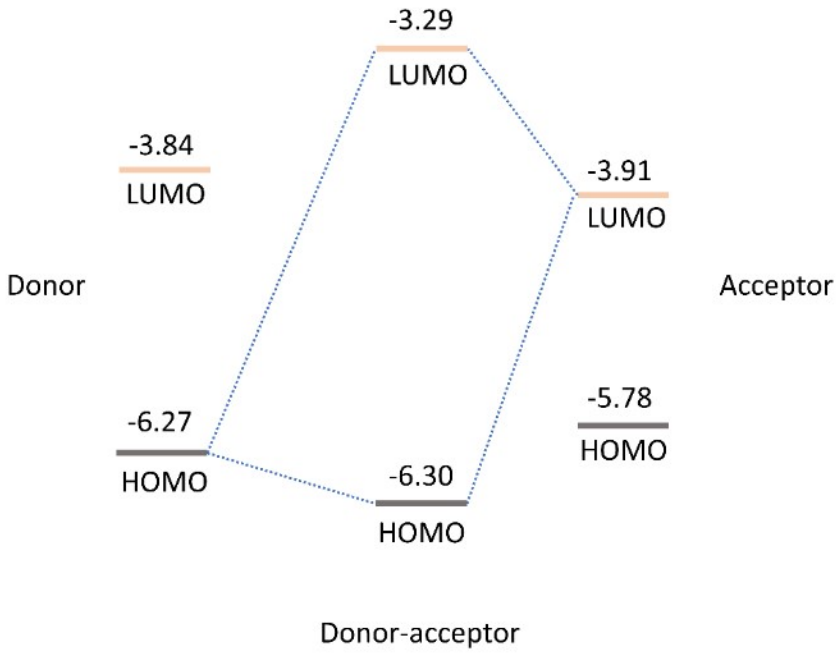

Fig S15. Orbital energy diagram for donor and acceptor

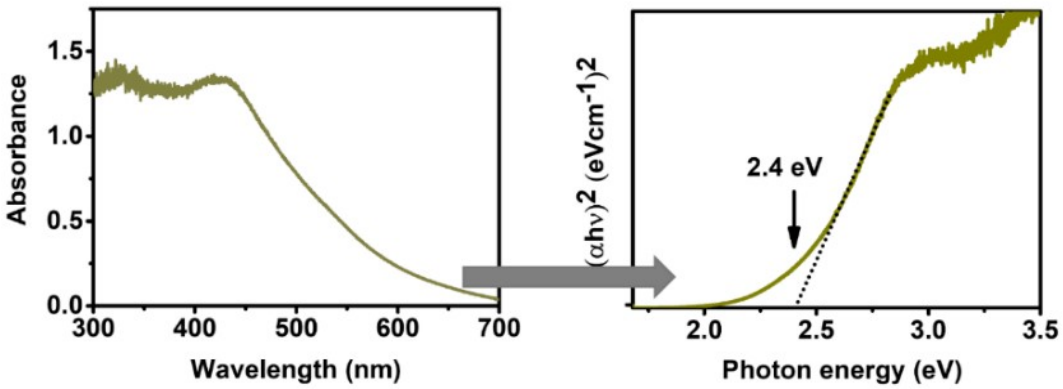

Fig S16. UV-vis spectrum and corresponding Tauc plot of TBB-phen

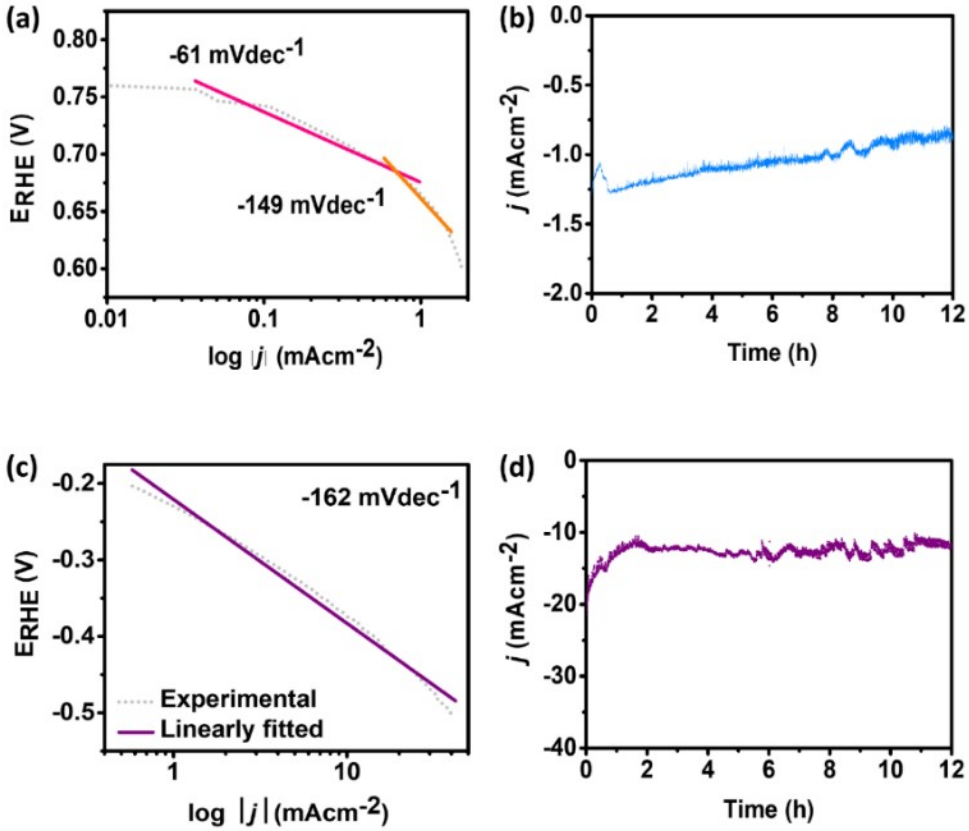

Fig S17(a). Tafel plot by recording LSV in O_2-purged 0.1 M KOH at 1 mVs^{-1} and 1600 rpm, (b) chronoamperometric plot recorded at 0.67 V vs. RHE in O_2-purged 0.1 M KOH and 1600 rpm for ORR, (c) Tafel plot by recording LSV in N_2-purged 0.5 M H_2SO_4 at 1 mVs^{-1} and 1600 rpm, and (d) *i-t* chronoamperometric plot recorded at -0.35 V vs. RHE in N_2-purged 0.5 M H_2SO_4 at 1600 rpm for HER

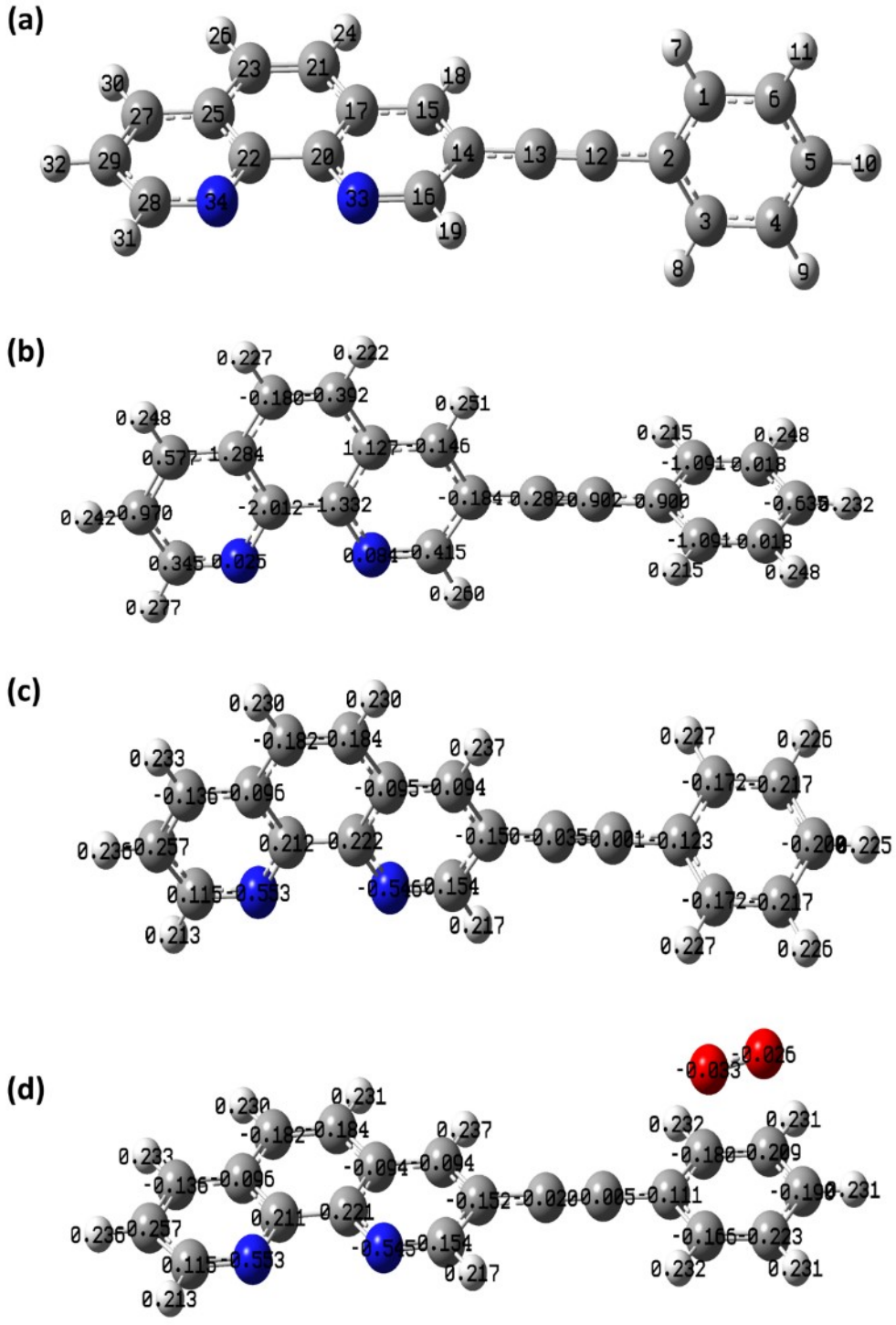

Fig S18. Model structure of TBB-phen (a) illustrating labeled atoms for identification of atoms, (b) illustrating Mulliken charge distribution, (c) NBO charge illustration before oxygen chemisorption, and (d) NBO charge distribution after oxygen chemisorption.

Table S1: Second Order Perturbation Theory Analysis of Fock Matrix in NBO Basis From TBB-phen to O_2

Donor NBO (i)	Acceptor NBO (j)	$E^{(2)}$ kcal/mol
1. BD (1) C 1 - C 2	187. RY*(2) O 36	0.27
1. BD (1) C 1 - C 2	239. BD*(1) O 35 - O 36	0.10
2. BD (2) C 1 - C 2	184. RY*(3) O 35	0.06
2. BD (2) C 1 - C 2	187. RY*(2) O 36	0.92
2. BD (2) C 1 - C 2	**239. BD*(1) O 35 - O 36**	**7.36**
3. BD (1) C 1 - C 6	187. RY*(2) O 36	0.06
5. BD (1) C 2 - C 3	187. RY*(2) O 36	0.11
6. BD (1) C 2 - C 12	187. RY*(2) O 36	0.06
7. BD (1) C 3 - C 4	183. RY*(2) O 35	0.08
8. BD (2) C 3 - C 4	182. RY*(1) O 35	0.10
8. BD (2) C 3 - C 4	183. RY*(2) O 35	0.17
8. BD (2) C 3 - C 4	239. BD*(1) O 35 - O 36	0.72
10. BD (1) C 4 - C 5	183. RY*(2) O 35	0.34
10. BD (1) C 4 - C 5	239. BD*(1) O 35 - O 36	0.12
12. BD (1) C 5 - C 6	183. RY*(2) O 35	0.18
13. BD (2) C 5 - C 6	182. RY*(1) O 35	0.10
13. BD (2) C 5 - C 6	183. RY*(2) O 35	0.37
13. BD (2) C 5 - C 6	**239. BD*(1) O 35 - O 36**	**3.39**
18. BD (3) C 12 - C 13	239. BD*(1) O 35 - O 36	0.10
191. BD*(2) C 1 - C 2	186. RY*(1) O 36	0.07

i = donor filled orbitals, j = acceptor unfilled orbitals, $E^{(2)}$ = stabilization energy, BD(1) = σ orbitals, BD*(1) = σ* orbitals, BD(2) = π orbitals, BD*(2) = π* orbitals, RY* = Rydberg orbitals

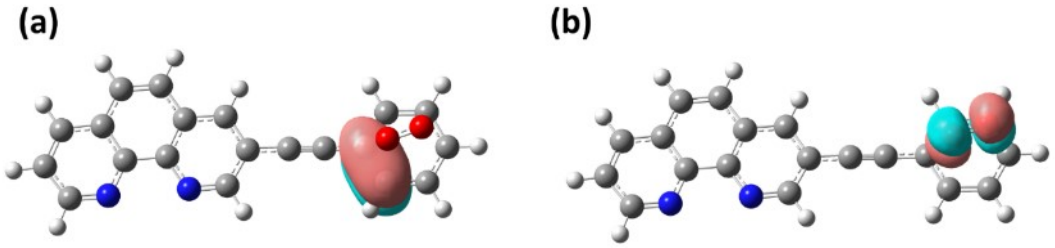

Fig S19 (a) HOMO and (b) LUMO NBO orbitals in TBB-phen-O_2 (isovalue = 0.04)

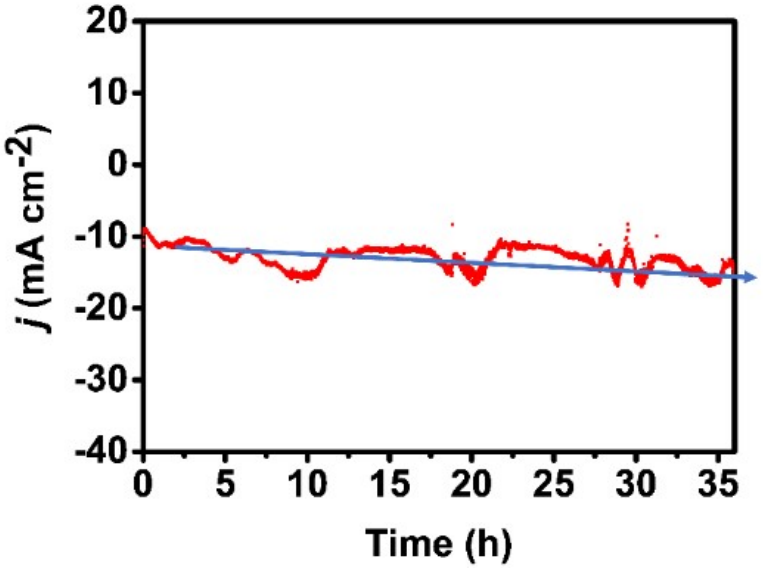

Fig S20. *i-t* chronoamperometric plot recorded at @10 $mAcm^{-2}$ in N_2-purged 0.5 M H_2SO_4 at 1600 rpm

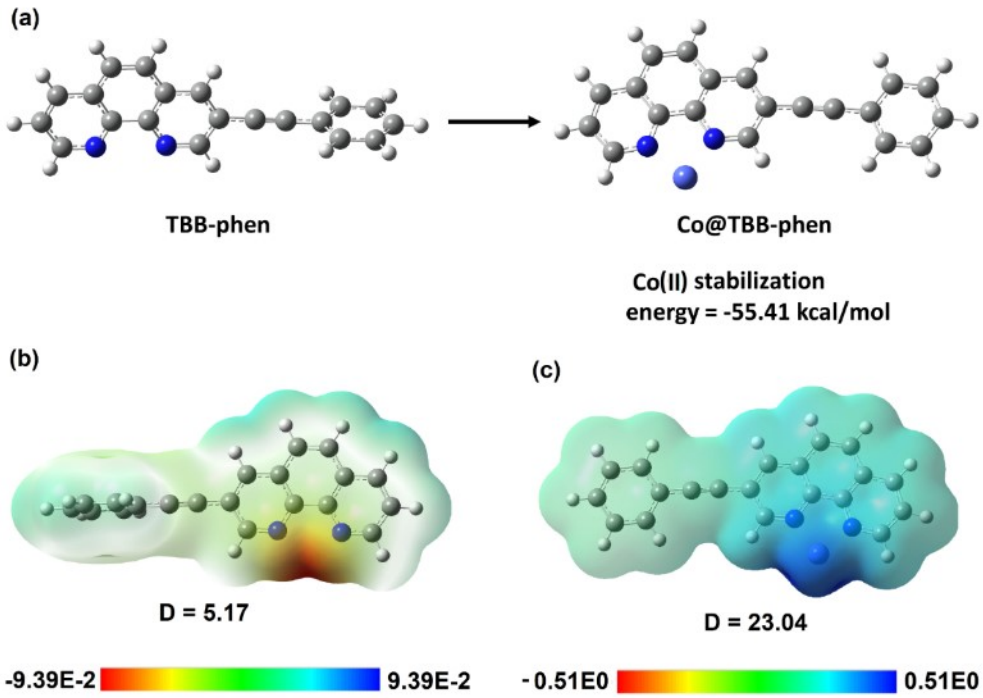

Fig S21. (a) Co(II) stabilization energy in Co@TBB-phen, MEP in (b) TBB-phen, and (c) Co@TBB-phen

Table S2: Second Order Perturbation Theory Analysis of Fock Matrix in NBO Basis From TBB-phen to Co in Co@TBB-phen

Donor NBO (i)	Acceptor NBO (j)	$E^{(2)}$ kcal/mol	Spin state
76. LP (1) N 33	81. LP*(4)Co 35	22.38	alpha
76. LP (1) N 33	82. LP*(5)Co 35	18.53	alpha
77. LP (1) N 34	81. LP*(4)Co 35	23.34	alpha
77. LP (1) N 34	82. LP*(5)Co 35	18.00	alpha
233. BD*(2) C 22 - N 34	85. LP*(8)Co 35	1.44	alpha
76. LP (1) N 33	82. LP*(5)Co 35	24.23	beta
76. LP (1) N 33	83. LP*(6)Co 35	15.08	beta
77. LP (1) N 34	82. LP*(5)Co 35	24.90	beta
77. LP (1) N 34	83. LP*(6)Co 35	14.76	beta
77. LP (1) N 34	191. RY*(5)Co 35	1.04	beta
233. BD*(2) C 22 - N 34	85. LP*(8)Co 35	1.57	beta

i = donor filled orbitals, j = acceptor unfilled orbitals, $E^{(2)}$ = stabilization energy, LP = lone pair orbitals, LP* = valence lone pair orbitals, BD*(2) = π* orbitals, RY* = Rydberg orbitals

From Co to TBB-phen in Co@TBB-phen

Donor NBO (i)	Acceptor NBO (j)	$E^{(2)}$ kcal/mol	Spin state
72. CR (1)Co 35	221. BD*(1) C 16 - N 33	1.08	alpha
72. CR (1)Co 35	243. BD*(1) C 28 - N 34	1.10	alpha
82. LP*(5)Co 35	132. RY*(1) C 16	3.77	alpha
82. LP*(5)Co 35	136. RY*(1) C 17	1.48	alpha
82. LP*(5)Co 35	142. RY*(1) C 20	3.16	alpha
82. LP*(5)Co 35	143. RY*(2) C 20	2.30	alpha
82. LP*(5)Co 35	150. RY*(1) C 22	3.35	alpha
82. LP*(5)Co 35	151. RY*(2) C 22	3.03	alpha
82. LP*(5)Co 35	159. RY*(1) C 25	1.34	alpha
82. LP*(5)Co 35	160. RY*(2) C 25	1.02	alpha
82. LP*(5)Co 35	164. RY*(1) C 27	3.76	alpha
82. LP*(5)Co 35	168. RY*(1) C 28	2.78	alpha
82. LP*(5)Co 35	179. RY*(1) N 33	4.11	alpha
82. LP*(5)Co 35	183. RY*(1) N 34	4.12	alpha
82. LP*(5)Co 35	243. BD*(1) C 28 - N 34	1.02	alpha
72. CR (1)Co 35	221. BD*(1) C 16 - N 33	1.08	beta
72. CR (1)Co 35	243. BD*(1) C 28 - N 34	1.10	beta

i = donor filled orbitals, j = acceptor unfilled orbitals, $E^{(2)}$ = stabilization energy, CR = 1-center core orbitals, LP* = valence lone pair orbitals, BD*(1) = σ* orbitals, RY* = Rydberg orbitals

Estimation of Cobalt (II) coverage in TBB-phen

The total percentage of Co(II) that could ideally coordinate with the TBB-phen is determined based on the asymmetric unit of TBB-phen (as it is challenging to calculate the molecular weight of a conjugated organic polymer). The asymmetric unit of TBB-phen ($C_{14}H_{17}N$) contains one pyridinic N of the phenanthroline.

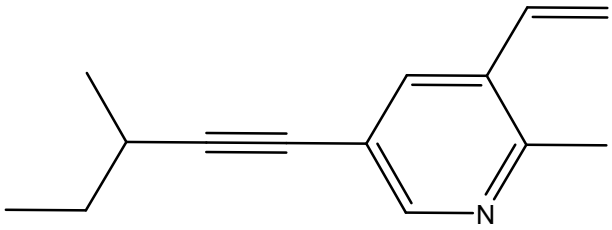

Fig S22. Asymmetric Unit of TBB-phen

Based on the XPS analysis, DFT computations, and pieces of literature, the Co(II) ions bind only to the phenanthroline N-atoms in TBB-phen. The asymmetric unit of TBB-phen contains only one pyridine N. Therefore, in the present study, ideally, one asymmetric unit (containing ½ phen unit) would coordinate to ½ Co(II) ion.

Let us take 100 g of TBB-phen. The molecular weight of the asymmetric unit is 199.30 g/mole. Hence, 100 g of TBB-phen will contain 0.501 moles of asymmetric units.

∴ 100 g of TBB-phen will contain and coordinate to 0.501/2 moles of Co(II) ions which is 0.250 moles.

Taking the molecular weight of cobalt as 58.93 $gmol^{-1}$, 100 g of TBB-phen will possibly coordinate with 14.78 g of Co(II) ions.

Considering ICP-MS data as a reference for the content of cobalt in the TBB-phen, which is 8.2 % Co(II) ions, on average, 55% of the phenanthroline N atoms are coordinated to the Co(II) ions. Though we tried to synthesize crystalline polymer, its amorphous structure lays a gigantic hindrance to visualizing the coordination of phen N-Co units within the TBB-phen and could be a reason for only 55% Co(II) coverage.

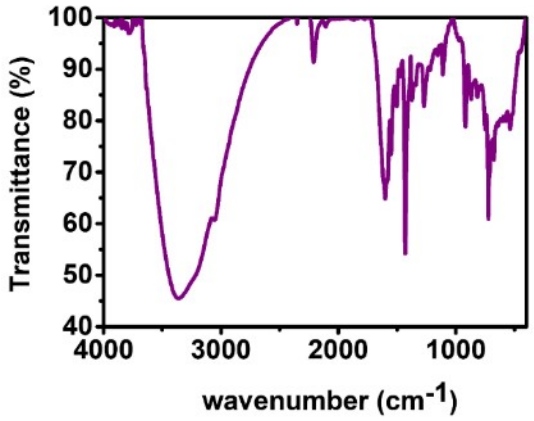

Fig S23. FTIR spectrum of Co@TBB-phen

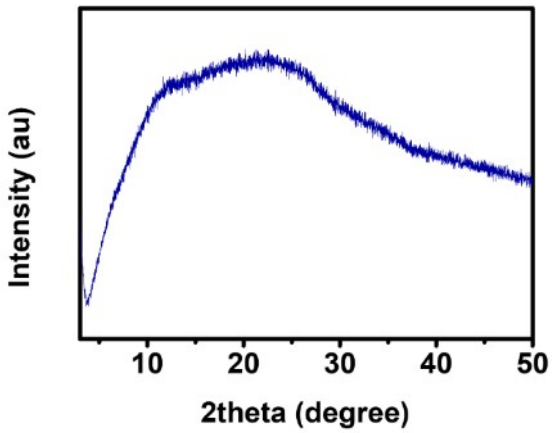

Fig S24. PXRD pattern of Co@TBB-phen

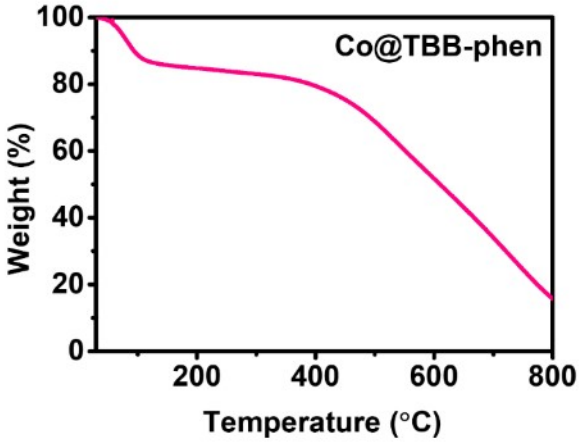

Fig S25. TGA profile of Co@TBB-phen

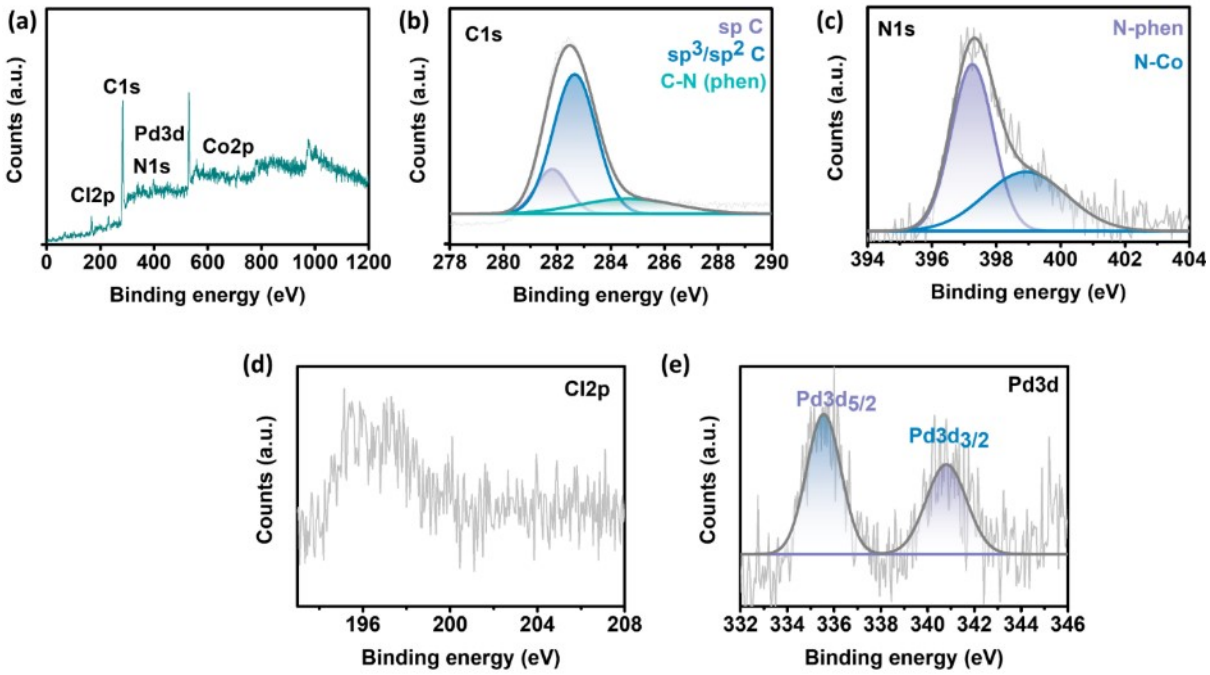

Fig S26. XPS spectrum of (a) complete elemental scan, (b) deconvoluted C1s, (c) deconvoluted N1s, (d) deconvoluted Cl2p, and (e) deconvoluted Pd3d

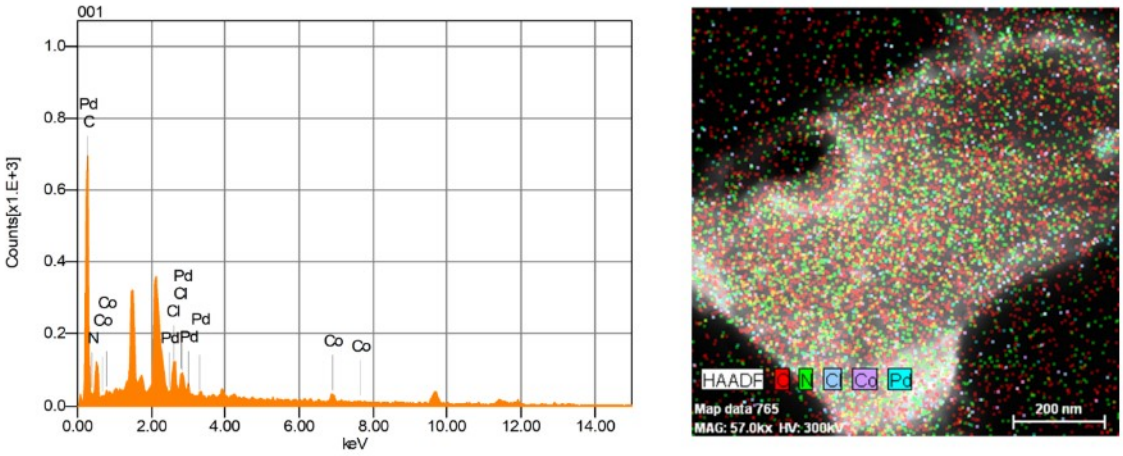

Fig S27. Energy dispersive spectrum (left) and HAADF elemental mapping (right) of Co@TBB-phen

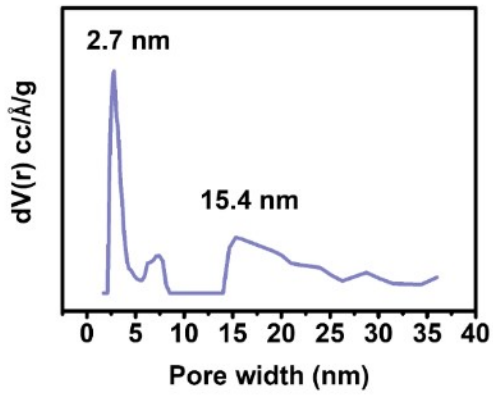

Fig S28. NLDFT pore width of Co@TBB-phen

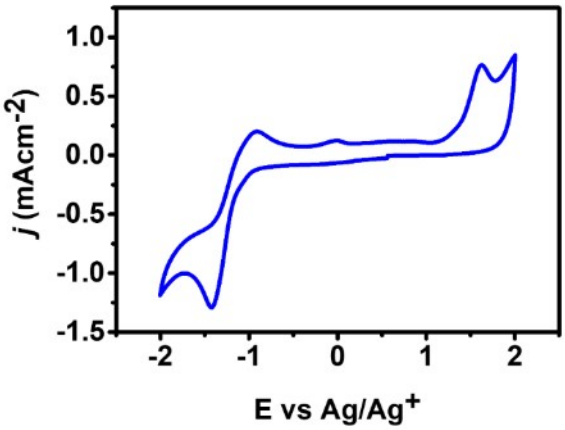

Fig S29. CV of Co@TBB-phen recorded in 0.1 M TBAP solution in anhydrous acetonitrile with respect to $Ag/AgNO_3$

The same procedure is adopted for bandgap determination of Co@TBB-phen as performed for TBB-phen by keeping all the testing parameters and conditions alike. Utilizing the eq. (10), (11), and (12), we obtained as follows

The onset oxidation and reduction potentials are found to be 2.47 V and 0.19 V vs. RHE, respectively.

$E_{oxRHE}^{onset} = 0.799 + (1.26) + 0.413 = 2.47$ V

$E_{redRHE}^{onset} = 0.799 + (-1.02) + 0.413 = 0.19$ V

The calculated HOMO and LUMO levels came out to be -6.49 eV and -3.83 eV, respectively, giving the bandgap of **2.66 eV**.

E (HOMO) = -e [2.47 - 0.42 + 4.44] = **-6.49 eV**

E (LUMO) = -e [-0.19 - 0.42 + 4.44] = **-3.83 eV**

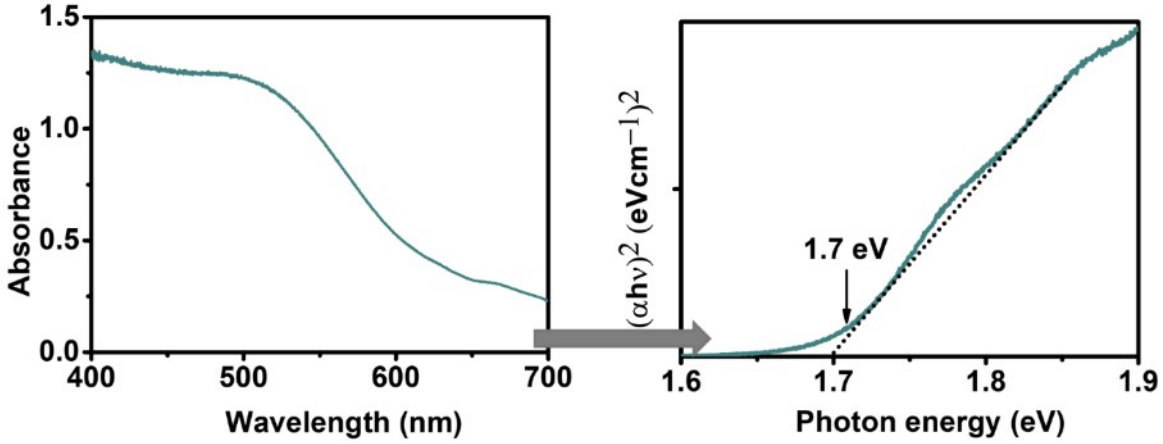

Fig S30. UV-vis spectrum and corresponding Tauc plot of Co@TBB-phen

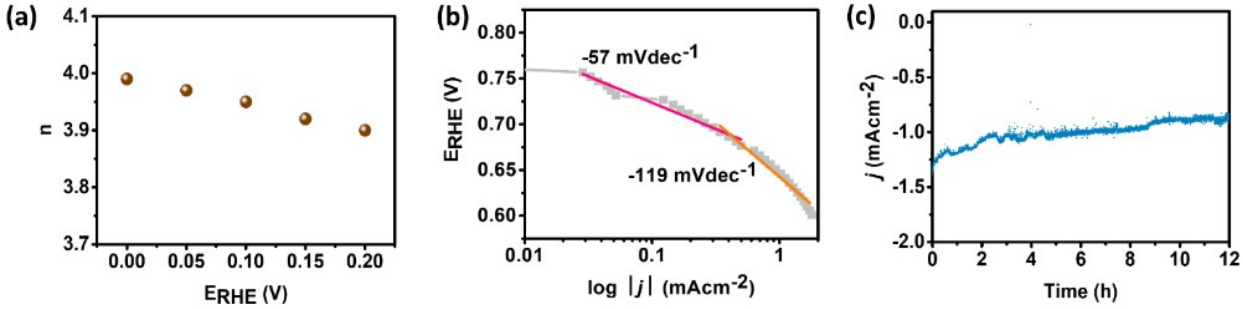

Fig S31. (a) number of electron transfer deduced from the K-L plot, (b) Tafel plot by recording LSV in O_2-purged 0.1 M KOH at 1 mVs^{-1} and 1600 rpm, and (c) chronoamperometric plot recorded at 0.67 V vs. RHE in O_2-purged 0.1 M KOH at 1600 rpm for ORR in Co@TBB-phen

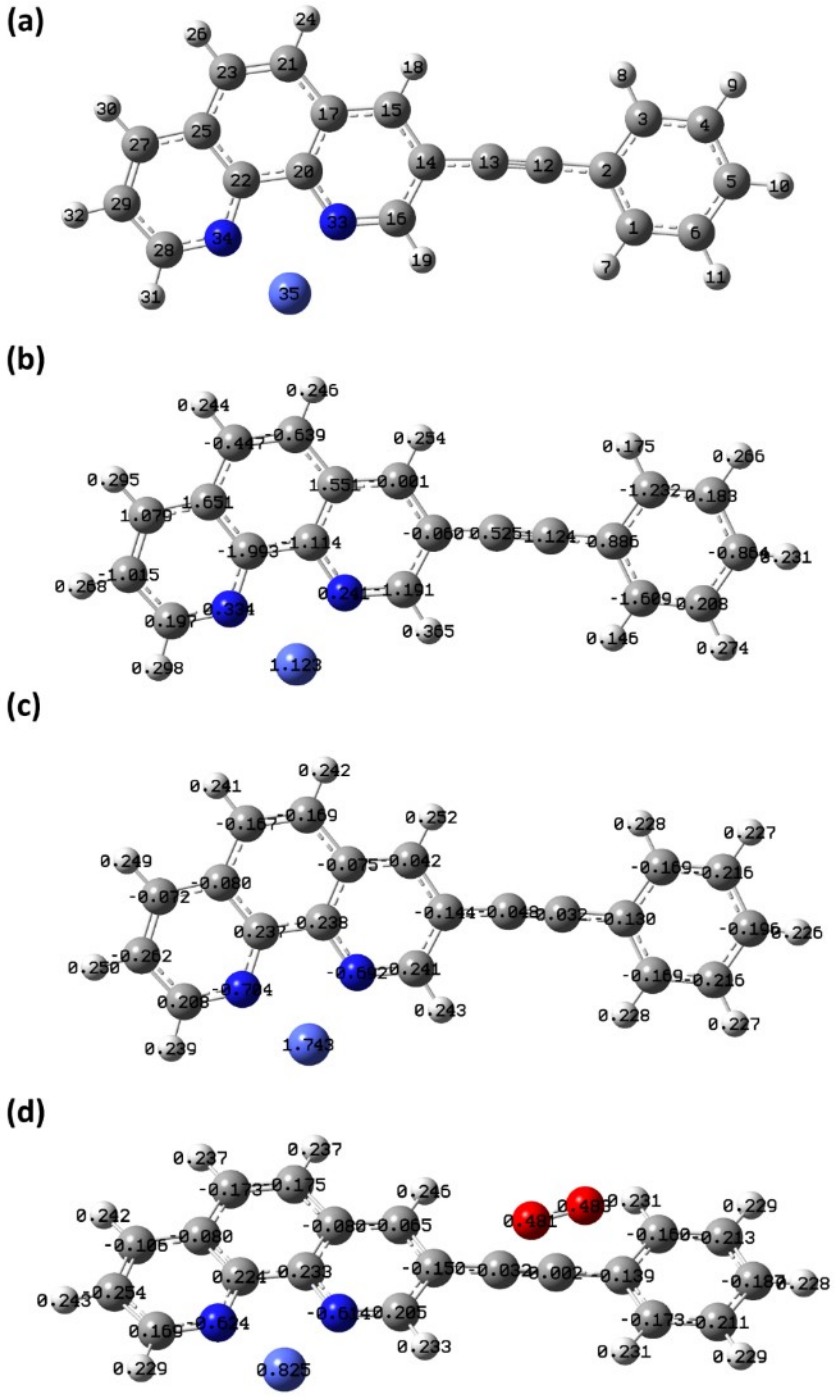

Fig S32. Model structure of Co@TBB-phen (a) illustrating labeled atoms for identification of atoms, (b) illustrating Mulliken charge distribution, (c) NBO charge illustration before oxygen chemisorption, and (d) NBO charge distribution after oxygen chemisorption.

Table S3 Second Order Perturbation Theory Analysis of Fock Matrix in NBO Basis From TBB-phen to O_2 in Co@TBB-phen

Donor NBO (i)	Acceptor NBO (j)	$E^{(2)}$ kcal/mol	Spin state
2. BD (2) C 1 - C 2	204. RY*(1) O 36	0.04	alpha
2. BD (2) C 1 - C 2	205. RY*(2) O 36	0.03	alpha
2. BD (2) C 1 - C 2	261. BD*(1) O 36 - O 37	0.16	alpha
6. BD (1) C 2 - C 12	204. RY*(1) O 36	0.04	alpha
8. BD (2) C 3 - C 4	261. BD*(1) O 36 - O 37	0.23	alpha
13. BD (2) C 5 - C 6	261. BD*(1) O 36 - O 37	0.07	alpha
16. BD (1) C 12 - C 13	208. RY*(1) O 37	0.03	alpha
18. BD (3) C 12 - C 13	208. RY*(1) O 37	0.04	alpha
18. BD (3) C 12 - C 13	261. BD*(1) O 36 - O	0.03	alpha
2. BD (2) C 1 - C 2	205. RY*(3) O 36	0.03	beta
2. BD (2) C 1 - C 2	260. BD*(1) O 36 - O 37	0.56	beta
2. BD (2) C 1 - C 2	261. BD*(2) O 36 - O 37	0.21	beta
2. BD (2) C 1 - C 2	262. BD*(3) O 36 - O 37	0.05	beta
6. BD (1) C 2 - C 12	203. RY*(1) O 36	0.03	beta
8. BD (2) C 3 - C 4	261. BD*(2) O 36 - O 37	0.03	beta
13. BD (2) C 5 - C 6	260. BD*(1) O 36 - O 37	0.10	beta
17. BD (2) C 12 - C 13	261. BD*(2) O 36 - O 37	0.03	beta
18. BD (3) C 12 - C 13	260. BD*(1) O 36 - O 37	0.56	beta
18. BD (3) C 12 - C 13	262. BD*(3) O 36 - O 37	0.04	beta
21. BD (2) C 14 - C 15	260. BD*(1) O 36 - O 37	0.04	beta

i = donor filled orbitals, j = acceptor unfilled orbitals, $E^{(2)}$ = stabilization energy, BD(1) = σ orbitals, BD(2) = π orbitals BD*(1) = σ* orbitals, BD*(2) = π* orbitals, RY* = Rydberg orbitals

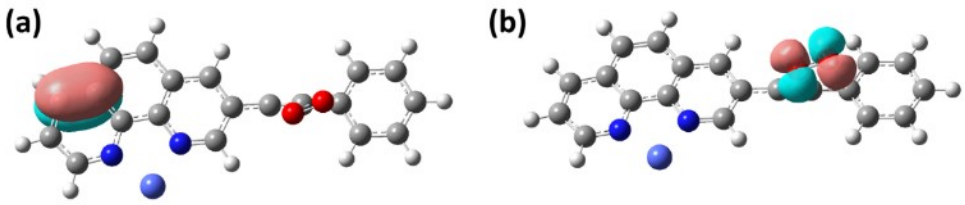

Fig S33 (a) HOMO and (b) LUMO NBO orbitals in Co@TBB-phen (isovalue = 0.04)

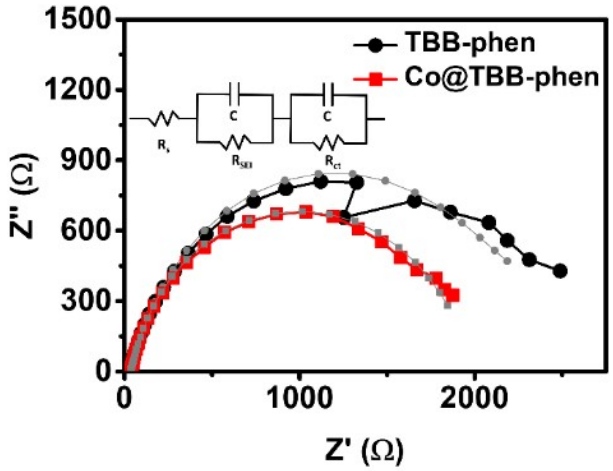

Fig S34. Nyquist plot for ORR recorded at 0.66 V vs. RHE in a frequency range of 0.1 to 10^5 Hz

Table S4 The EIS parameters of TBB-phen and Co@TBB-phen in ORR

	TBB-phen	**Co@TBB-phen**
R_s (Ω)	36.9	35.7
R_{ct} (Ω)	1810.0	1510.0
R_{SEI} (Ω)	215.0	168.0
$C_{dl}1$ (μF)	94.7	63.7
$C_{dl}2$ (μF)	56.0	92.7

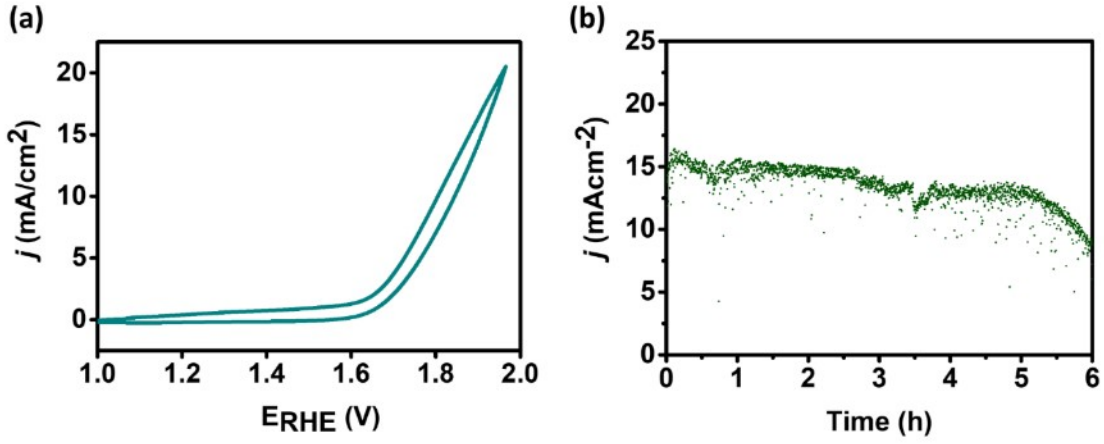

Fig S35. (a) CV recorded in 0.1 M KOH at a scan rate of 50 mVs^{-1}, and (b) chronoamperometric plot recorded at 1.8 V vs. RHE in 0.1 M KOH at 1600 rpm for OER

Table S5. Electronic configuration of chemisorbing atom in TBB-phen and Co@TBB-phen

TBB-phen (C25)

OH	[core]2S(0.90)2p(3.19)3p(0.02)
O	[core]2S(0.89)2p(2.86)3p(0.03)
OOH	[core]2S(0.90)2p(3.17)3p(0.02)
OO	[core]2S(0.90)2p(3.17)3p(0.02)

Co@TBB-phen (Co35)

OH	[core]3d(6.77)4p(0.04)5S(0.15)4d(0.01)5p(0.08
O	[core]4S(0.13)3d(6.64)4p(0.14)4d(0.01)
OOH	[core]3d(6.78)4p(0.10)5S(0.15)4d(0.02)5p(0.07)
OO	[core]4S(0.13)3d(8.00)4p(0.04)

Table S6 Second Order Perturbation Theory Analysis of Fock Matrix in NBO Basis in OER in TBB-phen

Donor NBO (i)	**Acceptor NBO (j)**	**$E^{(2)}$ kcal/mol**	**Spin state**
From O to TBB-phen			
77. LP (3) O 35	**/213. BD*(2) C 17 - C 20**	**1.29**	**alpha**
76. LP (2) O 35	/213. BD*(2) C 17 - C 20	1.10	beta
From O to H			
72. CR (1) O 35	/ 79. LP*(1) H 36	4.68	alpha
75. LP (1) O 35	/ 79. LP*(1) H 36	10.16	Alpha
77. LP (3) O 35	/ 79. LP*(1) H 36	7.34	Alpha
78. LP (4) O 35	/ 79. LP*(1) H 36	392.53	Alpha
78. LP (4) O 35	/184. RY*(1) H 36	15.11	alpha
72. CR (1) O 35	/ 79. LP*(1) H 36	4.45	Beta
75. LP (1) O 35	/ 79. LP*(1) H 36	7.14	Beta
76. LP (2) O 35	/ 79. LP*(1) H 36	10.55	Beta
77. LP (3) O 35	/ 79. LP*(1) H 36	513.09	Beta

77. LP (3) O 35	/184. RY*(1) H 36	17.29	Beta
From H to O			
79. LP*(1) H 36	/182. RY*(3) O 35	1.25	Alpha
79. LP*(1) H 36	/183. RY*(4) O 35	1.80	Alpha
79. LP*(1) H 36	/182. RY*(3) O 35	1.46	beta
79. LP*(1) H 36	/183. RY*(4) O 35	2.14	beta

Table S7 Second Order Perturbation Theory Analysis of Fock Matrix in NBO Basis in OER in Co@TBB-phen

Donor NBO (i)	**Acceptor NBO (j)**	**$E^{(2)}$ kcal/mol**
From O to Co		
76. CR (1) O 36	/ 82. LP*(4)Co 35	2.8
76. CR (1) O 36	/ 84. LP*(6)Co 35	3.01
76. CR (1) O 36	/ 85. LP*(7)Co 35	3.79
88. LP (1) O 36	/ 83. LP*(5)Co 35	1.22
88. LP (1) O 36	/ 86. LP*(8)Co 35	9.31
89. LP (2) O 36	/ 82. LP*(4)Co 35	14.09
89. LP (2) O 36	/ 84. LP*(6)Co 35	15.59
89. LP (2) O 36	/ 85. LP*(7)Co 35	29.06
90. LP (3) O 36	**/ 82. LP*(4)Co 35**	**188.27**
90. LP (3) O 36	/ 84. LP*(6)Co 35	51.32
90. LP (3) O 36	/ 85. LP*(7)Co 35	6.97
90. LP (3) O 36	/ 87. LP*(9)Co 35	1.69
91. LP (4) O 36	/ 82. LP*(4)Co 35	1.63
91. LP (4) O 36	/ 87. LP*(9)Co 35	2.54
91. LP (4) O 36	/201. RY*(9)Co 35	1.1
From O to H		
76. CR (1) O 36	/ 92. LP*(1) H 37	9.17
89. LP (2) O 36	/ 92. LP*(1) H 37	14.91
90. LP (3) O 36	/ 92. LP*(1) H 37	61.73

90. LP (3) O 36	/206. RY*(1) H 37	2.63
91. LP (4) O 36	/ 92. LP*(1) H 37	733.98
91. LP (4) O 36	/206. RY*(1) H 37	27.32
From H to O		
92. LP*(1) H 37	/205. RY*(4) O 36	2.90

i = donor filled orbitals, j = acceptor unfilled orbitals, $E^{(2)}$ = stabilization energy, BD*(2) = π* orbitals, CR = 1-centre core, LP = lone pair, LP* = antibonding lone pair, RY* = Rydberg orbitals

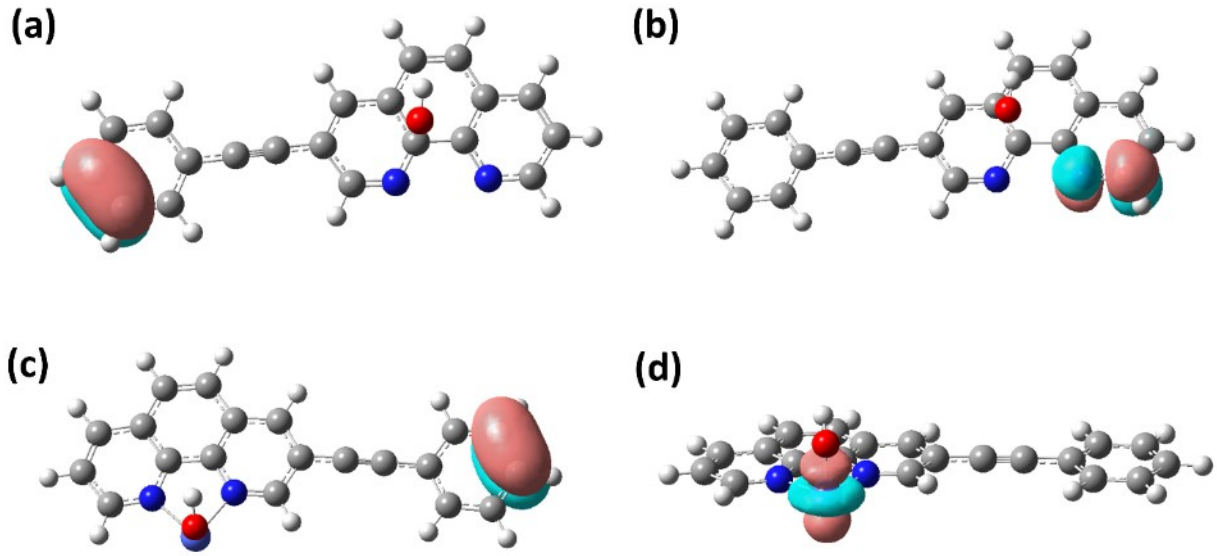

Fig S36. (a) HOMO NBO orbital, (b) LUMO NBO orbital in TBB-phen, (c) HOMO NBO orbital, and (d) LUMO NBO orbital in Co@TBB-phen (isovalue = 0.04)

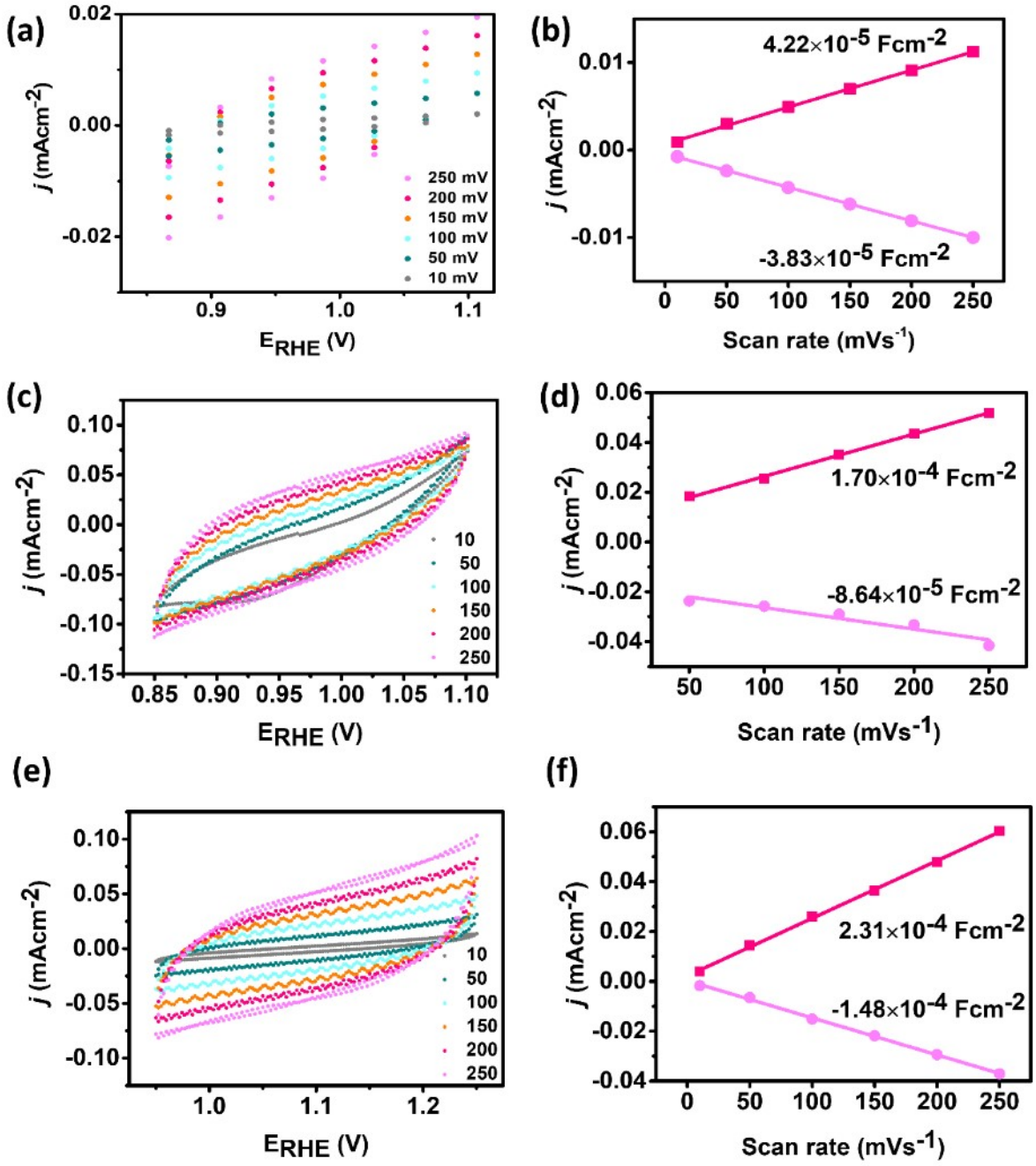

Fig S37. (a) Capacitance for bare GC, (b) corresponding j vs. scan rate plot for the capacitance of bare GC, (c) Capacitance for TBB-phen, (d) corresponding j vs. scan rate plot for the capacitance of TBB-phen, (e) OER activity for TBB-phen, and (f) corresponding j vs. scan rate plot for OER activity of TBB-phen

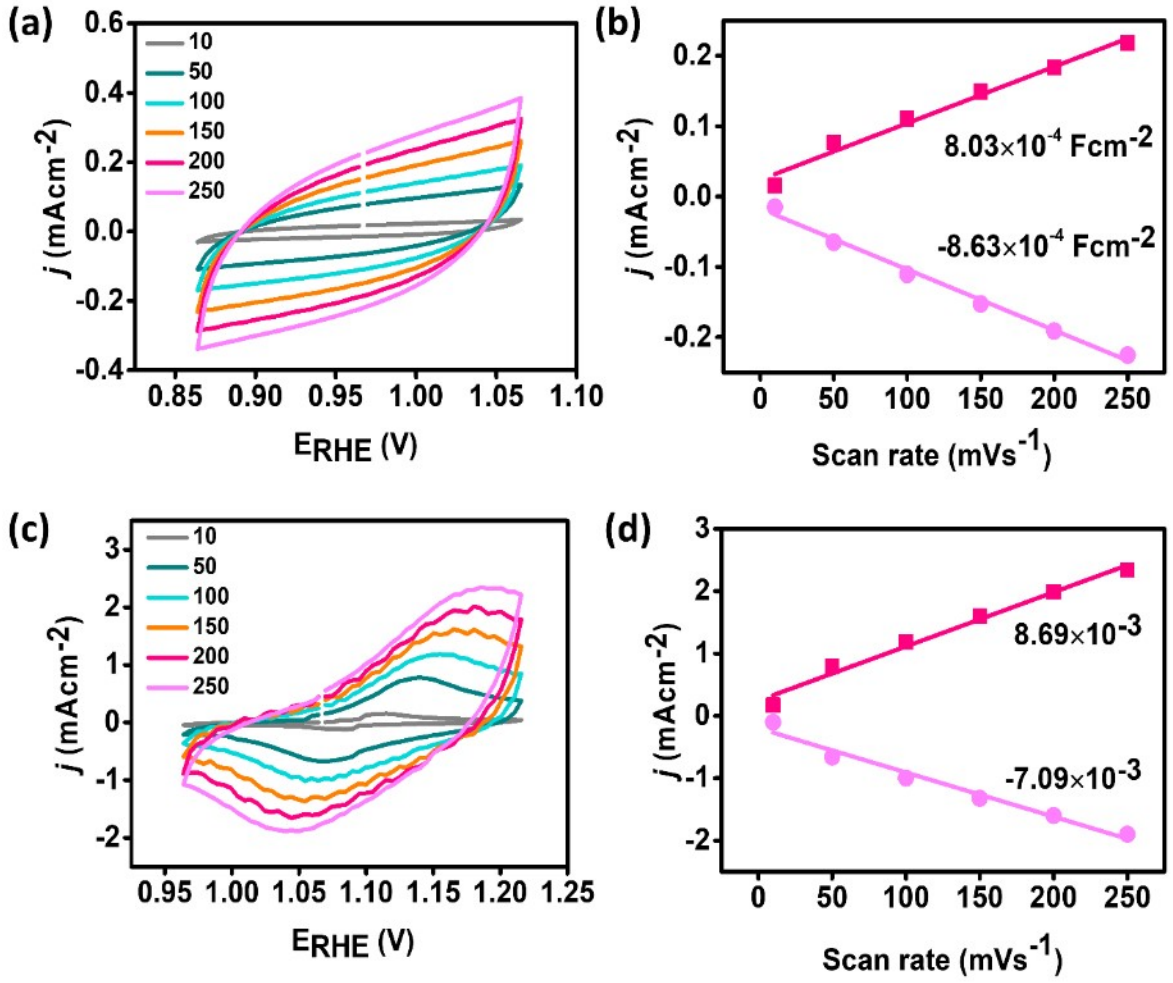

Fig S38. (a) Capacitance for Co@TBB-phen, (d) corresponding j vs. scan rate plot for the capacitance of Co@TBB-phen, (c) Cobalt peak for Co@TBB-phen, and (d) corresponding j vs. scan rate plot for cobalt peak of Co@TBB-phen

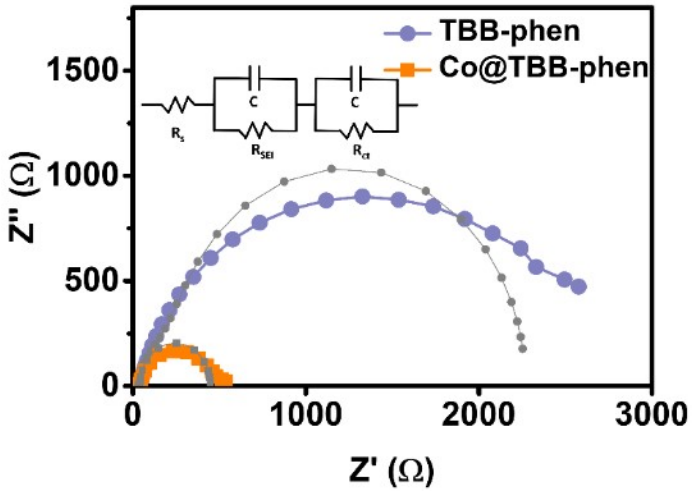

Fig S39. Nyquist plot for OER recorded at 1.76 V vs. RHE in a frequency range of 0.1 to 10^5 Hz

Table S8. The EIS parameters of TBB-phen and Co@TBB-phen in OER

	TBB-phen	**Co@TBB-phen**
R_s (Ω)	40.8	26.0
R_{ct} (Ω)	2050.0	409.0
R_{SEI} (Ω)	177.0	13.7
$C_{dl}1$ (µF)	45.8	0.112
$C_{dl}2$ (µF)	67.3	54.2

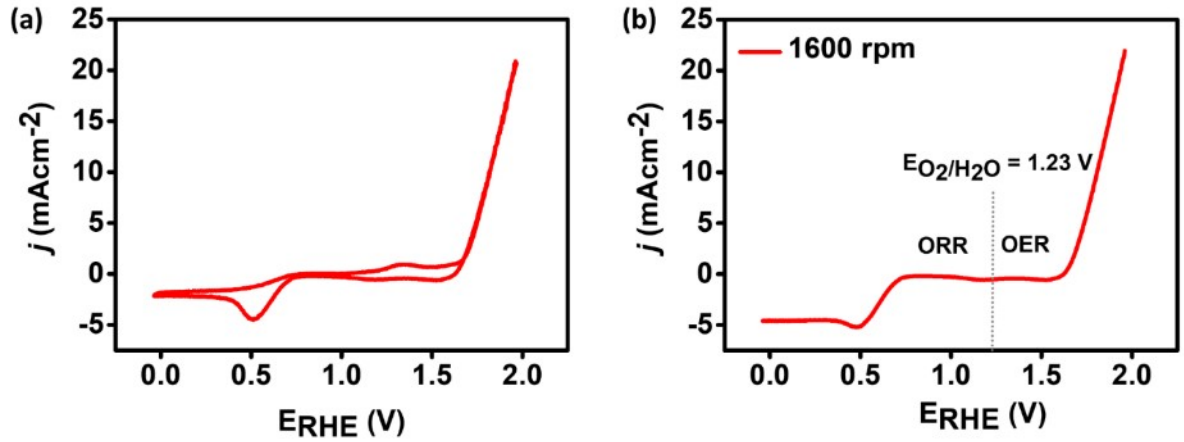

Fig S40. (a) CV recorded in O_2-saturated 0.1 M KOH at scan rate of 50 mVs^{-1}, and (b) LSV recorded in O_2-saturated 0.1 M KOH at scan rate of 5 mVs^{-1} and 1600 rpm of Co@TBB-phen towards overall bifunctionality

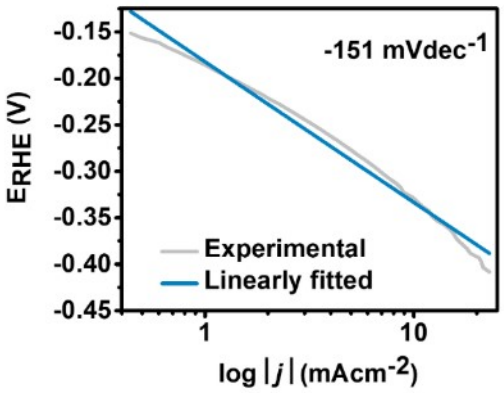

Fig S41. Tafel plot by recording LSV in N_2-purged 0.5 M H_2SO_4 at 1 mVs^{-1} and 1600 rpm for HER

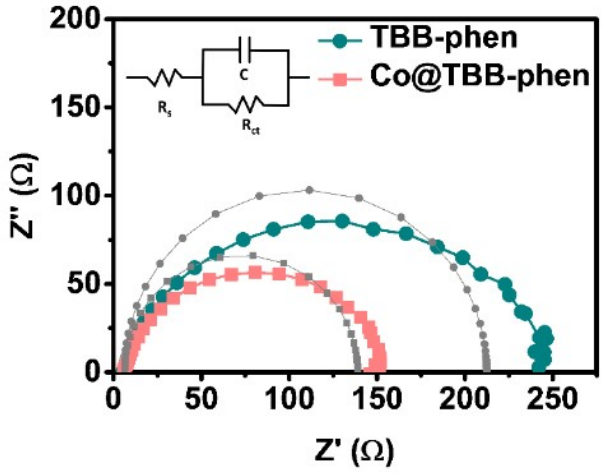

Fig S42. Nyquist plot for HER recorded at -0.48 V vs. RHE in a frequency range of 0.1 to 10^5 Hz

Table S9. The EIS parameters of TBB-phen and Co@TBB-phen in HER

	TBB-phen	**Co@TBB-phen**
R_s (Ω)	6.1	6.3
R_{ct} (Ω)	206.0	133.0
C_{dl} (μF)	35.6	51.1

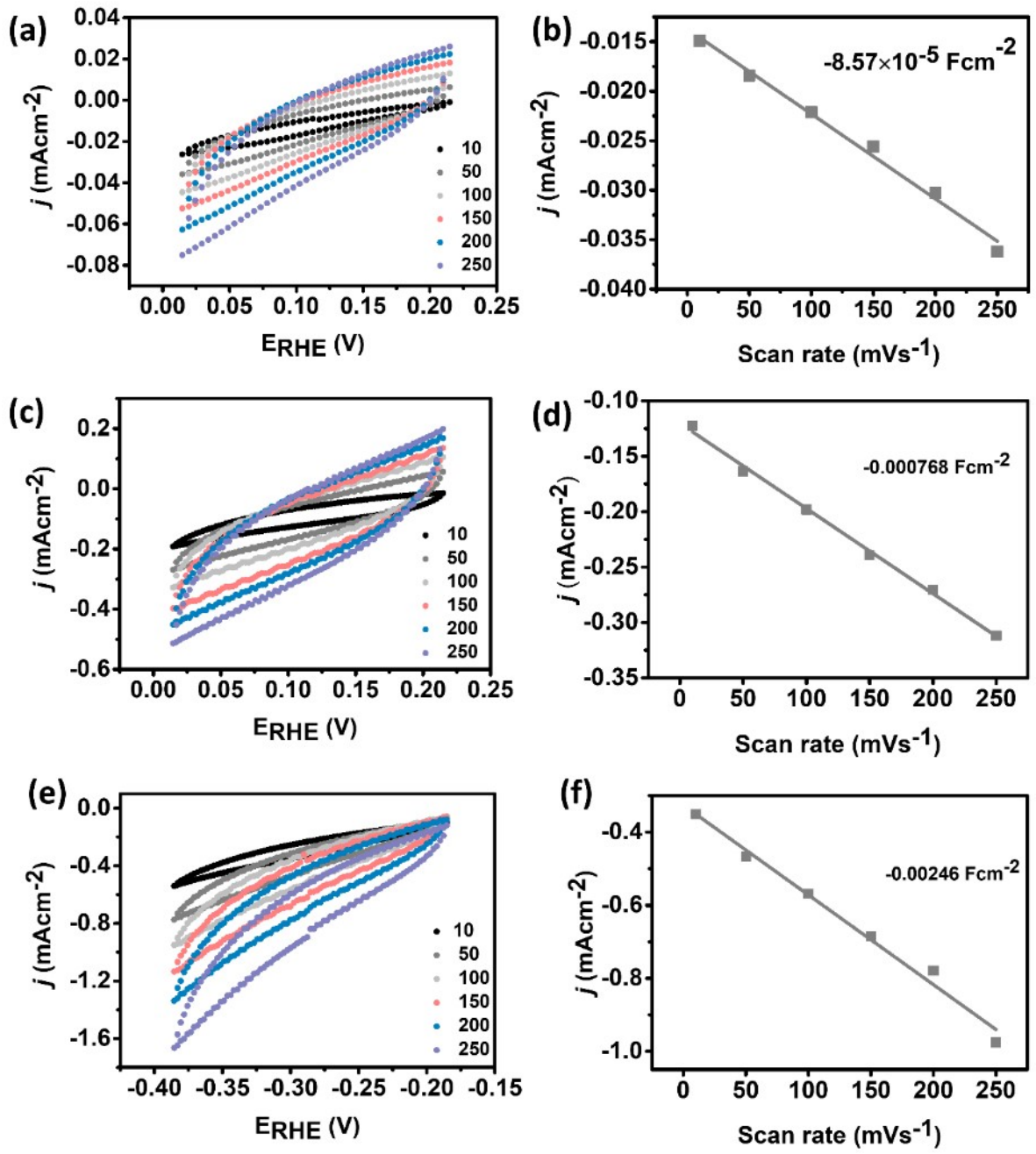

Fig S43. (a) Capacitance for bare GC, (b) corresponding j vs. scan rate plot for the capacitance of bare GC, (c) Capacitance for TBB-phen, (d) corresponding j vs. scan rate plot for the capacitance of TBB-phen, (e) HER activity for TBB-phen, and (f) corresponding j vs. scan rate plot for HER activity of TBB-phen

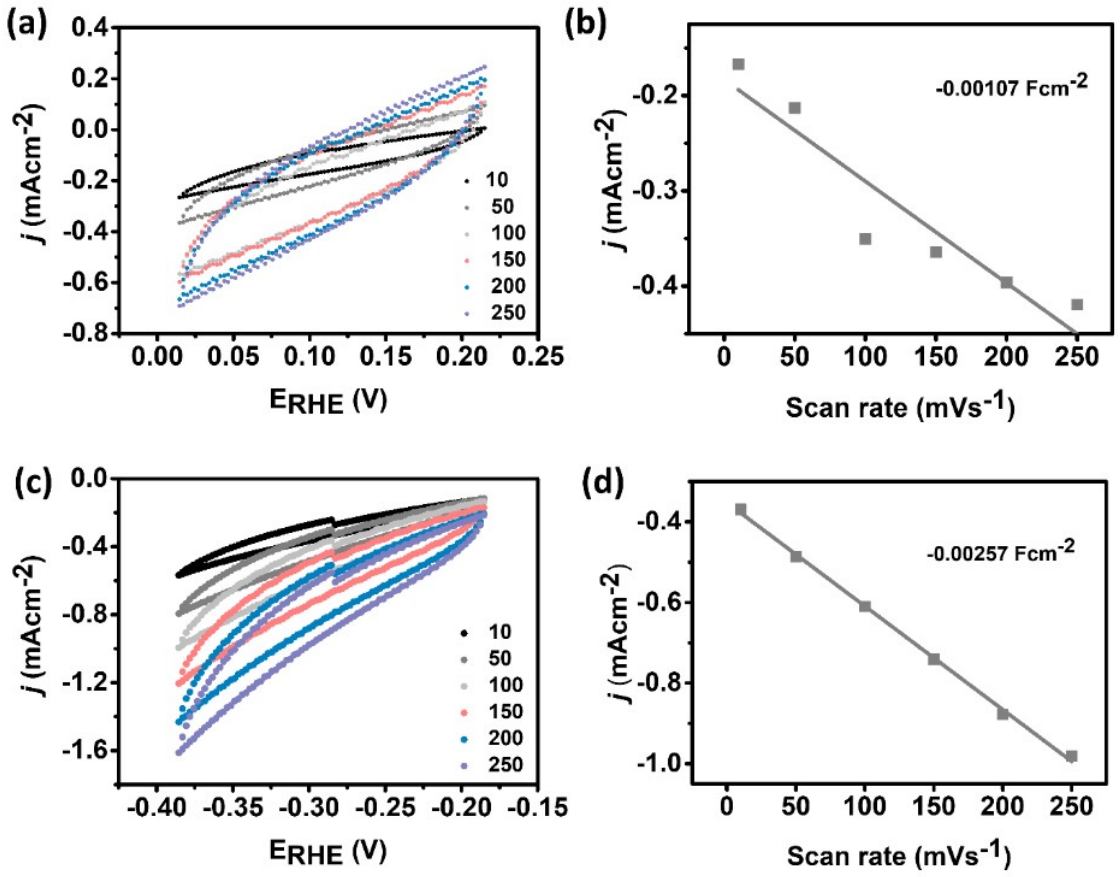

Fig S44. (a) Capacitance for Co@TBB-phen, (d) corresponding j vs. scan rate plot for the capacitance of Co@TBB-phen, (c) HER activity for Co@TBB-phen, and (d) corresponding j vs. scan rate plot for HER activity of Co@TBB-phen

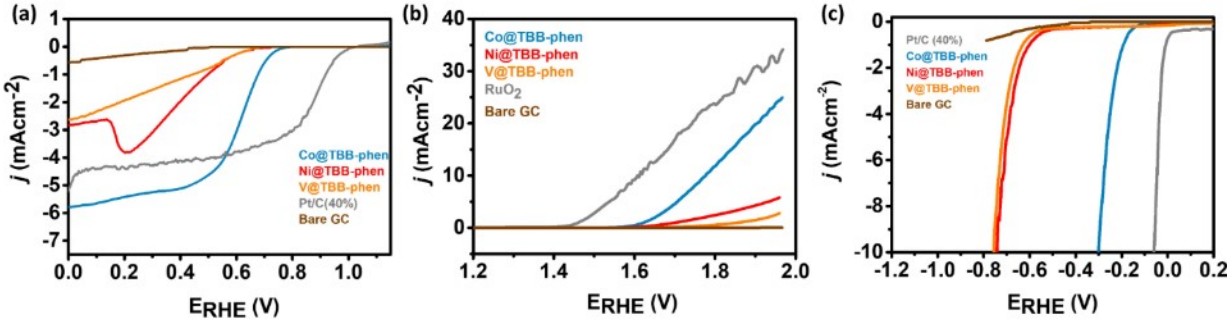

Fig S45. Material activity comparison towards (a) ORR recorded at a scan rate of 5 mVs^{-1} and 1600 rpm in O_2 saturated 0.1 M KOH, (b) OER recorded at a scan rate of 5 mVs^{-1} and 1600 rpm in N_2 saturated 0.1 M KOH, and (c) HER recorded at a scan rate of 5 mVs^{-1}, and 1600 rpm in N_2 saturated 0.5 M H_2SO_4

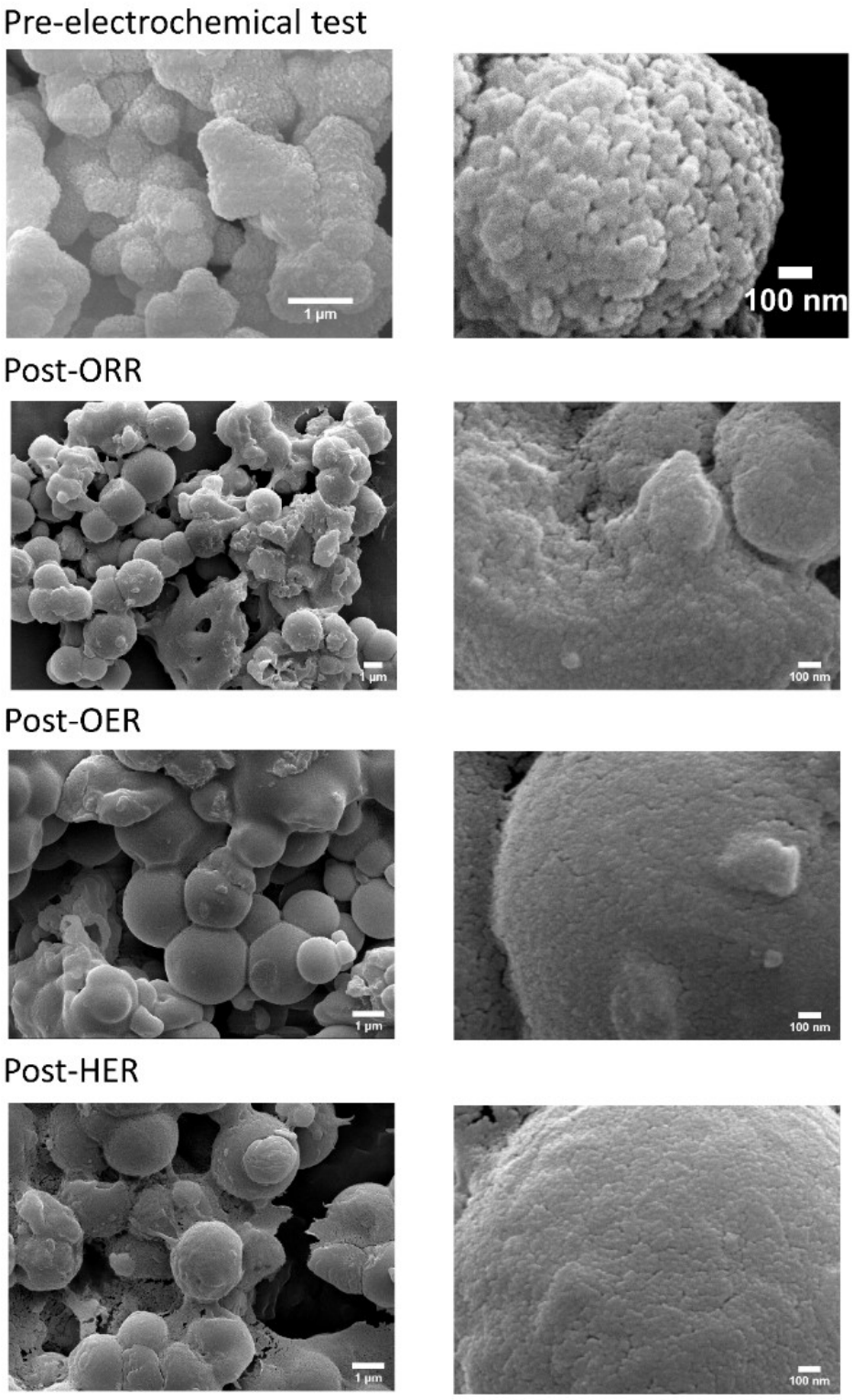

Fig S46. FESEM images of Co@TBB-phen before and after electrochemical tests

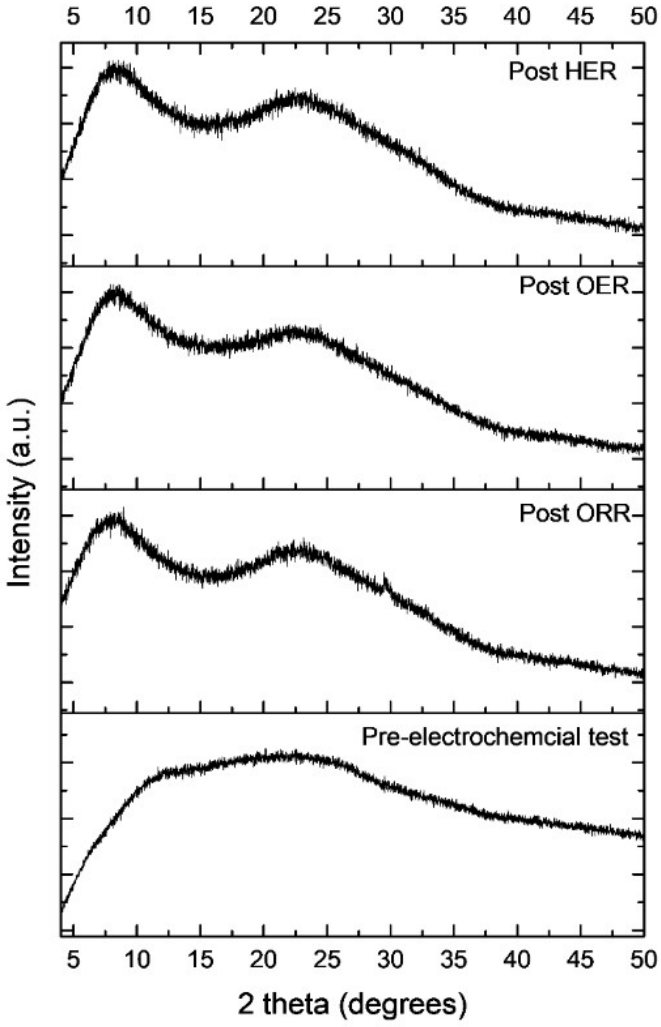

Fig S47. PXRD pattern of Co@TBB-phen before and after electrochemical tests

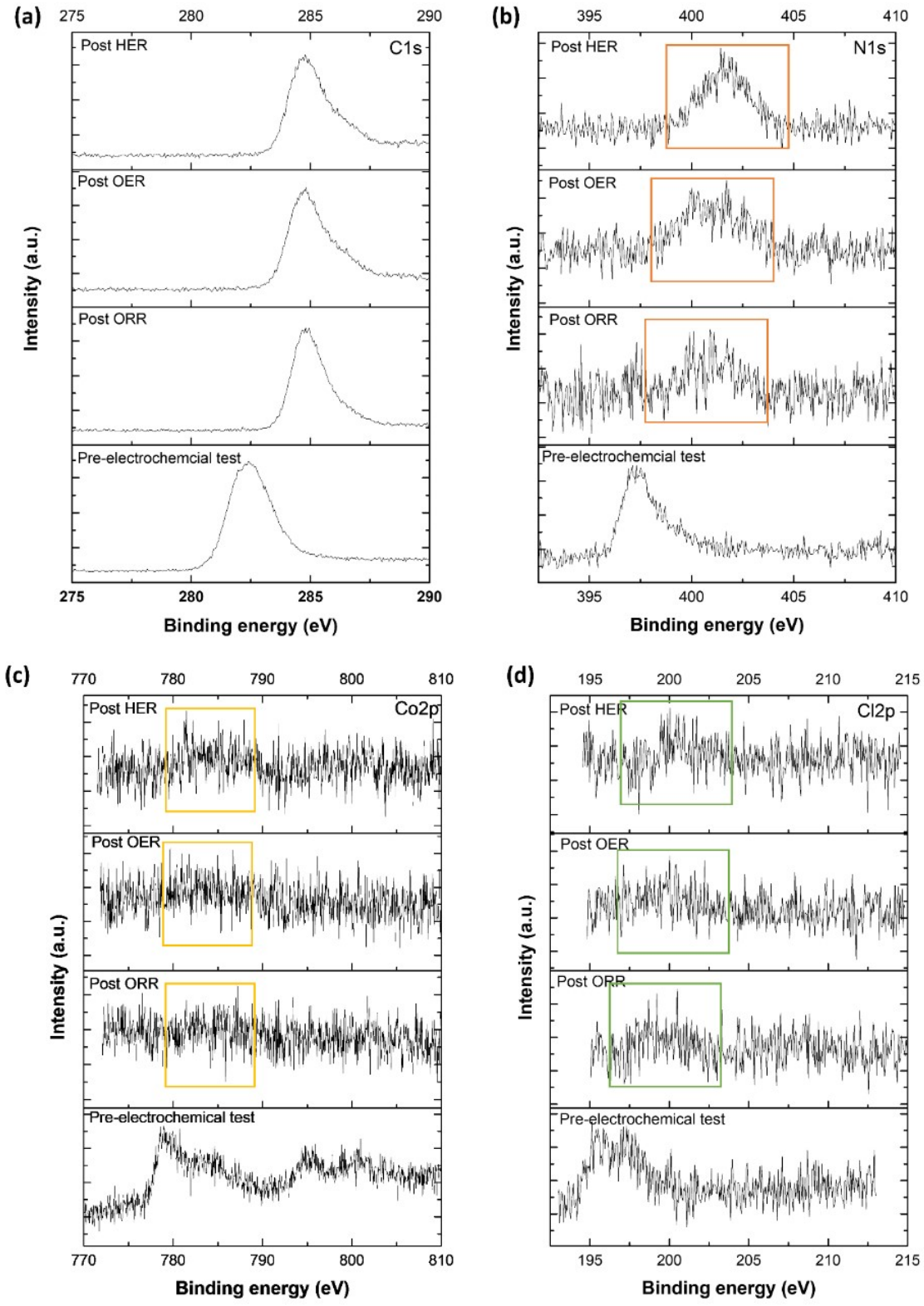

Fig S48. XPS spectrum of Co@TBB-phen (a) C1s, (b) N1s, (c) Co2p, and (d) Cl2p after electrochemical tests

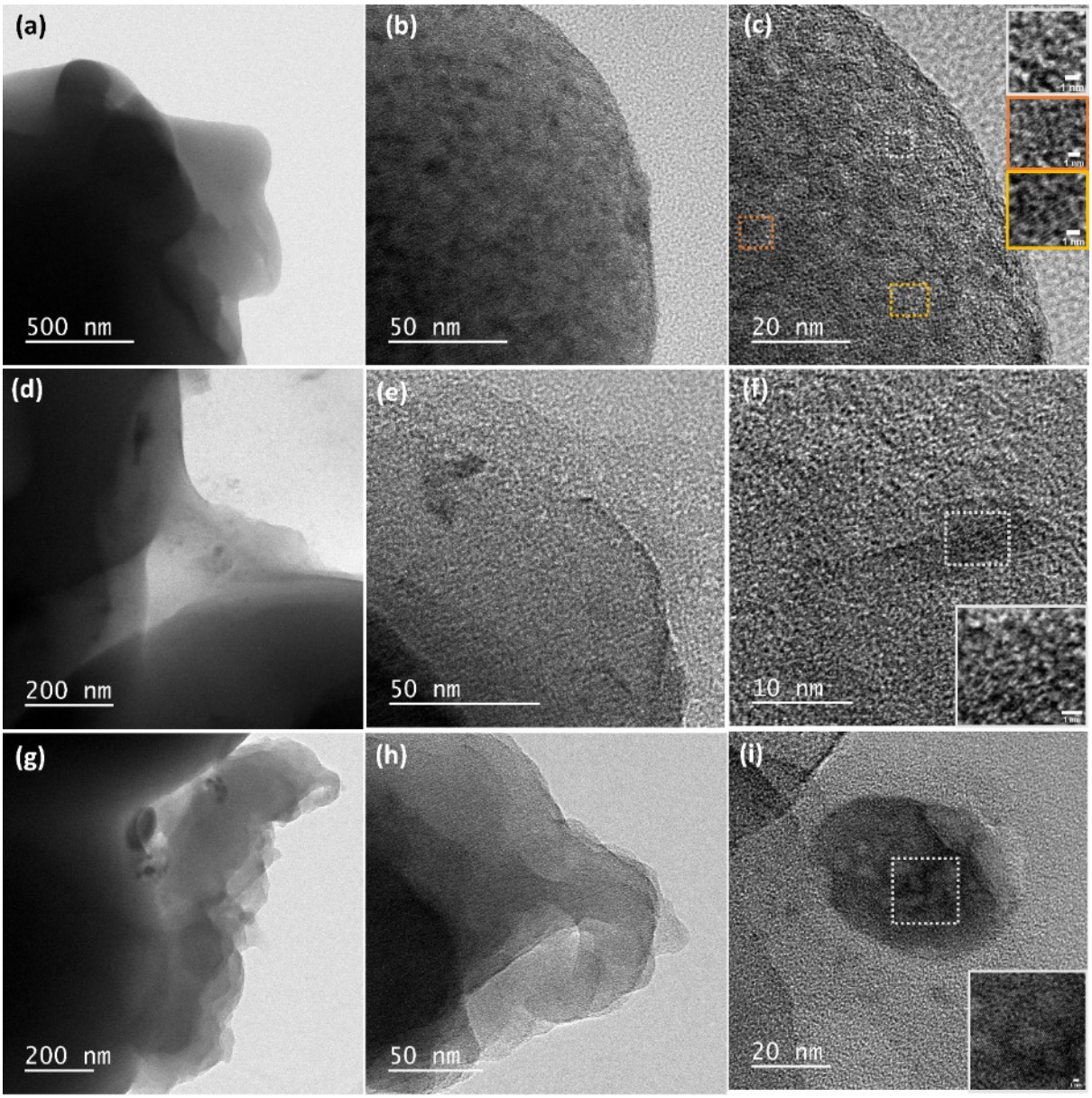

Fig S49. HRTEM images of Co@TBB-phen post (a), (b), (c) ORR, (d), (e), (f) OER, and (g), (h), (i) HER electrochemical tests

Table S10 Comparison of benchmark cobalt-based tri-functional materials for electrocatalysis

	ORR			OER		HER		
Materials	**Loading (μgcm^{-2}) /media**	**Onset potential (V vs RHE)**	**n**	**Loading (μgcm^{-2}) /media**	**η (j=10 $mAcm^{-2}$) mV, 1600 rpm**	**Loading (μgcm^{-2}) /media**	**η (j=-10 $mAcm^{-2}$) mV, 1600 rpm**	**Ref.**
Mn_3Co_7–$Co_2Mn_3O_8$@ CNTs/ CNFs (1000 ^oC)	215/0.1 M KOH	0.89	3.41 - 3.73	215/1 M KOH	374	215/0.5 M H2SO4	176	Energy Environ. Sci. 2017 10 321[1]
Co/CNFs	300/0.1 M KOH	1.01	4	300/1 M KOH	320	300/1 M KOH	190	Adv. Mater. 2019 31 1808043[2]
Co-N, P-HCS	430/0.1 M KOH	0.97	4	430/1 M KOH	320	430/1 M KOH	164	Adv. Mater. 2022 34 2204021[3]
Co@N-CNTF-2	280/ 0.1 M KOH	0.91	3.96	280/1 M KOH	350	280/0.5 M H_2SO_4	226	J. Mater. Chem. A, 2019 7 3664[4]
BrHT@CoNC	300/0.1 M KOH	1	~4	300/1 M KOH	254	300/1 M KOH	77	J. Mater. Chem. A 2020 8 10865[5]
CoFe/N_H-CNS	320/0.1 M KOH	~1	3.97	320/1 M KOH	321	320/1 M KOH	230	ACS Sustainable Chem. Eng. 2019 7 15278[6]
Co@IC/MoC@PC	400/0.1 M KOH	0.91	4	400/0.1 M KOH	282	400/1.0 M KOH	68	ACS Nano 2021 15 8 13399[7]
Co_9S_8/CoNSC-900	788/0.1 M KOH	0.87	3.86	394/1 M KOH	336	394/1 M KOH	136	Nanoscale 2022 14 9849[8]
$NiCoS_x/CoS_2$	0.1 M KOH	~0.83	4	0.1 M KOH	120	1 M KOH	253	CrystEngComm 2022 24 3894[9]
CoP/Co_2P/Co_3O_4	0.1 M KOH	0.95	4	1 M KOH	275	1 M KOH	170	New J. Chem. 2022 46 8786[10]

Fe_2P/Co@NPC	364/0.1 M KOH	1	4	364/1 M KOH	331	364/1 M KOH	235	J. Mater. Chem. A 2022 10 16037[11]
CoP-NC@NFP	76/0.1 M KOH	0.95	4	76/1 M KOH	270@j=50	76/1 M KOH	163@j=50	Chemical Engineering Journal 2022 428 131115[12]
Co@TBB-phen	**80/0.1 M KOH**	**0.81**	**3.9-3.99**	**160/0.1 M KOH**	**540**	**80/0.5 M H_2SO_4**	**299**	**This work**

Table S11. Performance comparison of recently proposed COFs and COPs

S. No.	Polymer and its structure	ORR (E_{onset}, V vs RHE)/media	OER ($\eta_{@10mAcm-2}$, mV)/media	HER ($\eta_{@10mAcm-2}$, mV)/media	Ref.
1.	Co-COP 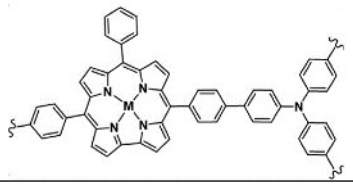	0.92 V/0.1 M KOH	560/0.1 M KOH	208/0.1 M KOH	Catal. Sci. Technol., 2023, 13, 6321[13]
2.	TP-COF-C700 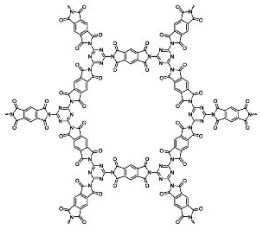	-	-	95/0.1 M KOH	Energy Adv.2023, 2, 1713[14]
3.	Ir-COF@ZIF800 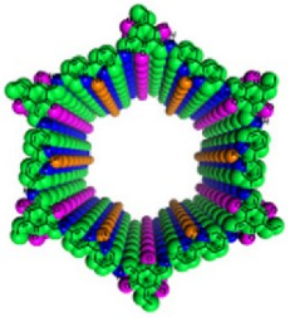	0.96/0.1 M KOH	-	48/0.5 M H_2SO_4	Chem. Commun., 2022, 58, 13214[15]
4.	COF@ZIF800	0.99/0.1 M KOH	-	159/0.1 M KOH	J. Mater. Chem. A, 2022, 10, 228[16]

	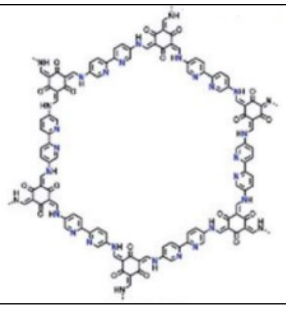				
5.	CoPor-GDY 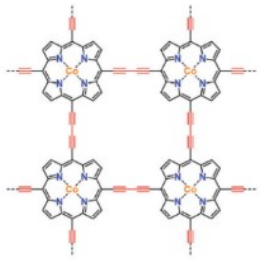	-	400/1 M KOH	308/1 M KOH	Mater. Chem. Front., 2021, 5, 4596[17]
6.	Co@rhm-PorBTD 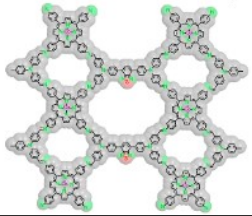	0.89/0.1 M KOH	-	-	ACS Nano 2023, 17, 3492[18]
7.	C-CMP-900 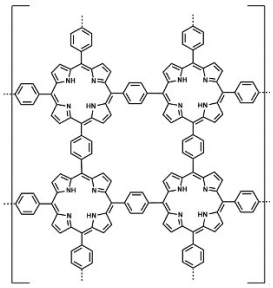		370/0.1 M PBS		ACS Appl. Nano Mater. 2023, 6, 3226[19]
8.	PDT-COF 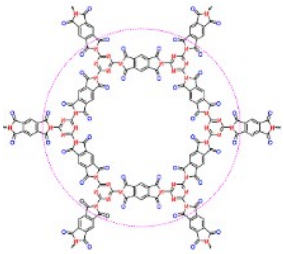			210/0.5 M H_2SO_4	ACS Appl. Eng. Mater. 2023, 1, 1799[20]
9.	TT-TPB	0.90/0.1 M KOH			ACS Appl. Energy Mater. 2022, 5, 13284[21]

	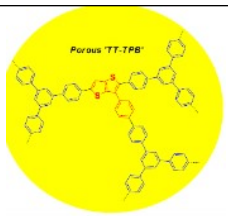				
10.	NiPcCOF 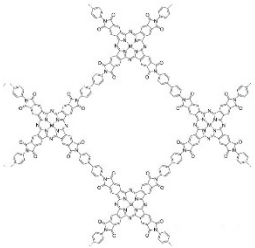		410/1 M NaOH		Materials Today Chemistry 2022, 26 101032[22]
11.	HNPC-900 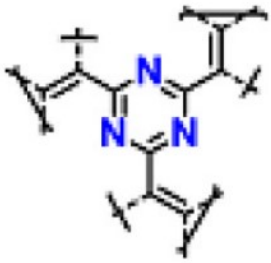	0.90/0.1 M KOH	370/0.1 M KOH		Applied Catalysis B: Environmental, 2023, 339 123088[23]
12.	FE-TTF-800 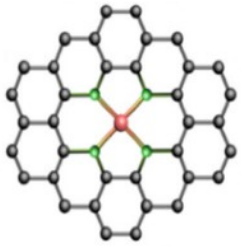	0.87/0.1 M KOH	313/0.1 M KOH		Journal of Power Sources, 2022, 542 231583[24]
13.	Ni-TTP 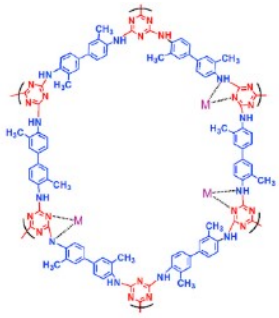		290/1 M KOH		Materials Chemistry and Physics, 2022, 285, 126104[25]
14.	S-POP/C	0.82/0.5 M H_2SO_4			Electrochimica Acta, 2021, 377, 138107[26]

	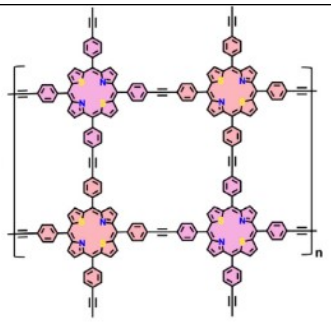				
15.	Co-PorBpy-Co 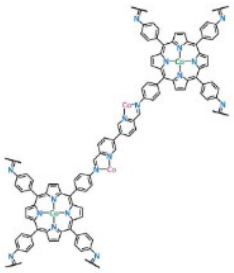	0.90/0.1 M KOH			Adv. Sci. 2023, 10, 2206165[27]
16.	Co-POP 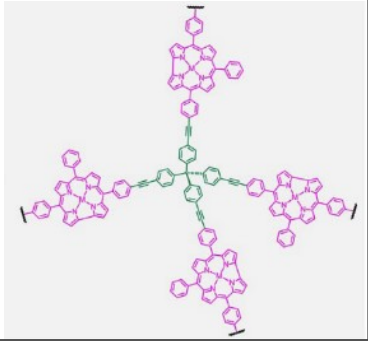	0.95/0.1 M KOH	340/0.1 M KOH		Angew. Chem. Int. Ed. 2022, 61, e202201104[28]

Density functional theory computations

The density functional theoretical (DFT) computations were performed to evaluate the energy gap between the highest occupied molecular orbital (HOMO) and the lowest unoccupied molecular orbital (LUMO) using the Gaussian 16[29] software package of program. The model structures (TBB-Phen and Co@TBB-Phen) were first optimized at UB3LYP|6-311++G(d,p) level (LanL2DZ: ECP and basis set of Co), and then orbital energies were evaluated using HSEH1PBE/6-311++G(d,p) level of theory[30–34]. Grimme's GD3BJ empirical dispersion was used to tackle weak interactions, and the solvation effect of water with a polarizable continuum model (PCM) was considered[35,36]. GaussView 6.0.16 was utilized for all molecular drawings and calculations setup. The reaction mechanism of each reaction intermediate was studied for OER and HER. The adsorbed reaction intermediates were also optimized at UB3LYP|6-311++G(d,p)

level (LanL2DZ: ECP and basis set of Co), and were subjected to harmonic frequency calculations to determine the thermochemistry data and also validate the stationary points. The energy barrier arising from thermodynamic free energy differences was considered for the study using the computational hydrogen electrode model. The kinetic barrier was not included in the calculations, and the approach of the study was to determine whether the proton-coupled electron transfer (PCET) reaction is thermodynamically feasible or not. The natural bonding orbital (NBO) analysis was performed for ORR with LanL2DZ/6-311++G(d,p) level of theory.

The oxygen evolution reaction was studied in alkaline media following the associative pathway.

$$* + OH^- \rightarrow HO^* + e^- \quad \text{Eq. (13)}$$

$$HO^* + OH^- \rightarrow O^* + H_2O\,(l) + e^- \quad \text{Eq. (14)}$$

$$O^* + OH^- \rightarrow HOO^* + e^- \quad \text{Eq. (15)}$$

$$HOO^* + OH^- \rightarrow OO^* + H_2O(l) + e^- \quad \text{Eq. (16)}$$

$$OO^* \rightarrow * + O_2(g) \quad \text{Eq. (17)}$$

Where * denotes the adsorption site on the electrocatalyst. (g) and (l) represents phases of gases and liquids. The free energy of each reaction intermediate (ΔG) is given by the following equation

$$\Delta G = \Delta E + \Delta ZPE - T\Delta S + \Delta G_U + \Delta G_{pH} + \Delta G_{field} \quad \text{Eq. (18)}$$

where the ΔE is the electronic energy, ΔZPE is the zero-point vibrational energy, ΔS is the entropy, and T is the temperature (298.15 K). $\Delta G_U = -eU$ is the applied electrode potential (SHE). $\Delta G_{pH} = -kTln10.pH$ is the free energy change corresponding to the pH conditions. Here, pH = 13 is considered for 0.1 M KOH. ΔG_{field} is the free energy correction for the electrochemical double layer and was neglected for this study. ΔE is determined from the DFT computations while ΔZPE and $T\Delta S$ were taken from literature and the free energy of OH^-, H_2O, and O_2 were determined accordingly [37–40].

HER

The change in the free energy of the proton adsorbed on the electrocatalyst surface is given as

$$\Delta G_{H*} = E_{H*} - E_{*} - 0.5E_{H_2} + \Delta E_{ZPE} - T\Delta S$$ Eq. (19)

Where the E_{H*} is the energy of the electrocatalyst with absorbed intermediate, E_{*} is the energy of the electrocatalyst, ΔE_{ZPE} is the difference in the zero-point vibrational energy of the intermediate-adsorbed site and gaseous molecular hydrogen. $E_{H_2}$is the energy of the hydrogen molecule. $T\Delta S$ is the change in entropy. The ΔG_{H*} is the descriptor and should be closer to zero for an efficient HER process [40–42]. The ΔG_{H*} is given as

$$\Delta G_{H*} = E_{H*} - E_{*} - 0.5E_{H_2} + 0.24\ eV$$ Eq. (20)

Plausible reaction mechanism for TBB-phen

$$TBB - phen + H_3O^+ \rightarrow [TBB - phen - H]^+ + H_2O$$

$$\Delta G = 5.55\ eV$$

$$[TBB - phen]^- + H_3O^+ \rightarrow [TBB - phen - H]^0 + H_2O$$

$$\Delta G = 3.5\ eV$$

Table S12. The values considered for the calculation of free energy of reaction intermediates

Polymer	Reaction	Intermediate	G (Ha)	E (Ha)	ZPE (Ha)	TS (Ha)
TBB-phen		*	-878.8484404	-879.04872	0.260332	0.060052
	ORR	OO*	-1029.1742	-1029.367034	0.264957	0.072123
	OER	HO*	-954.6170393	-954.82138	0.272295	0.067954
		O*	-954.009556	-954.205679	0.262144	0.066021
		HOO*	-1029.832141	-1030.034331	0.276348	0.074158
		OO*	-1029.17226	-1029.36535	0.264944	0.071854
	HER	H*		-879.605176		
Co@TBB-phen		*	-1023.730404	-1023.928743	0.264694	0.066355
	ORR	OO*	-1174.109284	-1174.302511	0.268315	0.075088
	OER	HO*	-1099.527643	-1099.738074	0.27912	0.068689
		O*	-1098.890932	-1099.085733	0.265319	0.070518
		HOO*	-1174.670631	-1174.883947	0.283789	0.070473

	OO*	-1174.108936	-1174.301842	0.269417	0.076511
HER	H*	-1024.44852			
	H_2	-1.183819167	-1.178674	0.009922822	0.01506799
	H_2O	-76.45121063	-76.447168	0.020580669	0.0246233 (0.035 bar)
	0.5 O_2	-75.0929848	-75.083062	0.00183756	0.011760382

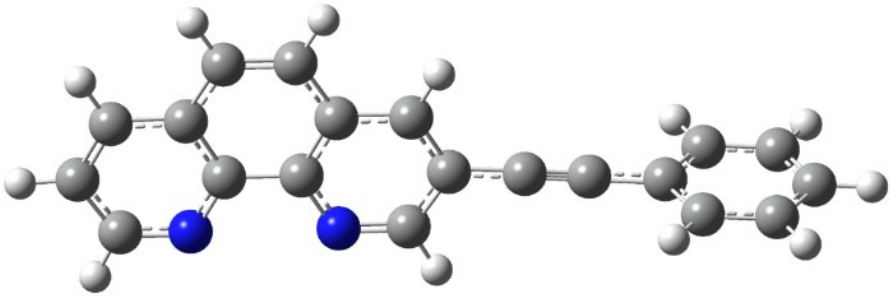

Fig S50. Optimized structure of the model system of **TBB-phen**, obtained from DFT computation at B3LYP/6-311++G(d,p) level, solvent = water, PCM

Charge 0, multiplicity 1

C,-5.3265844433,-0.0534894843,-1.2126030538
C,-4.6129169382,-0.055514899,-0.0003142124
C,-5.3260040361,-0.0511217779,1.2123107952
C,-6.7175617052,-0.0448017108,1.2077695168
C,-7.4175150059,-0.0427472045,0.0003464293
C,-6.7181396567,-0.0471661321,-1.2074056412
H,-4.7838034145,-0.0569338819,-2.1501881478
H,-4.7827735406,-0.0527365422,2.14964048
H,-7.2561199542,-0.0414545494,2.1484543825
H,-8.5013757799,-0.0378014574,0.0006007855
H,-7.2571487992,-0.0456600503,-2.1478368984
C,-3.1844670581,-0.0618188697,-0.0006539527
C,-1.973620424,-0.064007045,-0.0008304841
C,-0.5494669152,-0.0853670072,-0.0006053112
C,0.2118107775,1.0745505832,-0.0003754477
C,0.151727478,-1.3225327821,-0.000641935
C,1.6167994797,0.992490226,-0.000176631
H,-0.2688380244,2.0460715837,-0.0003452029
H,-0.415928192,-2.2488485197,-0.0008293715
C,2.2124691808,-0.2985609132,-0.0002279654
C,2.4373465269,2.1692198643,0.0000772935
C,3.6642375185,-0.4049049553,-0.0000227058

C,3.7918273078,2.070493459,0.0002732708
H,1.9522237486,3.1388061175,0.0001126507
C,4.4369188564,0.7897806917,0.0002294928
H,4.410299342,2.9612541786,0.000466322
C,5.8427015362,0.6641321348,0.0004318124
C,5.5575708732,-1.7096058643,0.0001143672
C,6.4105398611,-0.5899655264,0.0003743483
H,6.4583373074,1.5569397578,0.0006296563
H,5.9816912969,-2.7101757835,0.0000619905
H,7.4849358243,-0.7255333097,0.0005231777
N,1.4642831866,-1.4275233666,-0.0004657574
N,4.2367347856,-1.631342964,-0.0000760533

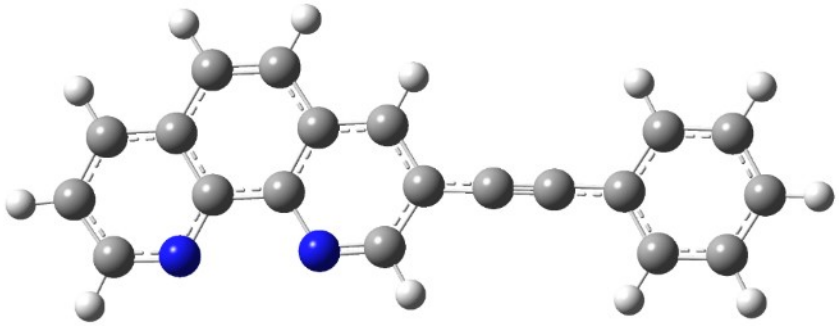

Fig S51. Optimized structure of the model system of **TBB-phen**, obtained from DFT computation at B3LYP/6-311++G(d,p) level, solvent = water, PCM

Charge = -1 Multiplicity = 2
C,5.3520504878,-1.1427374807,0.5713645453
C,4.6079972876,-0.0546650057,0.0470825212
C,5.3324401925,1.039731127,-0.4913848717
C,6.7214132044,1.0388949165,-0.5013498786
C,7.4407547684,-0.042376892,0.0199086989
C,6.7410593271,-1.1297131043,0.5546583846
H,4.8221074446,-1.9913917168,0.9885712225
H,4.7872293623,1.8836935289,-0.8983554062
H,7.2500910694,1.8891142052,-0.9193957123
H,8.5244198845,-0.0376448722,0.0094923069
H,7.2850505969,-1.9752668681,0.9623901471
C,3.1975896855,-0.0606761823,0.0603679924
C,1.9723210635,-0.0683157207,0.0730816394
C,0.5735410466,-0.0729717664,0.0854636802
C,-0.2231372733,0.9938529722,-0.4282550928
C,-0.1483591199,-1.177876646,0.6287388098
C,-1.6111713858,0.9113225304,-0.3779352652
H,0.2503013108,1.8697801162,-0.8582789008
H,0.4246794748,-2.0128589318,1.0313009092

C,-2.2333524457,-0.2526645396,0.1934388197
C,-2.4495193177,1.9682473791,-0.8864664242
C,-3.6565709392,-0.3454422901,0.2489384963
C,-3.8032947151,1.8835622146,-0.8353866585
H,-1.9695895394,2.842501347,-1.3156065361
C,-4.4559878188,0.7351228364,-0.2714579997
H,-4.4201652087,2.688696263,-1.2229081528
C,-5.8489399457,0.6294973144,-0.2099849403
C,-5.5788709648,-1.507301838,0.8286471924
C,-6.4336693697,-0.5051535692,0.3467559098
H,-6.4609950472,1.4374380101,-0.5989912297
H,-6.0077927071,-2.4059366232,1.2693877055
H,-7.5084656039,-0.6214398168,0.4111107613
N,-1.4549365137,-1.2856134801,0.6907949012
N,-4.2536842908,-1.4559294173,0.7940834253

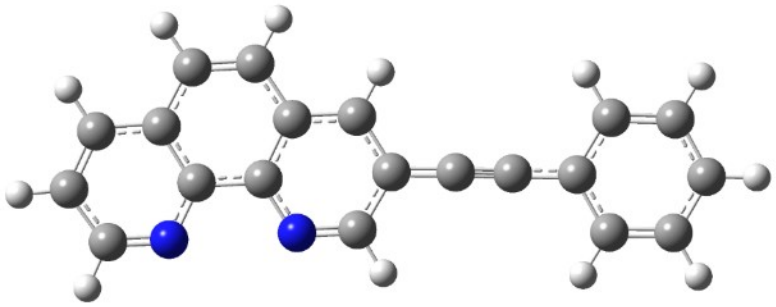

Fig S52. Optimized structure of the model system of **TBB-phen**, obtained from DFT computation at B3LYP/6-311++G(d,p) level, solvent = water, PCM

Charge = 1 Multiplicity = 2

C,5.2861566564,-1.1415001873,0.5998567712
C,4.5647704923,-0.0408708484,0.053642515
C,5.2717278039,1.0645854048,-0.5016031615
C,6.6509544686,1.05935076,-0.5054366262
C,7.349169168,-0.0314821321,0.0359513137
C,6.6652562684,-1.1269550864,0.586140104
H,4.7391266172,-1.9759162027,1.0190557411
H,4.7137778323,1.895272382,-0.9137549537
H,7.1959797341,1.8951558867,-0.925311466
H,8.4326219843,-0.0278362497,0.0290774262
H,7.2212381835,-1.9590241637,0.9989999055
C,3.1770198477,-0.0455954822,0.0625091206
C,1.9489437062,-0.0454392282,0.0682233315
C,0.5640030502,-0.0659150127,0.0850152645
C,-0.2023318254,0.9906529784,-0.4390721893
C,-0.1374016732,-1.1892625432,0.6493631391
C,-1.592842746,0.9150049259,-0.3947653507

H,0.2878391724,1.8538862058,-0.8725304195
H,0.4382871976,-2.013844219,1.0583847829
C,-2.1863039171,-0.2501150603,0.1899499127
C,-2.4174585806,1.9695147362,-0.9175920547
C,-3.6231584998,-0.3462559611,0.2447830948
C,-3.768999054,1.8743049999,-0.8636590394
H,-1.9344988725,2.836047991,-1.3527054398
C,-4.4026536032,0.7242583927,-0.2862276172
H,-4.3950184025,2.6668955251,-1.2565965524
C,-5.8071140172,0.6065375101,-0.2207711845
C,-5.5008540223,-1.5234368066,0.8416498381
C,-6.3615761256,-0.5184049808,0.3437436936
H,-6.4303587161,1.4009116049,-0.6145979074
H,-5.9233321391,-2.417831856,1.290395307
H,-7.4346847137,-0.6450437219,0.4120743719
N,-1.4377759761,-1.2719907999,0.6967933389
N,-4.1859652986,-1.4501807613,0.79883599

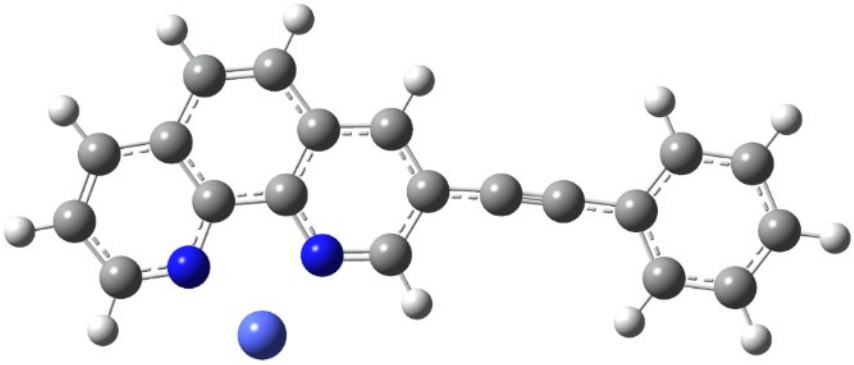

Fig S53. Optimized structure of the model system of **Co@TBB-phen** obtained from DFT computation at B3LYP/6-311++G(d,p) level, empirical dispersion=GD3BJ (LANL2DZ: basis set and electron core potential of Co; solvent = water, PCM)

Charge 2, multiplicity 2

C,-5.533547438,-1.2159645739,-0.0205413643
C,-5.0148797199,0.0919726691,0.0147955846
C,-5.8987755299,1.1859288372,0.0160179884
C,-7.2714527233,0.9704816447,-0.0179995758
C,-7.7788819108,-0.3291800391,-0.0537702867
C,-6.9074629968,-1.4194434361,-0.0548748389
H,-4.8526360628,-2.0578710116,-0.021896286
H,-5.5004240324,2.1923224898,0.0429776403
H,-7.9472188347,1.8171091468,-0.0171569339
H,-8.8495865696,-0.4921392318,-0.080975315
H,-7.299670251,-2.4288983334,-0.0829744229
C,-3.6097769962,0.293060439,0.0437492935
C,-2.4086871046,0.4388304185,0.0615329455

C,-0.9970599817,0.5238561705,0.0656288796
C,-0.3062258145,1.7361712031,0.056276452
C,-0.2531372976,-0.68696708,0.070926692
C,1.1010527093,1.7441569832,0.0407568035
H,-0.8558398766,2.6687040911,0.0556094633
H,-0.7510749556,-1.6474865604,0.0835898588
C,1.7428594115,0.4972212613,0.0370141373
C,1.9329381006,2.9167991361,0.0219978332
C,3.1506179229,0.392934775,0.0047049192
C,3.2936782258,2.8185065712,-0.0045666401
H,1.4556994735,3.8885272931,0.0282296606
C,3.9540742968,1.5421284837,-0.017289996
H,3.9039626402,3.7126525359,-0.0185968453
C,5.3492939375,1.3329359451,-0.0512276161
C,4.9660663552,-1.0528770314,-0.0393055351
C,5.8446800723,0.0429988463,-0.0625515335
H,6.0223736338,2.1812884412,-0.0684216149
H,5.325698588,-2.0734459131,-0.0467010021
H,6.9088137936,-0.1454803907,-0.0886713225
N,1.0672943616,-0.6801679566,0.0577712935
N,3.6506802262,-0.871461785,-0.0065786947
Co,2.251760347,-2.2066340389,0.0518063786

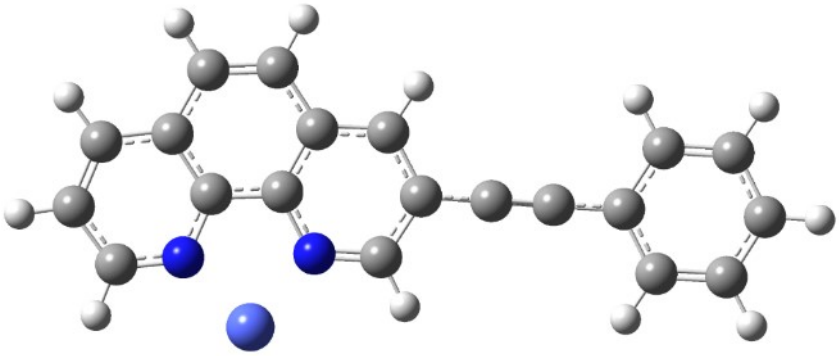

Fig S54. Optimized structure of the model system of **Co@TBB-phen** obtained from DFT computation at B3LYP/6-311++G(d,p) level, empirical dispersion=GD3BJ (LANL2DZ: basis set and electron core potential of Co; solvent = water, PCM)

Charge = 1 Multiplicity = 1

C,5.6070848685,-1.1923582939,0.0141912705
C,4.974090439,0.0640619591,0.0091500307
C,5.7608055295,1.2304205878,0.0035590234
C,7.1476461687,1.1368001609,0.0029821831
C,7.7682569195,-0.1132051489,0.0079471816
C,6.9946192697,-1.2747997502,0.0135524193

H,5.0034543748,-2.0913643747,0.0185521585
H,5.2758022846,2.1985850425,-0.000275527
H,7.7458182921,2.0401288553,-0.001342612
H,8.8495087107,-0.1817679157,0.0074792679
H,7.4737997695,-2.246499608,0.017433996
C,3.5558765971,0.1544017132,0.0098459243
C,2.348537257,0.2353119605,0.0104354623
C,0.9337096681,0.3242696603,0.0113212174
C,0.2778129443,1.5556981065,0.0050120785
C,0.1654586273,-0.8681526432,0.0189460477
C,-1.1277666773,1.5887292809,0.0062406625
H,0.8487688177,2.4751451266,-0.0007646312
H,0.6522313639,-1.8346264978,0.0240017883
C,-1.7989629395,0.3558038558,0.0139521217
C,-1.9265884062,2.7844814531,0.0001701788
C,-3.212454575,0.2943358588,0.0156222773
C,-3.2893986649,2.7254763265,0.0017601421
H,-1.4213396579,3.7426058651,-0.0057508069
C,-3.9844323696,1.4677324963,0.0095714841
H,-3.8743505801,3.6372167752,-0.0029092923
C,-5.3860313925,1.3086132235,0.0116677324
C,-5.0681658133,-1.0874467587,0.0250870573
C,-5.9155572365,0.0312338814,0.0193985075
H,-6.0317654795,2.1780679262,0.0072632974
H,-5.4651585389,-2.0945725452,0.0311714204
H,-6.9857052699,-0.1264610976,0.0211742243
N,-1.1632269962,-0.8549257333,0.0202660025
N,-3.73909935,-0.9656293541,0.0232961641
Co,-2.391446955,-2.2918893941,0.0299955476

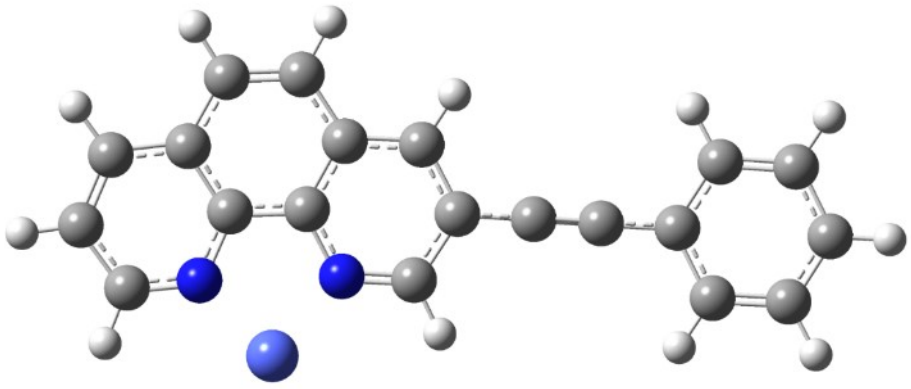

Fig S55. Optimized structure of the model system of **Co@TBB-phen** obtained from DFT computation at B3LYP/6-311++G(d,p) level, empirical dispersion=GD3BJ (LANL2DZ: basis set and electron core potential of Co; solvent = water, PCM)

Charge = 3 Multiplicity = 1

C,5.5798662569,-1.2119049224,0.0267761407
C,4.9337700412,0.0561561721,-0.0180977248
C,5.7050775181,1.2528567673,0.0143571877
C,7.0782466531,1.1721695857,0.0957573018
C,7.7043495888,-0.0837343076,0.1391099502
C,6.9546600572,-1.2701004267,0.1025629479
H,4.9794268049,-2.111221634,0.0000448284
H,5.1990789054,2.2083330123,-0.0198033129
H,7.6753312584,2.0739652346,0.1267048015
H,8.7841610551,-0.1381148114,0.2026011785
H,7.4574502006,-2.2276200621,0.1356164989
C,3.5502346613,0.1277890724,-0.0815720562
C,2.3292739157,0.1987766741,-0.117197266
C,0.9442944735,0.2848974613,-0.129807578
C,0.2916080282,1.5358286598,-0.1251815159
C,0.1658812804,-0.9155535484,-0.1594444398
C,-1.1030404445,1.5901561459,-0.1257619486
H,0.8816226144,2.4425439324,-0.0982609479
H,0.6387076424,-1.8879670684,-0.1970388262
C,-1.7822589183,0.3555819328,-0.1113708677
C,-1.8912958925,2.7928221615,-0.0731255555
C,-3.1778464741,0.3044836938,0.0125892962
C,-3.2510079688,2.7377441776,0.0125092462
H,-1.380209504,3.7462904822,-0.0997355424
C,-3.9445915756,1.4820642989,0.0629251526
H,-3.8331933795,3.6492247085,0.0504152421
C,-5.3444247467,1.3153009304,0.1404402873
C,-5.0368704248,-1.0879083164,0.1141459432
C,-5.878391696,0.0423755408,0.160717258
H,-5.9903645651,2.1830792398,0.1788052274
H,-5.4289309219,-2.0963919746,0.1398217404
H,-6.9461017451,-0.1134055255,0.224133761
N,-1.145918237,-0.8552011628,-0.1643130502
N,-3.7225131387,-0.9434449075,0.0561830776
Co,-2.3942503229,-2.3044502162,-0.0755024355

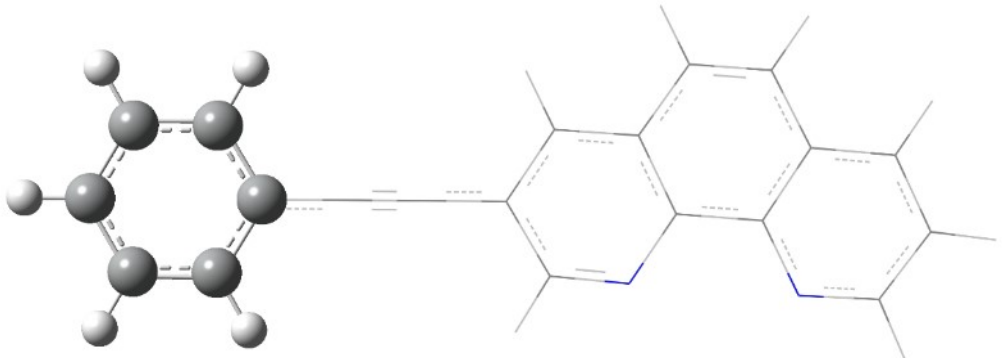

Fig S56. Optimized structure of the charge-separated model system of **TBB-phen**, obtained from DFT computation at B3LYP/6-311++G(d,p) level, solvent = water, PCM

Overall: Charge 0 and multiplicity 1, TBB-layer: Charge +1 and multiplicity 2, and phen-layer: Charge -1 and multiplicity 2
C,5.3520489279,-1.1427555367,0.5713411659
C,4.6079974502,-0.0546743218,0.0470755127
C,5.3324411467,1.0397230317,-0.4913876919
C,6.7214142269,1.0388815249,-0.5013607069
C,7.440754269,-0.0423975622,0.0198845687
C,6.7410577747,-1.1297363441,0.5546276132
H,4.8221048373,-1.9914120233,0.9885419372
H,4.7872312616,1.8836906806,-0.8983485887
H,7.250093036,1.8891023897,-0.9194020494
H,8.5244193768,-0.0376697949,0.0094620587
H,7.2850481258,-1.9752962576,0.9623477464
C,3.1975896092,-0.0606812406,0.0603660325
C,1.9723210242,-0.0683184941,0.0730832069
C,0.5735408459,-0.0729713288,0.0854655154
C,-0.2231359174,0.9938631564,-0.4282354928
C,-0.148360798,-1.1778836065,0.6287234567
C,-1.6111702373,0.9113340349,-0.3779158711
H,0.2503033328,1.869796574,-0.8582457651
H,0.424676835,-2.0128729126,1.031272424
C,-2.2333529614,-0.2526608861,0.1934402776
C,-2.4495165414,1.9682685619,-0.8864295037
C,-3.6565715308,-0.3454370654,0.2489397588
C,-3.8032921174,1.8835852315,-0.8353497998
H,-1.969585461,2.8425283201,-1.3155563619
C,-4.4559869233,0.7351381544,-0.271438815
H,-4.4201614584,2.6887265272,-1.2228580332
C,-5.8489390934,0.629514568,-0.2099659127
C,-5.5788734849,-1.5073021831,0.8286308675
C,-6.4336703369,-0.5051442846,0.3467571539
H,-6.4609929314,1.4374628392,-0.5989584558
H,-6.0077965716,-2.4059432536,1.2693572407

H,-7.5084667249,-0.6214292814,0.4111114607
N,-1.4549383495,-1.2856192266,0.6907792238
N,-4.2536866412,-1.4559319908,0.794066827

ORR (TBB-phen-OO*)

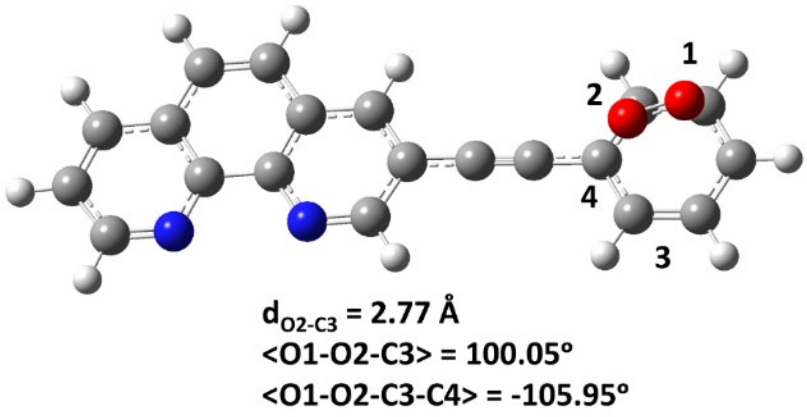

Fig S57. Optimized structure of the model system of **TBB-phen-OO*** obtained from DFT computation at B3LYP/6-311++G(d,p) level, solvent = water, PCM)

Charge = 0 Multiplicity = 1

C,-5.1938904142,0.8297782973,1.4957331693
C,-4.5137956724,0.4194681743,0.3183129883
C,-5.2626769559,0.0671527652,-0.8231085418
C,-6.6451912688,0.0518053566,-0.7612451889
C,-7.3082737178,0.4327129075,0.4196510241
C,-6.5778730859,0.863448185,1.5283092842
H,-4.6142460021,1.123655285,2.3618326349
H,-4.7469582488,-0.2239188251,-1.7294553747
H,-7.2213528629,-0.2541593338,-1.6260879332
H,-8.3910347866,0.4198241502,0.4545147668
H,-7.0901165533,1.1792457413,2.4288834736
C,-3.0963858446,0.4137386073,0.2809112599
C,-1.8849062335,0.4083231187,0.2456135583
C,-0.4671014773,0.41325964,0.2146698781
C,0.2516914954,0.051821461,-0.9178981503
C,0.2771716236,0.7984416172,1.3651426908
C,1.6571538642,0.0810352235,-0.893363121
H,-0.2644960367,-0.2512566887,-1.8213801954
H,-0.257588692,1.083745161,2.2667024923
C,2.2981786423,0.4865917383,0.3102230247
C,2.4353910116,-0.2835926113,-2.0421947638
C,3.751672608,0.5286011339,0.3539784185
C,3.7921418843,-0.24652209,-2.0003515727

H,1.9163157526,-0.5889051825,-2.9436543548
C,4.4815880985,0.1579877775,-0.8097842535
H,4.3790621492,-0.5223289851,-2.8694360163
C,5.8907001875,0.2049175913,-0.7450824722
C,5.6887593699,0.9507059447,1.5178534861
C,6.5017911379,0.6025669664,0.4225642018
H,6.4745308145,-0.0726267966,-1.6157915003
H,6.1478224631,1.2685884764,2.4501376113
H,7.5800995284,0.6510342336,0.5096083745
N,1.5913607067,0.8341426298,1.4130205192
N,4.3664352535,0.9184140664,1.495066507
O,-6.5237983503,-2.082645427,1.0711807708
O,-5.3431796183,-1.942310469,1.3953853345

ORR(Co@TBB-phen-OO*)

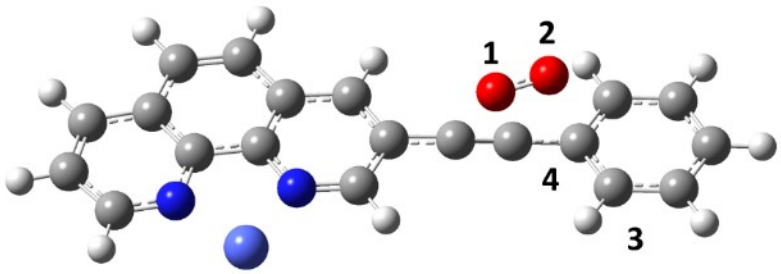

$d_{O2\text{-}C3}$ = 3.54 Å
<O1-O2-C3> = 106.95°
<O1-O2-C3-C4> = 84.19°

Fig S58. Optimized structure of the model system of **Co@TBB-phen-OO*** obtained from DFT computation at B3LYP/6-311++G(d,p) level, empirical dispersion=GD3BJ (LANL2DZ: basis set and electron core potential of Co; solvent = water, PCM)

Charge = 2 Multiplicity = 2
C,5.6261781348,-1.1661317926,0.1438817285
C,5.0025033175,0.0759770814,0.3623173361
C,5.7860895116,1.1894795777,0.7165600616
C,7.1630541545,1.0569893693,0.8479933945
C,7.7746234785,-0.1788856716,0.6302894701
C,7.0035214096,-1.2878262641,0.2786974719
H,5.02204997,-2.0233121027,-0.1257801751
H,5.3067348096,2.1459514212,0.8831978987
H,7.7611786254,1.9183598742,1.1197122513
H,8.8484256313,-0.2774040529,0.7350536653
H,7.4766811756,-2.2475225064,0.1094126487
C,3.5955916544,0.2000086397,0.2319219121
C,2.39379335,0.2954957551,0.1327051475

C,0.9891179049,0.3785978094,0.0020097341
C,0.2866632175,1.5628251275,0.2304547681
C,0.2667838199,-0.7815614202,-0.3875331384
C,-1.1092255577,1.5956324496,0.0663211243
H,0.8216134262,2.4556364948,0.5277015845
H,0.7744160479,-1.7191765727,-0.5712799346
C,-1.7298253972,0.4015134218,-0.3288658013
C,-1.9467257942,2.7481686617,0.260550092
C,-3.1254951797,0.3358118625,-0.5365433393
C,-3.2951287219,2.684188241,0.0649773271
H,-1.4821784712,3.6767742688,0.5666603242
C,-3.9353778606,1.4651243658,-0.3458502064
H,-3.9103306176,3.5621843162,0.2155522919
C,-5.3163569947,1.2959833865,-0.5802056511
C,-4.9115916044,-1.0165331682,-1.1477624945
C,-5.7947611531,0.0615226622,-0.9773101009
H,-5.9926527937,2.1316603315,-0.4489163975
H,-5.2549206671,-1.9944320886,-1.4591410271
H,-6.848117966,-0.0949565427,-1.1628356889
N,-1.0451409944,-0.7523898562,-0.5433209767
N,-3.6090185525,-0.8707945978,-0.9302619717
Co,-2.2142727243,-2.1936724974,-1.0975529484
O,3.8049307198,-1.411321313,3.1784877975
O,2.6679567615,-1.6853094413,2.8850757518

OER

OER(TBB-phen-HO*)

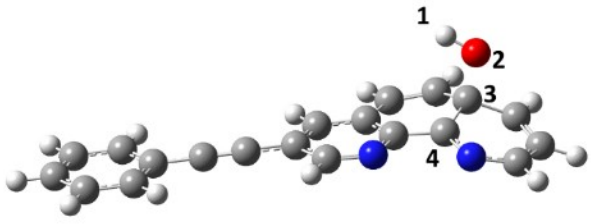

d_{O2-C3} = 1.48 Å
<H1-O2-C3> = 107.65°
<H1-O2-C3-C4> = -77.86°

Fig S59. Optimized structure of the model system of **TBB-phen-HO*** obtained from DFT computation at B3LYP/6-311++G(d,p) level, solvent = water, PCM)

Charge = 0 Multiplicity = 2
C,-5.5532304957,1.1777250593,-0.2068758043
C,-4.8730116302,-0.0413755104,-0.0188719475
C,-5.620997042,-1.2223464871,0.1544049634

C,-7.0108095672,-1.1796829285,0.1391052533
C,-7.6762103474,0.0334049146,-0.0481471179
C,-6.943354681,1.209253964,-0.2205815935
H,-4.983725416,2.089493349,-0.3406620932
H,-5.1038757905,-2.1631438762,0.2994483334
H,-7.5764276484,-2.0944713284,0.2733788895
H,-8.7595866699,0.0622720261,-0.0595733102
H,-7.456424408,2.1528411244,-0.3661964294
C,-3.4513773435,-0.0794284328,-0.0049783494
C,-2.2389285152,-0.1095675949,0.0057805773
C,-0.824814243,-0.1576362645,0.0183464269
C,-0.0365087548,0.9875557405,-0.1516405993
C,-0.1444129637,-1.3888740353,0.2032110609
C,1.3522069165,0.8852890523,-0.1246221738
H,-0.5061793441,1.9518899738,-0.3067780499
H,-0.7235762612,-2.2968992155,0.3437815422
C,1.9314768249,-0.4010922165,0.0624377505
C,2.2046924315,2.0498028048,-0.3192356535
C,3.3728187346,-0.5330812771,0.0307068639
C,3.5371528487,1.9779662083,-0.1993446928
H,1.7239563438,2.9919340624,-0.560494753
C,4.2327631893,0.7106800684,0.2126442681
H,4.1619915465,2.8551788551,-0.3285042716
C,5.5663632663,0.5421898678,-0.4580392831
C,5.2055580053,-1.8304829251,-0.4467142084
C,6.032682487,-0.6952447003,-0.7294876551
H,6.1559687527,1.43508566,-0.6326605857
H,5.6168754666,-2.831621528,-0.5330039435
H,7.0204064791,-0.8513742607,-1.1468801109
N,1.1689818113,-1.5098443056,0.2169081244
N,3.9184333037,-1.7409356867,-0.1364006921
O,4.5738465164,0.8268936929,1.653839201
H,3.7983451976,1.1815811499,2.1113100632

OER(TBB-phen-O*)

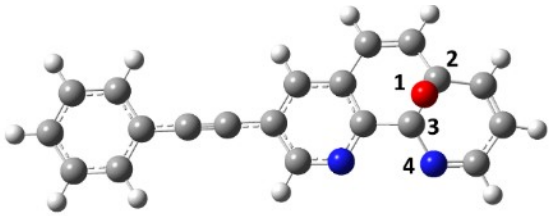

d_{O1-C2} = 1.43 Å
<O1-C2-C3> = 55.38°
<O1-C2-C3-N4> = -105.00°

Fig S60. Optimized structure of the model system of **TBB-phen-O*** obtained from DFT computation at B3LYP/6-311++G(d,p) level, solvent = water, PCM)

Charge = 0 Multiplicity = 1
C,-5.5175404315,1.1738197007,-0.0499569808
C,-4.8304769505,-0.0549834647,-0.0300881171
C,-5.5713362909,-1.2522359077,-0.0283496561
C,-6.9617135758,-1.2161257616,-0.0460171627
C,-7.6343726049,0.0069747756,-0.0656270085
C,-6.9081241151,1.199215155,-0.067346358
H,-4.9536094705,2.0988140408,-0.0512447873
H,-5.0490697546,-2.201254568,-0.0130979624
H,-7.5216472009,-2.1442111284,-0.0445977784
H,-8.717861988,0.030892067,-0.0792749991
H,-7.4262557023,2.1511593404,-0.082404554
C,-3.4067208261,-0.0859889185,-0.0117243369
C,-2.1957793335,-0.109283886,0.0040296092
C,-0.7756703857,-0.1457096491,0.0246736626
C,-0.0031777863,1.0184518683,-0.0002280606
C,-0.0850386583,-1.3755932141,0.0550024442
C,1.3931452758,0.9378374285,0.0316340317
H,-0.4848962491,1.9876669844,-0.0563934484
H,-0.6448050795,-2.3055902133,0.0572361625
C,1.9707471148,-0.3534137181,0.1026425472
C,2.2047657692,2.1374075893,-0.1147595313
C,3.4517430145,-0.4872661554,0.2177087064
C,3.5481258703,2.1109784358,-0.1614797285
H,1.6777580139,3.0731155639,-0.2664496416
C,4.2925988889,0.8712108322,0.0885685384
H,4.1163425907,3.0017682581,-0.4064366948
C,5.6483608881,0.6808969678,-0.4030627079
C,5.3290576395,-1.7199824118,-0.3158234263
C,6.1809755658,-0.5617536743,-0.4554955307
H,6.192463637,1.5473687834,-0.7636255052
H,5.7690905652,-2.6938144137,-0.5210598158
H,7.2007674492,-0.7187176431,-0.7849939623
N,1.2387336119,-1.4738732925,0.0872262396
N,4.0455542302,-1.6927712429,-0.1370874359
O,3.9990502784,0.2078294717,1.328826249

OER(TBB-phen-HOO*)

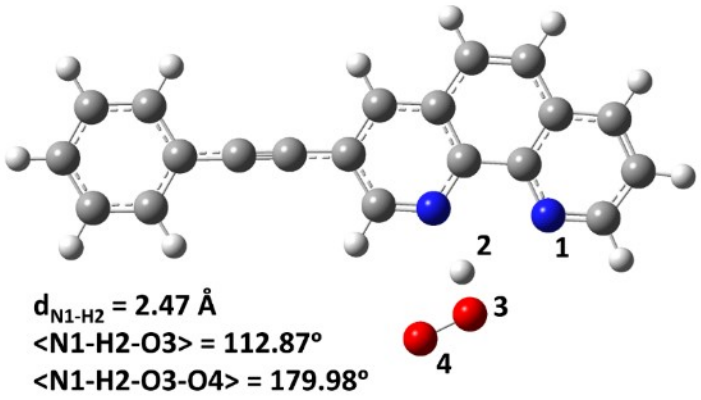

Fig S61. Optimized structure of the model system of **TBB-phen-HOO*** obtained from DFT computation at B3LYP/6-311++G(d,p) level, solvent = water, PCM)

Charge = 0 Multiplicity = 2
C,-5.2499575578,-1.0102622096,1.0434058066
C,-4.3134853135,-0.0922257625,1.5558986871
C,-4.6924847048,0.7513118308,2.6176489299
C,-5.9753990478,0.6747874673,3.1492736219
C,-6.8974468564,-0.2385368662,2.6348299091
C,-6.5303826403,-1.0788295528,1.5821557805
H,-4.964464145,-1.6620299594,0.2265332691
H,-3.976352839,1.4597307361,3.0162261351
H,-6.2564254791,1.3289543,3.9665233626
H,-7.8962418262,-0.2951216013,3.0518463385
H,-7.2434311864,-1.7892275071,1.1800406611
C,-3.0012832958,-0.0173345263,1.0086142538
C,-1.8852966178,0.0451274088,0.5418885271
C,-0.5733651697,0.1315507146,0.00679313
C,-0.1384513489,-0.6722993609,-1.0402305661
C,0.3538993454,1.0653425869,0.5402266287
C,1.1731890317,-0.5431606519,-1.5305518044
H,-0.8072422888,-1.4011215682,-1.4827766971
H,0.0587017766,1.7132084738,1.3576915418
C,2.0224079676,0.4211666936,-0.9280094364
C,1.6623820663,-1.35297467,-2.6096622332
C,3.3793727812,0.5765192908,-1.4125291027
C,2.9340261109,-1.2093687377,-3.0657924772
H,0.99392028,-2.0821294168,-3.0527077892
C,3.8222249663,-0.2460672501,-2.482892478
H,3.2991650641,-1.8235098384,-3.881366705
C,5.1484879846,-0.0718319151,-2.933040749
C,5.4122762502,1.6356031896,-1.2751810995
C,5.9494136738,0.8717413639,-2.3291356183

H,5.5212036403,-0.682088828,-3.7481649062
H,6.0254820718,2.385773602,-0.7838314563
H,6.9715595623,1.0328037461,-2.648082145
N,1.5886935126,1.2018924649,0.0942688674
N,4.1749803936,1.5001553,-0.8269147125
O,1.9694643094,3.4482924218,2.2588647885
O,2.9445045724,3.0986134285,1.4292723948
H,2.554662756,2.3544018528,0.837769412

OER(TBB-phen-OO*)

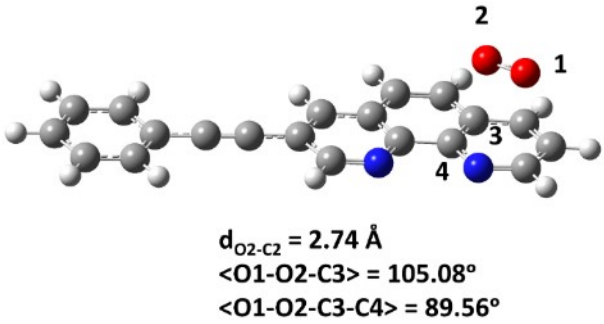

Fig S62. Optimized structure of the model system of **TBB-phen-OO*** obtained from DFT computation at B3LYP/6-311++G(d,p) level, solvent = water, PCM

Charge = 0 Multiplicity = 1
C,5.8166187368,-1.1151405048,0.2338837812
C,5.0973778429,0.0778518665,0.0280949638
C,5.8033653086,1.2899714325,-0.0948564935
C,7.1917274103,1.3030996366,-0.0137728466
C,7.896440057,0.115352333,0.1903460636
C,7.2048847273,-1.091120181,0.3136237251
H,5.2791684114,-2.0508540351,0.3294376094
H,5.2557391653,2.2111566796,-0.2532002448
H,7.7251199665,2.2417250492,-0.1099726812
H,8.9783607612,0.1298379211,0.2529489339
H,7.7484986743,-2.015293897,0.4723206799
C,3.6764668624,0.0582693763,-0.054458542
C,2.4670669138,0.0368000061,-0.1248443176
C,1.0508236072,0.027657959,-0.2069457364
C,0.3058394759,-1.1426562511,-0.1027187848
C,0.3327659037,1.2389838327,-0.4026537989
C,-1.0945936871,-1.0887779784,-0.1897648824
H,0.8002148548,-2.0955319134,0.045360503
H,0.8846496312,2.1703255943,-0.4905518521
C,-1.7060936111,0.1779798545,-0.3810365142
C,-1.8993252349,-2.2775203729,-0.0936607688
C,-3.1599168768,0.2544930111,-0.4665132942
C,-3.2515367939,-2.2152360984,-0.1788291996

H,-1.3982188224,-3.2284946583,0.0472476232
C,-3.9191639016,-0.9597988628,-0.3643759125
H,-3.8534787553,-3.1139201876,-0.1085209683
C,-5.3203217321,-0.8733606715,-0.4825659869
C,-5.0653656273,1.5015133719,-0.7117972299
C,-5.9042404636,0.3627876415,-0.6237977941
H,-5.9188192887,-1.7753064895,-0.4280257309
H,-5.5098160613,2.4829004114,-0.8497207748
H,-6.9785591486,0.4804489217,-0.6862630748
N,-0.9802466327,1.3131233495,-0.4851018437
N,-3.7447767969,1.4517252632,-0.6741719998
O,-4.063733692,0.3248236971,2.054414065
O,-5.0472391844,1.0583818931,1.9689503246

OER(Co@TBB-phen-HO*)

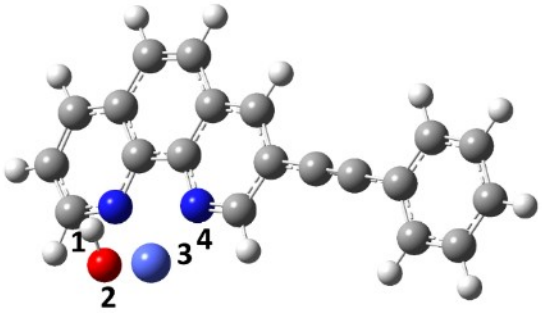

$d_{O2\text{-}Co3}$ = 1.73 Å
<H1-O2-Co3> = 117.27°
<H1-O2-Co3-N4> = 43.57°

Fig S63. Optimized structure of the model system of **Co@TBB-phen-HO*** obtained from DFT computation at B3LYP/6-311++G(d,p) level, empirical dispersion=GD3BJ (LANL2DZ: basis set and electron core potential of Co; solvent = water, PCM)

Charge = 2 Multiplicity = 1
C,5.4344225909,-1.1424123479,0.8523344185
C,4.8655785302,0.0577602315,0.3873982079
C,5.7049646981,1.1183388685,-0.0000507592
C,7.0848249563,0.9755626935,0.0778218169
C,7.6427957286,-0.2179744054,0.5386202362
C,6.8155968019,-1.2738906704,0.9246966214
H,4.7872432718,-1.9579749623,1.149521541
H,5.2661585374,2.0412524386,-0.3576658688
H,7.7266385194,1.7951849959,-0.2216321689
H,8.7192987529,-0.3250866959,0.5964560453
H,7.2483155963,-2.2004616915,1.2819643311
C,3.4558206354,0.1925078183,0.3050934822
C,2.2530732835,0.3022668985,0.2297354611

C,0.8480279979,0.4009388275,0.1323413354
C,0.2136745141,1.5230771444,-0.4079427204
C,0.0549471099,-0.6844180533,0.5979538794
C,-1.1889974177,1.5683555023,-0.4992377657
H,0.8100144807,2.3552075651,-0.758552443
H,0.5045767676,-1.566260796,1.0334050723
C,-1.8838742716,0.4488005243,-0.0262519186
C,-1.9748715631,2.6458765422,-1.0384762442
C,-3.2866795945,0.3761351445,-0.0792097637
C,-3.3379255952,2.5772375,-1.0866821128
H,-1.4608533542,3.5223404986,-1.4115936124
C,-4.0500608763,1.4260918375,-0.6034092919
H,-3.9093174436,3.3994322396,-1.4979625669
C,-5.449303038,1.2389997292,-0.6013770083
C,-5.1493409405,-0.9402796869,0.4097243202
C,-5.9851993493,0.0657922327,-0.1005155024
H,-6.0982147777,2.0140851976,-0.9894474231
H,-5.5338060253,-1.8667977548,0.8145994003
H,-7.0533190868,-0.0985519955,-0.0882338174
N,-1.2617554754,-0.6358873429,0.5046254781
N,-3.8318331029,-0.7684371203,0.4061924571
Co,-2.5087452905,-1.9577476339,1.0086716666
O,-2.5830655166,-1.5646012029,2.6995803029
H,-2.6340544337,-0.6263897901,2.9354446638

OER(Co@TBB-phen-O*)

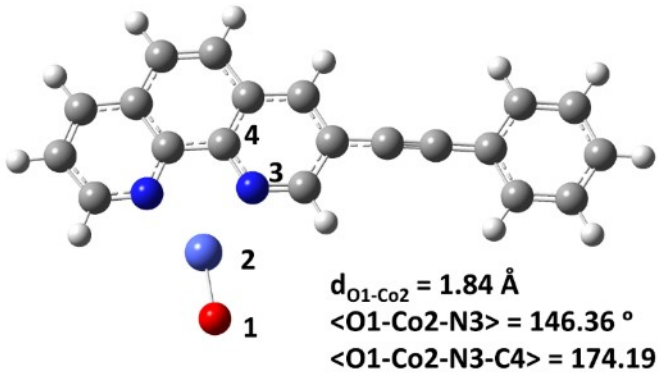

Fig S64. Optimized structure of the model system of **Co@TBB-phen-O*** obtained from DFT computation at B3LYP/6-311++G(d,p) level, empirical dispersion=GD3BJ (LANL2DZ: basis set and electron core potential of Co; solvent = water, PCM)

Charge = 2 Multiplicity = 2
C,5.7367751715,-0.5141908962,0.1477252288
C,4.9621476808,0.6524375985,-0.1308086474
C,5.6091898715,1.8768103821,-0.4776620503
C,6.9825463776,1.9210148886,-0.5409003282

C,7.7338709553,0.7647266682,-0.2654482515
C,7.1087644641,-0.4472408472,0.0773784363
H,5.2289483286,-1.4328070242,0.4085556749
H,5.0058247558,2.7501983953,-0.6850065008
H,7.4866531322,2.8418592602,-0.8021832995
H,8.8146616941,0.8083553916,-0.318488511
H,7.7087300043,-1.3233323102,0.2845607021
C,3.5836013345,0.5927588599,-0.0662549254
C,2.3596812201,0.5353266263,-0.0114059687
C,0.9756869994,0.4403925241,0.0524387078
C,0.1462900609,1.5377849189,-0.2314741126
C,0.3733446214,-0.8058729363,0.4127258225
C,-1.2413869701,1.3871923306,-0.1624971447
H,0.5852402677,2.4888434386,-0.5035633241
H,0.990948516,-1.6653709034,0.6400073851
C,-1.7404798424,0.1110881278,0.1984477175
C,-2.1656783055,2.4496931025,-0.4395799266
C,-3.145022534,-0.1059410566,0.2777183437
C,-3.5071301428,2.2385381014,-0.3618036346
H,-1.7722561147,3.4205960587,-0.7120826465
C,-4.0344704132,0.9552286997,-0.0026895816
H,-4.2024028303,3.0414933041,-0.5719372613
C,-5.4161195375,0.6782855431,0.0902221426
C,-4.8712750444,-1.5837406302,0.7044965159
C,-5.8306589725,-0.5863354185,0.4414896841
H,-6.1351085385,1.4614739828,-0.1152866618
H,-5.1721563289,-2.5855458379,0.9838438767
H,-6.8809866359,-0.8306723329,0.5208037886
N,-0.9282000882,-0.947188001,0.4788662614
N,-3.5708454047,-1.349708778,0.6251839481
Co,-2.0175509156,-2.7449762936,1.0251271771
O,-1.588837187,-4.4452729268,1.6127223333

OER(Co@TBB-phen-HOO*)

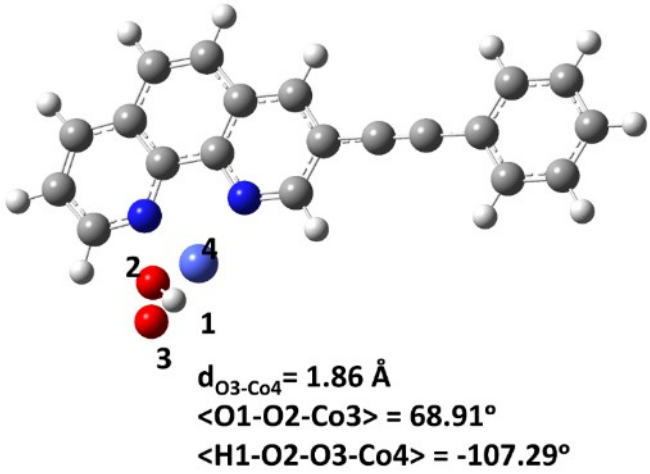

Fig S65. Optimized structure of the model system of **Co@TBB-phen-HOO*** obtained from DFT computation at B3LYP/6-311++G(d,p) level, empirical dispersion=GD3BJ (LANL2DZ: basis set and electron core potential of Co; solvent = water, PCM)

Charge = 2 Multiplicity = 1
C,5.4759933651,-1.0965353365,0.9826842162
C,4.8891338587,0.0382525732,0.3932190394
C,5.7136950132,1.0501095562,-0.1321056604
C,7.0958989526,0.9236893029,-0.0676186102
C,7.6715322987,-0.2043247982,0.5191882733
C,6.8593886345,-1.2111764956,1.0433974536
H,4.8410590939,-1.8749413172,1.3867095662
H,5.2613473999,1.9225812803,-0.5864548832
H,7.7255273402,1.7051652058,-0.4754298613
H,8.7497020637,-0.2986013095,0.5676237771
H,7.3056450301,-2.0866663588,1.4992610539
C,3.4769053652,0.1594852837,0.3244338424
C,2.2730514663,0.2630041622,0.2593729696
C,0.8673101714,0.3734191256,0.170849513
C,0.2446646994,1.5178632524,-0.3322306266
C,0.0599800269,-0.717390034,0.5963211234
C,-1.1581065328,1.5786546783,-0.414615635
H,0.8462629907,2.3552551097,-0.6611413959
H,0.5036136053,-1.6217405144,0.9914756708
C,-1.8614547378,0.4515508759,0.0289598473
C,-1.9262600317,2.6832293539,-0.9205833229
C,-3.2673555838,0.4014753695,-0.022266693
C,-3.2892582061,2.6341047244,-0.9698172707
H,-1.3990725015,3.561317694,-1.2708032718
C,-4.0151011628,1.4796549792,-0.517555409
H,-3.8511187912,3.4725530208,-1.3612999156

C,-5.4166320295,1.3194135123,-0.5331345527
C,-5.1662693223,-0.8959753205,0.4029062981
C,-5.9783836802,0.1402394419,-0.0801802492
H,-6.0472561265,2.1194323868,-0.900226247
H,-5.5682597754,-1.8269431029,0.7748062174
H,-7.0492583978,-0.0064522455,-0.081635392
N,-1.2577041591,-0.6615381204,0.5178382749
N,-3.8437116392,-0.7490526562,0.4165819323
Co,-2.5770024533,-2.0203271284,0.980866719
O,-3.7762468241,-3.1297607223,1.8813149268
O,-3.3299559294,-2.0714804413,2.7197586384
H,-2.7178497014,-2.4766686775,3.3722466533

OER(Co@TBB-phen-OO*)

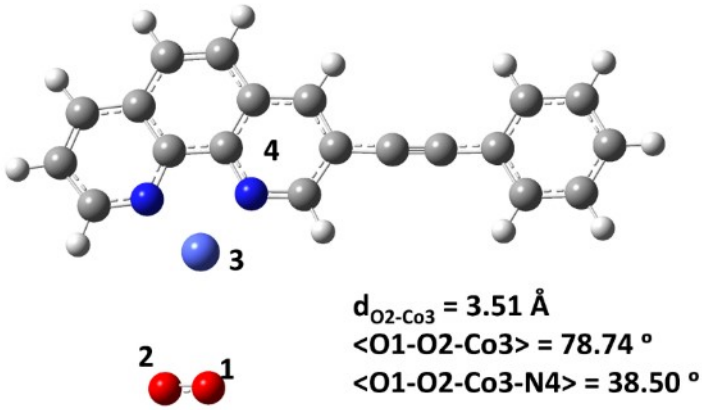

Fig S66. Optimized structure of the model system of **Co@TBB-phen-OO*** obtained from DFT computation at B3LYP/6-311++G(d,p) level, empirical dispersion=GD3BJ (LANL2DZ: basis set and electron core potential of Co; solvent = water, PCM)

Charge = 2 Multiplicity = 2
C,5.4957906134,-1.0042412743,1.0366958673
C,4.8800425405,0.0621217548,0.3569067874
C,5.6792828231,1.0504893712,-0.2471064212
C,7.0641509381,0.9693537547,-0.1693278866
C,7.6685228064,-0.0913439079,0.5071989328
C,6.8819433682,-1.0752217284,1.108220884
H,4.8814253985,-1.7647930362,1.5019194341
H,5.2047603416,1.8713263777,-0.7700235337
H,7.6731592948,1.7340099184,-0.6362381593
H,8.7486734719,-0.1506986694,0.5659868356
H,7.3503598221,-1.8986277239,1.6336288448
C,3.4652135526,0.1506973353,0.2794401042
C,2.2615762717,0.2493507884,0.2052535057
C,0.8600464567,0.4096000799,0.1057099451

C,0.2994055563,1.4984133513,-0.5636099061
C,-0.0043951781,-0.5479695664,0.7022003781
C,-1.0968245717,1.6386544797,-0.6333638628
H,0.944521537,2.2354016472,-1.0243670805
H,0.3916740369,-1.407095607,1.2268993716
C,-1.8648650669,0.6458998349,-0.0081552788
C,-1.7952088324,2.7133552706,-1.2847057761
C,-3.2757852592,0.7073308782,-0.0136658187
C,-3.157909678,2.7701083542,-1.2925358009
H,-1.2126009626,3.4842894736,-1.7725586734
C,-3.9513072682,1.7596834342,-0.649375955
H,-3.667321675,3.5869470083,-1.7879500121
C,-5.3610684617,1.7266135647,-0.5951079413
C,-5.2400994449,-0.3232220434,0.6746308093
C,-5.9951313016,0.6902085953,0.0631919064
H,-5.9381072901,2.511584155,-1.0681591835
H,-5.7062134944,-1.1477557851,1.1982448758
H,-7.0735279291,0.6408060326,0.1193855634
N,-1.3186622493,-0.4190532787,0.6377332945
N,-3.9124836538,-0.3030740972,0.6307344632
Co,-2.6814275322,-1.5825374495,1.3860682037
O,-2.7364535701,-4.6088345437,3.1192118024
O,-3.8483379705,-4.6475850691,2.6549329406

HER(TBB-phen-H*)

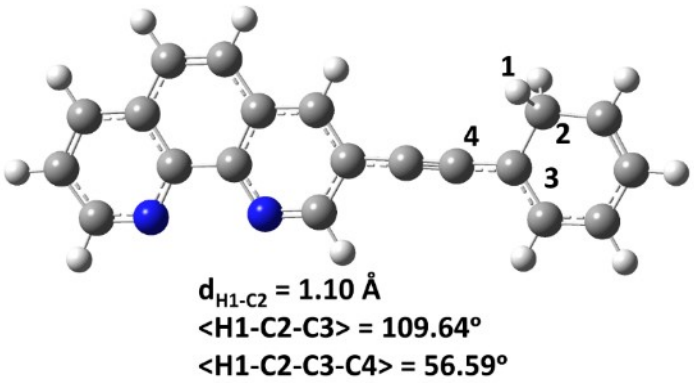

Fig S67. Optimized structure of the model system of **TBB-phen-H*** obtained from DFT computation at B3LYP/6-311++G(d,p) level, solvent = water, PCM

Charge = 0 Multiplicity = 2
C,5.2216189457,1.246882366,-0.8330729999
C,4.5095929123,-0.0916569375,-0.7852164692
C,5.221251422,-1.2754168284,-0.9959972134
C,6.5892744958,-1.2719156596,-1.2536767668
C,7.3145640688,-0.0391998366,-1.3107372603
C,6.6907112345,1.14849316,-1.116327978
H,5.0624768059,1.7849897892,0.1146714035

H,4.6865815929,-2.2180705493,-0.9561735326
H,7.1088428085,-2.2089565916,-1.412109623
H,8.379852783,-0.0653170384,-1.5133684119
H,7.2482298321,2.0778604985,-1.1617101532
C,3.1360800328,-0.1059147136,-0.5270540763
C,1.9380842374,-0.0795270555,-0.2988326522
C,0.5501108718,-0.0841131789,-0.0372081486
C,-0.1808085572,1.081793713,0.1760508265
C,-0.1689765791,-1.3150691741,0.0189696247
C,-1.5610606323,1.0090061177,0.4318157262
H,0.3093100668,2.0480829619,0.1459765375
H,0.3707085497,-2.2442118382,-0.1429242853
C,-2.1736899759,-0.2746735074,0.4644708204
C,-2.3459561124,2.1895331745,0.6562166911
C,-3.6004050516,-0.3699024809,0.727510912
C,-3.6786195644,2.1015350824,0.9019646156
H,-1.8508641255,3.1536581838,0.625111546
C,-4.3377052535,0.8285679076,0.9440295708
H,-4.268904853,2.9954449385,1.071099218
C,-5.7208703039,0.7141147444,1.1975410097
C,-5.4873278307,-1.6568573769,1.0001954555
C,-6.3038272628,-0.5331330346,1.226881548
H,-6.3083214152,1.610028885,1.3662679237
H,-5.9236190602,-2.6521055979,1.0182064339
H,-7.3621179656,-0.6599394767,1.4183139304
N,-1.4585855959,-1.4082943666,0.2562899661
N,-4.1879610917,-1.5896172587,0.7594567184
H,4.7423903312,1.8947674486,-1.5837041071

HER(Co@TBB-phen-H*)

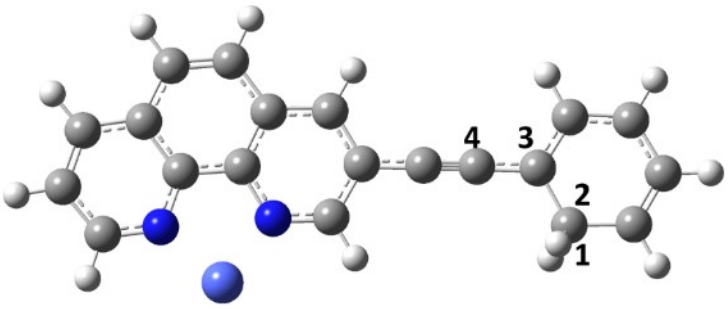

Fig S68. Optimized structure of the model system of **Co@TBB-phen-H*** obtained from DFT computation at B3LYP/6-311++G(d,p) level, empirical dispersion=GD3BJ (LANL2DZ: basis set and electron core potential of Co; solvent = water, PCM)

Charge = 2 Multiplicity = 1
C,5.6857081473,-0.840976807,-0.2699416887
C,4.9443855057,0.3656347071,0.1891300347
C,5.6524454664,1.471976886,0.6540185882
C,7.0423081317,1.4421955426,0.6862579553
C,7.8008174592,0.3225614995,0.2624720239
C,7.1549261303,-0.781149541,-0.1994074919
H,5.3817016607,-1.0862752473,-1.3004653504
H,5.1197110837,2.351368974,0.9888539168
H,7.5679220072,2.316423347,1.0526578521
H,8.8805146656,0.3601106528,0.3116907796
H,7.7037425514,-1.6540957843,-0.5311363526
C,3.5547999066,0.3653066838,0.1451190292
C,2.3409460851,0.3583599251,0.1040934257
C,0.9338328653,0.3518971596,0.0572116448
C,0.1951802592,1.4620431264,0.4777123341
C,0.2633209378,-0.8026958036,-0.4253151402
C,-1.2057308531,1.4109291991,0.4132438488
H,0.7017164248,2.344345466,0.8462764548
H,0.82312909,-1.6683569069,-0.7537562224
C,-1.7808572121,0.2259643257,-0.0783598389
C,-2.0885974052,2.473649562,0.8101187053
C,-3.1825190321,0.087689146,-0.1777296569
C,-3.442049975,2.3381705795,0.7132748357
H,-1.6551793278,3.3903682255,1.1901397357
C,-4.0391070465,1.1314505843,0.2122131007
H,-4.0940863004,3.14808063,1.0163460387
C,-5.4241212889,0.9027506728,0.0769308601
C,-4.928854416,-1.3014159735,-0.7880935673
C,-5.8554880692,-0.3123293719,-0.4223116194
H,-6.1326159252,1.6706137141,0.3613326993
H,-5.2508932533,-2.2575241473,-1.1802727309
H,-6.910461327,-0.5207093695,-0.5390954482
N,-1.0597764116,-0.8648150671,-0.4916600158
N,-3.6133322302,-1.1120896521,-0.6706919554
Co,-2.1809839401,-2.2667504427,-1.0862606002
H,5.3312224856,-1.7219303849,0.2893373756

Model systems with considering residual Pd in the COPs

To incorporate the role of Pd in OER and HER, DFT computations have been performed following the same methodology. In both the model systems, TBB-phen and Co@TBB-phen, Pd was stabilized at three positions, (i) near TBB, (ii) in the middle near alkyne, and (iii) near phen. In

TBB-phen-Pd, in all of the three positions, the most stable system was found to be in the middle, near alkyne, and in Co@TBB-phen-Pd, the most stable system was found to be near phen. Therefore, further DFT computations were performed on model (b) for TBB-phen-Pd and on a model (c) for Co@TBB-phen-Pd as illustrated in Figs S69 and S70, respectively. Table S13 displays the Pd stabilization energy of model systems where model (b) for TBB-phen-Pd and model (c) for Co@TBB-phen-Pd have maximum negative value leading to the most feasibility.

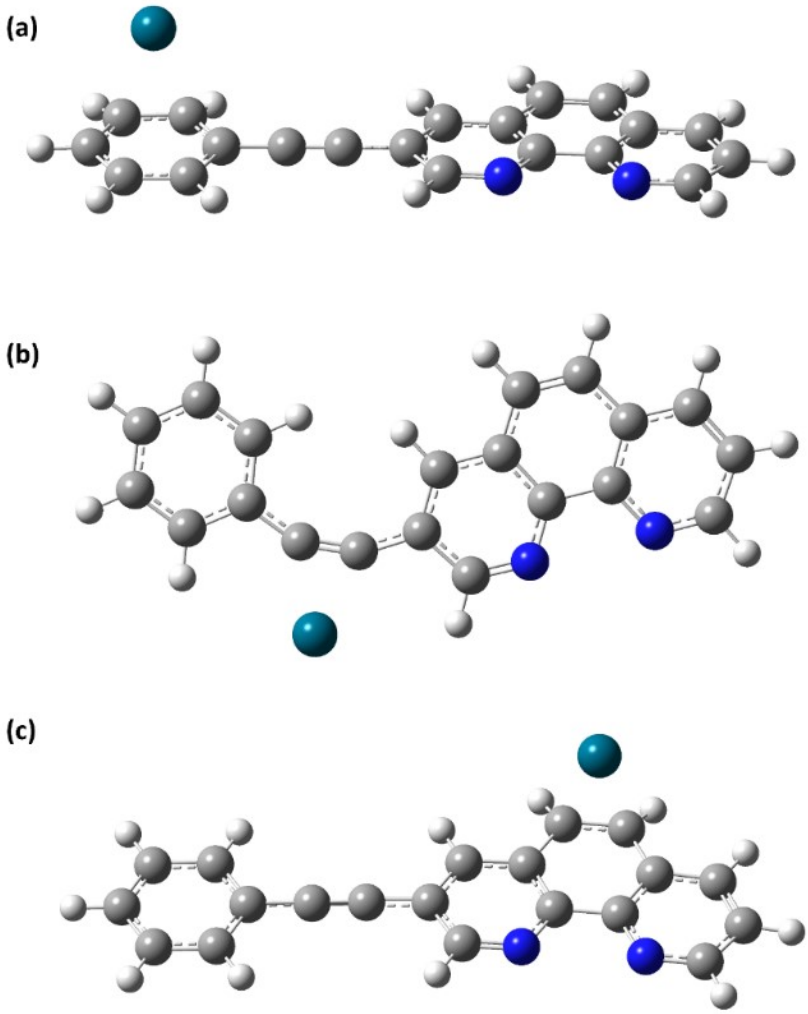

Fig S69. Optimized structure of the model system of TBB-phen-Pd, obtained from DFT computation at B3LYP/6-311++G(d,p) level, solvent = water, PCM (a) Pd near TBB, (b) Pd near alkyne, and (c) Pd near phen

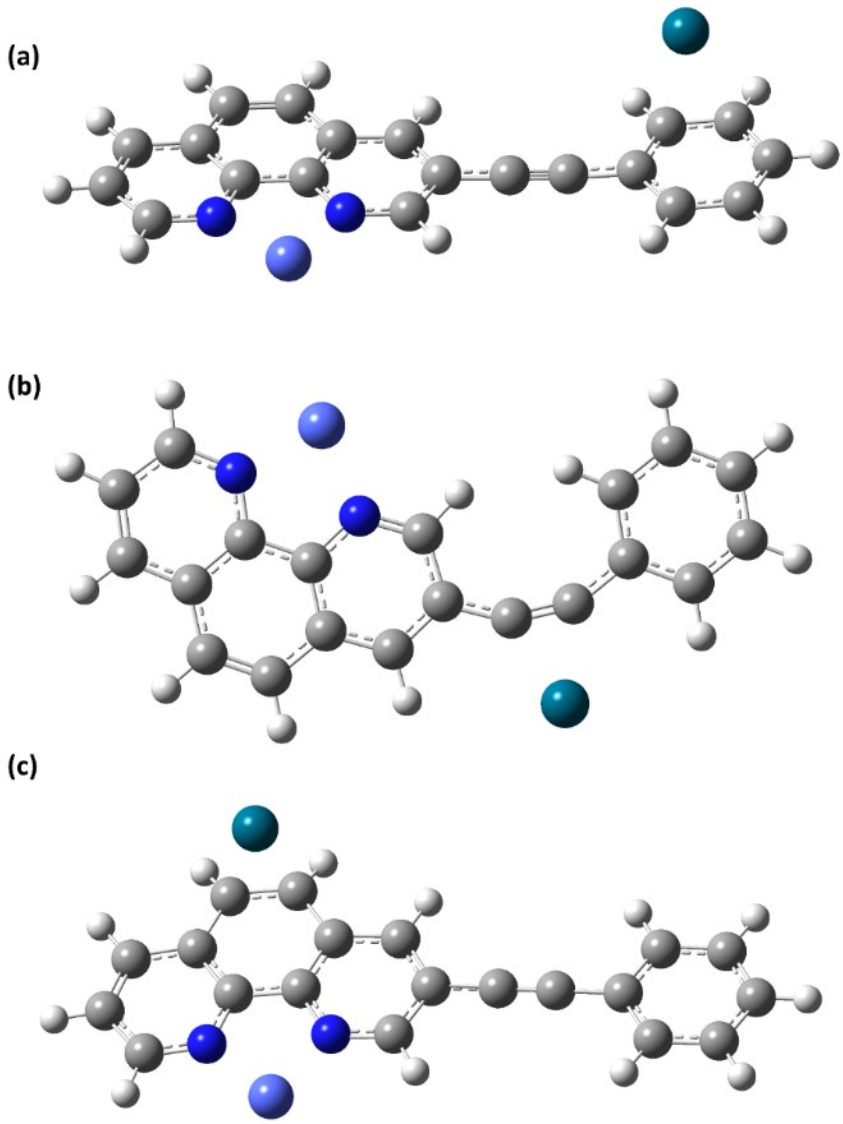

Fig S70. Optimized structure of the model system of Co@TBB-phen-Pd, obtained from DFT computation at B3LYP/6-311++G(d,p) level, solvent = water, PCM (a) Pd near TBB, (b) Pd near alkyne, and (c) Pd near phen

Table S13. Palladium stabilization energy in the model systems (kcal/mol)

	TBB-phen-Pd	Co@TBB-phen-Pd
Near TBB	-37.57027872	-27.26091693
Near alkyne	-60.61809351	-24.39445125
Near phen	-45.04329531	-57.26154252

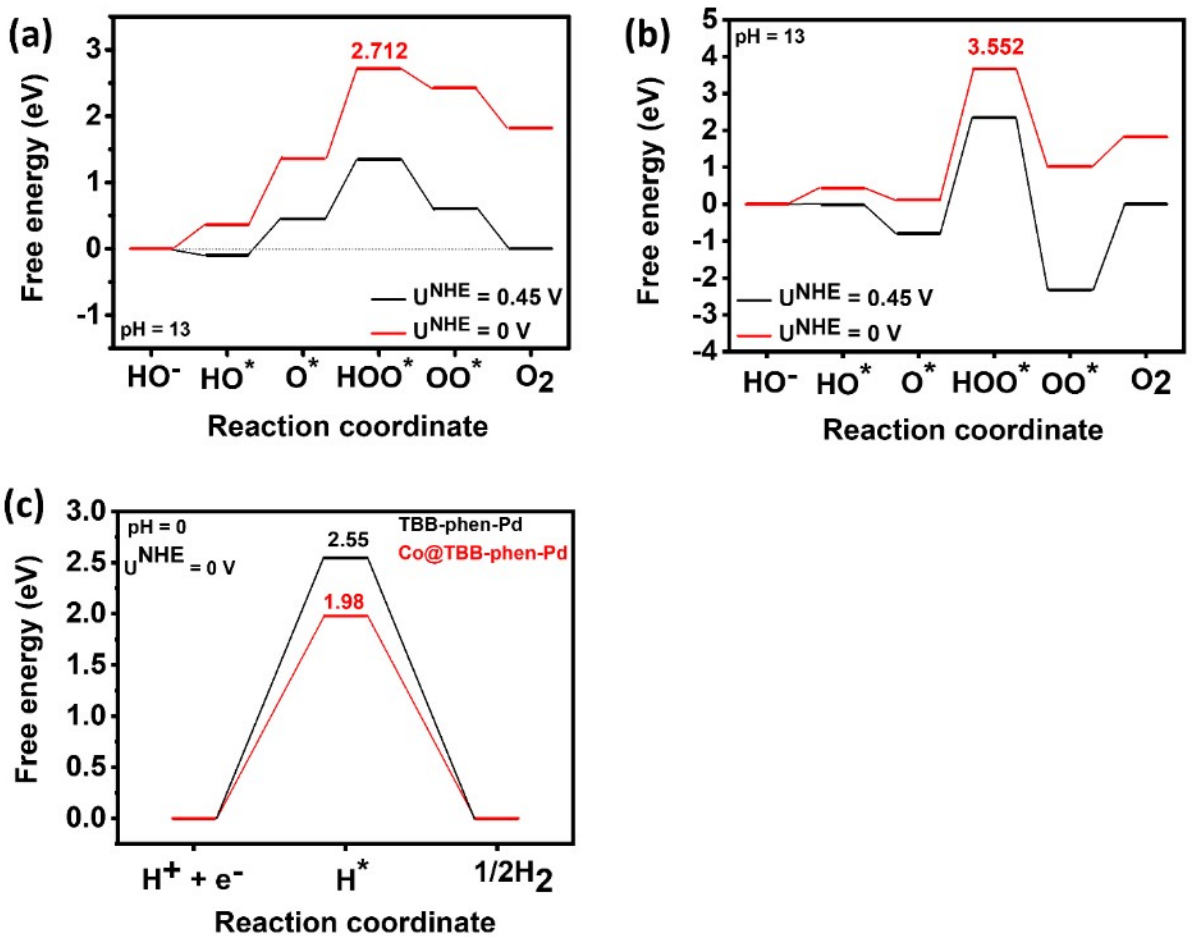

Fig S71. Free energy profile of (a) TBB-phen-Pd, (b) Co@TBB-phen-Pd for oxygen evolution reaction, (c) hydrogen evolution reaction (ub3lyp/6-311++G(d,p), LanL2DZ: ECP and basis set of Co and Pd, empirical dispersion = GD3BJ, solvent=water, PCM)

Table S14. The values considered for the calculation of free energy of reaction intermediates

Polymer	Reaction	Intermediate	G (Ha)	E (Ha)	ZPE (Ha)	TS (Ha)
TBB-phen-Pd		*	-1005.714915	-1005.905951	0.260574	0.069537925
	OER	HO*	-1081.549429	-1081.752002	0.275244	0.07267142
		O*	-1080.912816	-1081.105382	0.263594	0.071027938
		HOO*	-1156.694349	-1156.887687	0.275324	0.08198638
		OO*	-1156.05192	-1156.242006	0.265482	0.075396301
	HER	H*	-1006.410125			
Co@TBB-phen-Pd		*	-1150.442987	-1150.706988	0.264001	0.072842962
	OER	HO*	-1226.274816	-1226.476075	0.27774	0.076481048

	O*	-1225.683965	-1225.874707	0.26687	0.0761285
	HOO*	-1301.428878	-1301.710565	0.281687	0.080105355
	OO*	-1300.894348	-1301.08426	0.26989	0.079978494
HER	H*	-1151.223469			
	H_2	-1.183819167	-1.178674	0.009922822	0.01506799
	H_2O	-76.45121063	-76.447168	0.020580669	0.0246233 (0.035 bar)
	0.5 O_2	-75.0929848	-75.083062	0.00183756	0.011760382

Optimized models and XYZ coordinates of OER and HER reaction intermediates

TBB-phen-Pd

OER (TBB-phen-Pd-OH*)

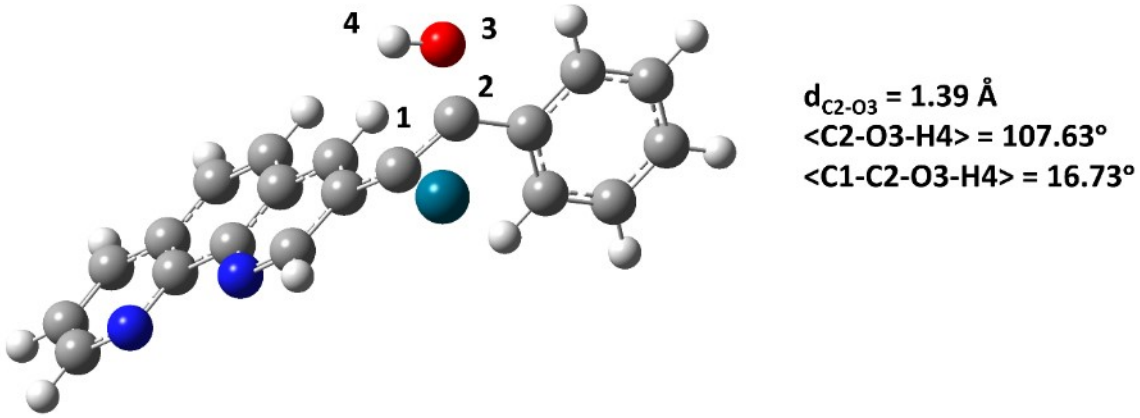

Fig S72. Optimized structure of the model system of **TBB-phen-Pd-OH*** obtained from DFT computation at B3LYP/6-311++G(d,p) level, LanL2DZ: ECP and basis set of Pd, empirical dispersion = GD3BJ solvent = water, PCM

Charge = 0 Multiplicity = 2

C,-2.9424595644,-1.2711839788,-0.9711311472
C,-3.3187493219,-0.9196875236,0.3358305932
C,-4.4113508376,-1.5736003441,0.9216097875
C,-5.1142800458,-2.5477591923,0.2137584373
C,-4.7349322327,-2.8889708559,-1.0825594101
C,-3.6410190621,-2.246515176,-1.670116096
H,-2.1024973386,-0.7672576936,-1.4335982333
H,-4.7071779181,-1.3164862513,1.9295964722
H,-5.9595025602,-3.0414417638,0.679691055
H,-5.2821905874,-3.6463670077,-1.6313276793
H,-3.3346052316,-2.5080697566,-2.6764243382

C,-2.5504598335,0.0997711254,1.0859506029
C,-1.3976486992,0.7272927769,0.6070646432
C,-0.0396842696,0.4580465543,0.4349670324
C,0.5486714451,-0.7751793312,0.781138107
C,0.8472122598,1.4394418538,-0.1269541339
C,1.9165888567,-0.987185467,0.5682987336
H,-0.0583345506,-1.5642713641,1.2099695045
H,0.4250175071,2.4027781837,-0.4042443724
C,2.6920346418,0.0653999619,0.0013513394
C,2.5440557442,-2.2333264771,0.9079648433
C,4.1053011033,-0.1389839303,-0.2248801301
C,3.8709794931,-2.4272339906,0.6972329367
H,1.9310998881,-3.0175848787,1.337761492
C,4.6843369923,-1.393465183,0.1291766592
H,4.340542336,-3.3697852684,0.9555436788
C,6.0622455453,-1.5731344373,-0.0981705337
C,6.1376483723,0.6524782285,-0.9642638231
C,6.8001715426,-0.5473168845,-0.6480729056
H,6.5255250727,-2.5181281214,0.163037399
H,6.6966532716,1.4766315154,-1.3993223471
H,7.8612511458,-0.6491522777,-0.8368912422
N,2.1269451032,1.2626583254,-0.3328121195
N,4.8459851852,0.8603319544,-0.7661773837
Pd,-2.7532330033,2.0595104003,0.1733160872
O,-2.8315377158,0.0619727339,2.4535212129
H,-2.2820741739,0.7293429412,2.8836506379

OER(TBB-phen-Pd-O*)

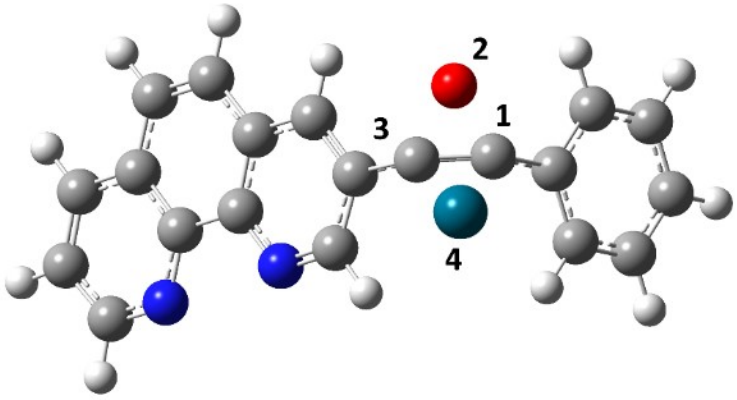

Fig S73. Optimized structure of the model system of **TBB-phen-Pd-O*** obtained from DFT computation at B3LYP/6-311++G(d,p) level, LanL2DZ: ECP and basis set of Pd, empirical dispersion = GD3BJ solvent = water, PCM

Charge = 0 Multiplicity = 1

C,-3.5186469628,-0.306621878,-1.3076499369

C,-3.3994566287,-0.6778360997,0.041369076
C,-3.9531696453,-1.8889013166,0.4783778578
C,-4.5975982204,-2.726433467,-0.4292293707
C,-4.7042683112,-2.3610107884,-1.7708503292
C,-4.161749669,-1.1483188879,-2.206175477
H,-3.1070499869,0.6418667576,-1.6333107837
H,-3.8671869837,-2.1654403493,1.5217135779
H,-5.020275816,-3.6640481654,-0.087277825
H,-5.210716789,-3.0123200977,-2.4732659713
H,-4.2449387245,-0.860149185,-3.2476051824
C,-2.7075813872,0.1886066813,0.971511054
C,-1.435891977,0.5959817603,1.3244228752
C,-0.0691249019,0.2947659009,0.9817094296
C,0.7202009094,-0.5407243913,1.7523041803
C,0.5115146151,0.8629173849,-0.1816521907
C,2.0406647491,-0.8154330984,1.3485262876
H,0.3239520171,-0.9870270821,2.6562739094
H,-0.0846559718,1.5413065816,-0.786401378
C,2.5206751488,-0.2073000668,0.1567124136
C,2.8915236468,-1.6817127217,2.1098970117
C,3.8802980568,-0.4787263624,-0.2752656767
C,4.1628646426,-1.9373478011,1.7070430755
H,2.4957922204,-2.1292808899,3.0143615615
C,4.6874186011,-1.3473458469,0.5120941391
H,4.8048636395,-2.5939437765,2.2831871661
C,6.0040230324,-1.6007015216,0.0758838586
C,5.5851869025,-0.1648618704,-1.7875619873
C,6.4606545972,-1.0089660925,-1.0800289702
H,6.6397221569,-2.2589348444,0.6574066205
H,5.9221058317,0.3146377751,-2.7024605655
H,7.4650736993,-1.179683308,-1.4460251624
N,1.7408168398,0.6215025825,-0.5828143919
N,4.3444840629,0.0969699241,-1.4099799562
Pd,-2.6407503247,2.2337171443,1.1251541871
O,-2.2323697893,-0.2221608835,2.2915630536

OER (TBB-phen-Pd-OOH*)

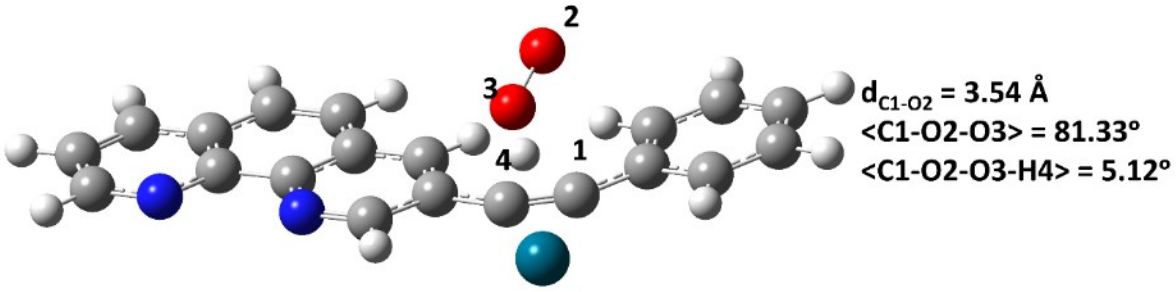

Fig S74. Optimized structure of the model system of **TBB-phen-Pd-OOH*** obtained from DFT computation at B3LYP/6-311++G(d,p) level, LanL2DZ: ECP and basis set of Pd, empirical dispersion = GD3BJ solvent = water, PCM

Charge = 0 Multiplicity = 2

C,-3.0837873703,-2.4730927674,-0.3792720189
C,-3.440025289,-1.1610960279,-0.0117322458
C,-4.7938216717,-0.8678258751,0.2244013551
C,-5.7625154336,-1.857620913,0.1024146772
C,-5.3992964418,-3.155048027,-0.2618633978
C,-4.0573636882,-3.4574839998,-0.5020032581
H,-2.0448523869,-2.711262664,-0.5687661339
H,-5.0666767454,0.1421334722,0.5056738343
H,-6.8025467117,-1.6177661319,0.2900129654
H,-6.1554172253,-3.9250816836,-0.3583942981
H,-3.7699321503,-4.4630604527,-0.7861941803
C,-2.4331401995,-0.1473144368,0.1150926187
C,-1.2353457118,0.2809629356,0.1507420111
C,0.1865495743,0.1423652334,0.1028475552
C,0.8076940167,-1.0505791242,-0.246009665
C,1.0320238583,1.2416948508,0.4116990321
C,2.2101670947,-1.1278681236,-0.281121896
H,0.2205649996,-1.9257352481,-0.4957100633
H,0.5696769006,2.1857196709,0.6876650221
C,2.9569317174,0.0370402483,0.048097047
C,2.8839557055,-2.3413944426,-0.641323215
C,4.4079138525,-0.0237844849,0.0133170266
C,4.2396375046,-2.3984524123,-0.674768945
H,2.2853224067,-3.2111249086,-0.8865296959
C,5.0321391502,-1.2493661663,-0.3509007137
H,4.748720033,-3.3156759435,-0.9478932548
C,6.4411895015,-1.2881849434,-0.3801819767
C,6.4455679286,1.006593199,0.28731145
C,7.1566945503,-0.1565603596,-0.0602486244
H,6.9427044644,-2.2094513908,-0.6543815754
H,6.9875393956,1.912473084,0.544151623

H,8.239144231,-0.1482323615,-0.0718089409
N,2.3470644521,1.1979281427,0.3896700945
N,5.1251392013,1.0810502283,0.3256293168
Pd,-2.4910921398,1.8726439827,0.458254009
O,-2.4165956919,-0.1685126662,3.6551991826
O,-2.2246987804,1.1256346932,3.4627666785
H,-2.2941244712,1.2891048536,2.4570468597

OER (TBB-phen-Pd-OO*)

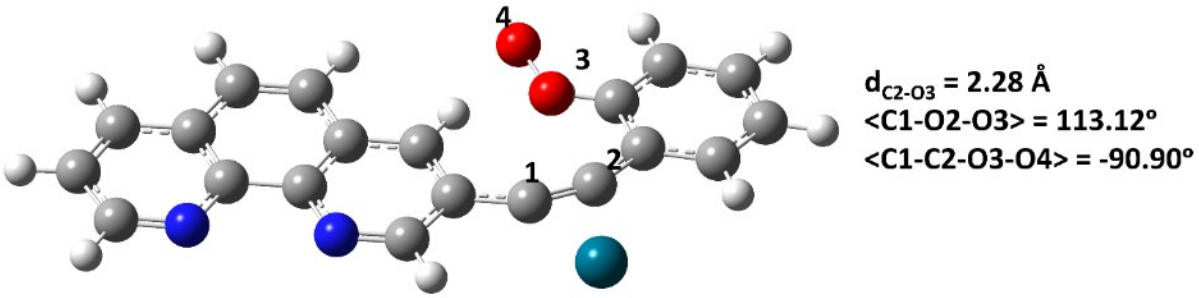

Fig S75. Optimized structure of the model system of **TBB-phen-Pd-OO*** obtained from DFT computation at B3LYP/6-311++G(d,p) level, LanL2DZ: ECP and basis set of Pd, empirical dispersion = GD3BJ, solvent = water, PCM

Charge = 0 Multiplicity = 1

C,-3.0587041124,-2.2452040754,-0.1041086107
C,-3.5078499894,-0.9137403425,0.0009936396
C,-4.8921103668,-0.6567307224,0.01898527
C,-5.8007818055,-1.7018377931,-0.0611487925
C,-5.3453503168,-3.0200022617,-0.1585938868
C,-3.976339236,-3.2871922245,-0.1795761131
H,-1.9989918716,-2.4529082716,-0.1311920312
H,-5.2304399349,0.3691523623,0.0997192034
H,-6.8641917969,-1.4952131115,-0.0470917286
H,-6.056755332,-3.8348060651,-0.2224332676
H,-3.6236034965,-4.3084828651,-0.2600424625
C,-2.5742555885,0.1593683437,0.111708873
C,-1.3537536215,0.6257022606,0.1119696543
C,0.0492283297,0.4256171084,0.0189915869
C,0.6124381062,-0.8461898287,0.0297954239
C,0.9386044668,1.534995289,-0.0111941535
C,2.0136562043,-0.9848753336,0.0148690724
H,-0.0097331518,-1.7289054286,0.0301086646
H,0.5147576277,2.5357276476,-0.015233502
C,2.8053296279,0.1936076994,-0.0198244147
C,2.6351270131,-2.2756170099,0.0258916974
C,4.2506763163,0.0681912433,-0.0447438061
C,3.9878194705,-2.3945498506,0.00503511

H,2.0009714677,-3.1541574278,0.0529432794
C,4.8250182596,-1.233739678,-0.030726874
H,4.4585456003,-3.3708554641,0.0144172946
C,6.2319557552,-1.3335191938,-0.0536123251
C,6.3266239299,1.0547848061,-0.0998572417
C,6.9908936741,-0.1864629352,-0.0883459454
H,6.696190061,-2.313208184,-0.0435817907
H,6.9048759751,1.9740952757,-0.1272133969
H,8.0726734095,-0.2230274474,-0.1066963878
N,2.2472060589,1.4332119969,-0.0346875619
N,5.0112112675,1.1882630813,-0.0793191368
Pd,-2.64959869,2.1554364725,0.0684972989
O,-1.6773813688,-0.1291772399,2.1886626255
O,-1.093433382,-1.2541814321,2.3301200956

HER (TBB-phen-Pd-H*)

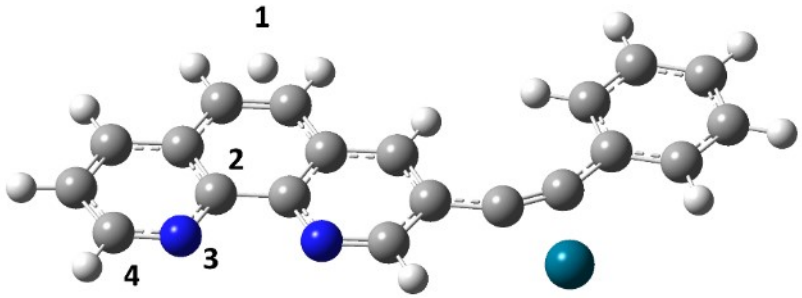

d_{H1-C3} = 3.00 Å
<H1-C2-N3> = 112.02°
<H1-C2-N3-C4> = 96.45°

Fig S76. Optimized structure of the model system of **TBB-phen-Pd-OO*** obtained from DFT computation at B3LYP/6-311++G(d,p) level, LanL2DZ: ECP and basis set of Pd, empirical dispersion = GD3BJ, solvent = water, PCM

Charge = 0 Multiplicity = 2

C,-3.1600135272,-2.2498529892,0.0323786434
C,-3.5405336878,-0.8936095299,0.0025671715
C,-4.9110437431,-0.5795938639,0.0027029816
C,-5.8693301484,-1.5865058797,0.0316128368
C,-5.4801548648,-2.9266609353,0.0611413314
C,-4.1222558281,-3.2525785319,0.0613990971
H,-2.1090718568,-2.5092456774,0.0327469012
H,-5.2048875931,0.4630010876,-0.0201807979
H,-6.9216459712,-1.327163955,0.0312443475
H,-6.2276837079,-3.710722763,0.0837816899
H,-3.8134320557,-4.2912847374,0.084258464
C,-2.5476367389,0.1434277149,-0.0271267949
C,-1.3437385278,0.5677551831,-0.0446920055
C,0.0749632209,0.3889854071,-0.0499092629
C,6768313409,-0.8639957281,-0.0207834378

C,0.9436198873,1.5140933559,-0.0857362677
C,2.0775954454,-0.9729765339,-0.0263046561
H,0.0753255822,-1.7641443594,0.0073031724
H,0.4982249814,2.5051685798,-0.1095781343
C,2.8462413956,0.2233241379,-0.0623645105
C,2.7301515103,-2.2494868888,0.0076374937
C,4.2954933123,0.1302613119,-0.0639637322
C,4.0847253655,-2.337269265,0.0070661815
H,2.1167576648,-3.1427631534,0.0360595901
C,4.8980992431,-1.1583466275,-0.0280326044
H,4.5770358414,-3.3026257419,0.0349507928
C,6.3060509282,-1.2279006526,-0.025264408
C,6.3512233568,1.1606164655,-0.0921799624
C,7.0417200589,-0.0646983899,-0.0570054634
H,6.7909637227,-2.1972575949,0.0023687066
H,6.9093481578,2.0923880018,-0.1182276243
H,8.1241881829,-0.0783264258,-0.0554352027
N,2.2576224145,1.4436819721,-0.0923866542
N,5.0322386729,1.2655941516,-0.0960323558
Pd,-2.5994600747,2.1798486482,-0.0708347825
H,3.4165291298,-0.5662062636,2.7292981458

Co@TBB-phen-Pd
OER (Co@TBB-phen-Pd-OH*)

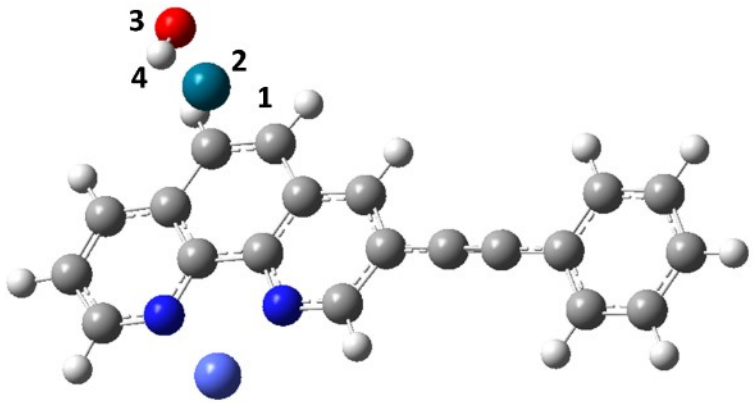

d_{Pd2-O3} = 1.98 Å
<Pd2-O3-H4> = 109.39°
<C1-Pd2-O3-H4> = -100.84°

Fig S77. Optimized structure of the model system of **Co@TBB-phen-Pd-OH*** obtained from DFT computation at B3LYP/6-311++G(d,p) level, LanL2DZ: ECP and basis set of Co and Pd, empirical dispersion = GD3BJ, solvent = water, PCM

Charge = 2 Multiplicity = 1

C,0,6.371396831,1.0770592713,-0.2965657616
C,0,5.6218061381,-0.0445248693,0.1031790733
C,0,6.283722783,-1.2541759717,0.3825720749
C,0,7.6657077018,-1.3350933478,0.2614338237
C,0,8.403107795,-0.2182019769,-0.1345792934

C,0,7.7531863045,0.9854921084,-0.4116103973
H,0,5.8621020667,2.0082186354,-0.5109624685
H,0,5.7068935566,-2.1176937477,0.6891562543
H,0,8.1690769406,-2.270121916,0.4756858598
H,0,9.4804372773,-0.2856201856,-0.2269785491
H,0,8.3244911351,1.853380506,-0.718125344
C,0,4.2096361648,0.0435021244,0.2195586623
C,0,3.0056831102,0.1172309198,0.3160677039
C,0,1.5981605817,0.2125520971,0.4118041236
C,0,0.8251691968,-0.8043531382,0.9809526748
C,0,0.9443337579,1.3680638736,-0.083109146
C,0,-0.5680780891,-0.6686172062,1.0288364327
H,0,1.3028711905,-1.6921756492,1.37420983
H,0,1.5101846105,2.1849770192,-0.5107719789
C,0,-1.1242635087,0.5034817127,0.4986637395
C,0,-1.4770303923,-1.6611633053,1.5700138478
C,0,-2.5349950034,0.7144865448,0.4780140708
C,0,-2.8549863766,-1.4588160102,1.5433919287
H,0,-1.0623163339,-2.4819865701,2.1425680289
C,0,-3.4199034017,-0.2484816835,0.9829732919
H,0,-3.5095691064,-2.1283246858,2.0878650048
C,0,-4.7937317867,0.0398287487,0.9063239764
C,0,-4.2495490114,2.1426426971,-0.1421469666
C,0,-5.2013501599,1.2342306947,0.3369745992
H,0,-5.5187684466,-0.6681074099,1.2876815788
H,0,-4.5369477347,3.0899251986,-0.5793730295
H,0,-6.2501927701,1.4842657341,0.2588254628
N,0,-0.3754770181,1.4978103371,-0.0388635505
N,0,-2.9428494567,1.8827921491,-0.0730656932
Co,0,-1.46063698,2.989973016,-0.5776913428
Pd,0,-2.2690530149,-2.7623228045,-0.258669119
O,0,-2.3303934301,-3.9501934681,-1.8446203132
H,0,-2.2507208209,-3.418256762,-2.6471172695

OER (Co@TBB-phen-Pd-O*)

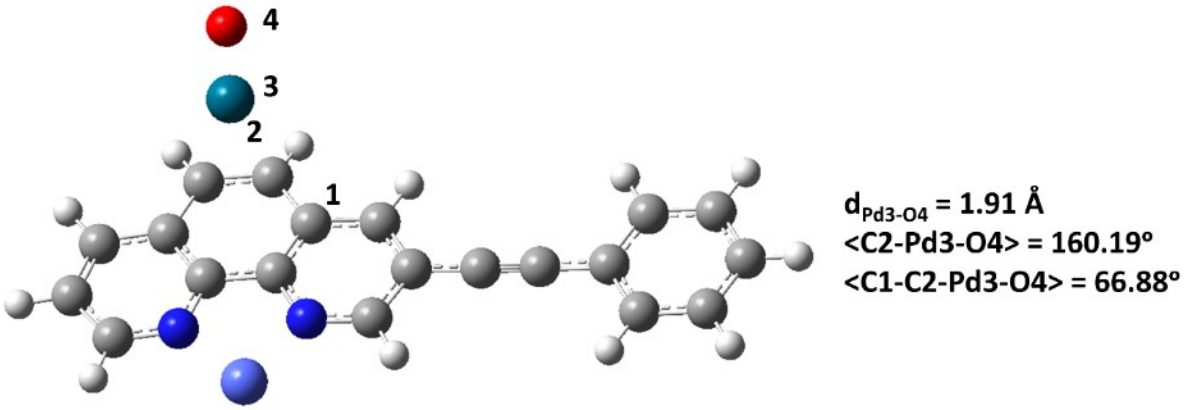

Fig S78. Optimized structure of the model system of **Co@TBB-phen-Pd-O*** obtained from DFT computation at B3LYP/6-311++G(d,p) level, LanL2DZ: ECP and basis set of Co and Pd, empirical dispersion = GD3BJ, solvent = water, PCM

Charge = 2 Multiplicity = 2

C,0,6.3581988101,1.0638167442,-0.3698342061
C,0,5.6003223279,-0.022282858,0.1050796368
C,0,6.2490591527,-1.2263105432,0.4356823459
C,0,7.6266103121,-1.3364797714,0.2909299239
C,0,8.3721941899,-0.2552861955,-0.181460796
C,0,7.7353183682,0.9423740625,-0.5101644303
H,0,5.8588373598,1.9900338435,-0.6250120575
H,0,5.6655539534,-2.0623812381,0.800143208
H,0,8.120021576,-2.2666008795,0.5457784306
H,0,9.4459364466,-0.3459728286,-0.2935832617
H,0,8.3131358306,1.7819790183,-0.8771959726
C,0,4.1919181923,0.0909923374,0.2398609189
C,0,2.989637392,0.17817149,0.3455629307
C,0,1.5820082516,0.2688937864,0.4342038415
C,0,0.8017746973,-0.7950150189,0.898298979
C,0,0.9344087909,1.4624675181,0.0273763508
C,0,-0.5940118264,-0.6794584335,0.9261803036
H,0,1.2799774234,-1.7106855118,1.2206821024
H,0,1.4990893141,2.3147054135,-0.3261203324
C,0,-1.1442484062,0.5321891871,0.4917429069
C,0,-1.5098032405,-1.7168365291,1.368710325
C,0,-2.5502176346,0.7489598265,0.4779644638
C,0,-2.8906549086,-1.5053685906,1.3514286418
H,0,-1.0987954652,-2.5641011835,1.9038974806
C,0,-3.4437843783,-0.2437323734,0.8976798982
H,0,-3.5497980421,-2.1935140869,1.8660112638
C,0,-4.8119813021,0.0802725298,0.864741682
C,0,-4.2491902963,2.2628804878,0.0032693597

C,0,-5.207627809,1.3281044532,0.4141057501
H,0,-5.5471157113,-0.6459423575,1.188064577
H,0,-4.5216376003,3.2479249027,-0.3522545016
H,0,-6.252939581,1.6006191256,0.3744879312
N,0,-0.3852490838,1.5716403335,0.0651140472
N,0,-2.9511350583,1.967771885,0.0424811561
Co,0,-1.4644671389,3.1115957979,-0.403510018
Pd,0,-2.3135187898,-2.7436114455,-0.4965289385
O,0,-2.3582509664,-3.7892510581,-2.095444031

OER (Co@TBB-phen-Pd-OOH*)

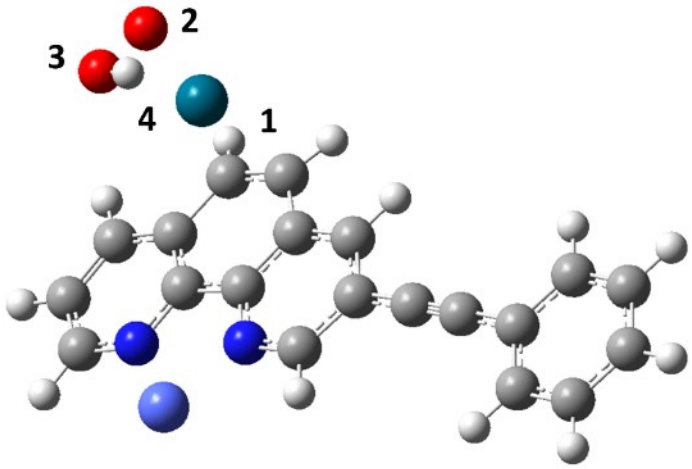

d_{Pd1-O2} =2.02 Å
<Pd1-O2-O3> = 105.18°
<Pd1-O2-O3-H4> = 95.59°

Fig S79. Optimized structure of the model system of **Co@TBB-phen-Pd-OH*** obtained from DFT computation at B3LYP/6-311++G(d,p) level, LanL2DZ: ECP and basis set of Co and Pd, empirical dispersion = GD3BJ, solvent = water, PCM

Charge = 2 Multiplicity = 1

C,0,6.2363277673,0.9840323193,-0.5160046964
C,0,5.5541383009,-0.1158821577,0.0363333981
C,0,6.2886709119,-1.2203302131,0.5049856445
C,0,7.6758245969,-1.2190601908,0.4208703942
C,0,8.3460163759,-0.1241898252,-0.1269000794
C,0,7.6235718797,0.9748929519,-0.5939479636
H,0,5.67081548,1.8341979953,-0.876341551
H,0,5.7641691431,-2.0669620121,0.9297633335
H,0,8.2358301303,-2.0726342618,0.7832333456
H,0,9.4275880841,-0.1272498578,-0.1894644039
H,0,8.1424852193,1.8256036625,-1.0189396348
C,0,4.1371534927,-0.1043759503,0.1207591914
C,0,2.929433649,-0.0831164819,0.192905011
C,0,1.5193312458,-0.0165671047,0.2672003492
C,0,0.7532469296,-1.0138388471,0.8796156721
C,0,0.8566649382,1.102426614,-0.2947384252

C,0,-0.6418430596,-0.8929619319,0.9320560465
H,0,1.2417867772,-1.8780767262,1.3106129794
H,0,1.4082442536,1.8943687545,-0.78333803
C,0,-1.2049353967,0.2573712681,0.3657276283
C,0,-1.5426175254,-1.85745125,1.5412551987
C,0,-2.6064490925,0.4994222492,0.3995376819
C,0,-2.9242884613,-1.6139488659,1.5867565385
H,0,-1.1098618847,-2.6273532207,2.1679984094
C,0,-3.4847803502,-0.4025332912,1.0126588129
H,0,-3.553028675,-2.1979238949,2.247513997
C,0,-4.8460619556,-0.0492968028,1.0254031259
C,0,-4.3085032786,1.9736852589,-0.1767813171
C,0,-5.2503875343,1.1342513063,0.4307284559
H,0,-5.5702992794,-0.7042375969,1.4937535467
H,0,-4.590201168,2.9029057563,-0.6541051588
H,0,-6.291102843,1.4265636054,0.4234008709
N,0,-0.4615596705,1.2168975247,-0.2357656173
N,0,-3.0157466465,1.6530057516,-0.1834617881
Co,0,-1.5512568879,2.6530673852,-0.9411287798
Pd,0,-2.5202898888,-2.9983531874,-0.1053207579
O,0,-2.8658242991,-4.195126737,-1.6995576402
O,0,-2.8545698626,-3.3163573325,-2.8403277103
H,0,-1.9507275857,-3.4142008335,-3.1758531179

OER (Co@TBB-phen-Pd-OO*)

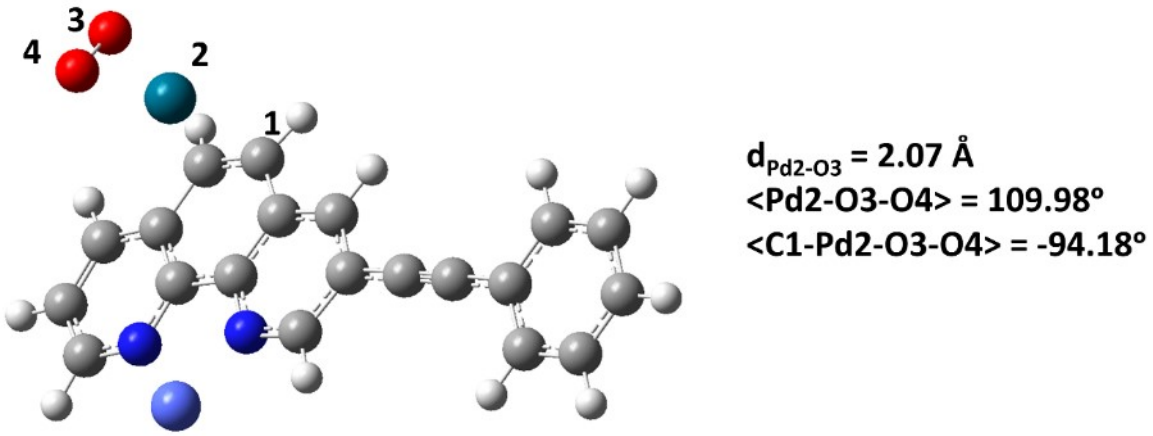

Fig S80. Optimized structure of the model system of **Co@TBB-phen-Pd-OOH*** obtained from DFT computation at B3LYP/6-311++G(d,p) level, LanL2DZ: ECP and basis set of Co and Pd, empirical dispersion = GD3BJ, solvent = water, PCM)

Charge = 2 Multiplicity = 2

C,0,6.3024664863,1.0821455342,-0.3028020077
C,0,5.5881626712,-0.0728932693,0.0655267698

C,0,6.2904157403,-1.2566436757,0.3562804717
C,0,7.6777213994,-1.2790972124,0.2779365698
C,0,8.3800151485,-0.1292037537,-0.0860573549
C,0,7.6896932607,1.0489610956,-0.3748533101
H,0,5.761724027,1.993331335,-0.5258611226
H,0,5.7409092649,-2.1457660127,0.6388208669
H,0,8.2127727571,-2.1941656165,0.5012723772
H,0,9.4616105376,-0.1510278207,-0.1442650825
H,0,8.2336170414,1.9425075201,-0.6564594581
C,0,4.1711316862,-0.0387819834,0.143852211
C,0,2.9636377945,-0.0008339771,0.212305867
C,0,1.5541367641,0.0784006768,0.285258195
C,0,0.7760732989,-0.9401546038,0.8436619598
C,0,0.9043763702,1.2318341636,-0.2215266442
C,0,-0.6182202945,-0.8066924819,0.8975832438
H,0,1.2537387847,-1.8299751578,1.2326776883
H,0,1.4665579261,2.0423176231,-0.6657192961
C,0,-1.1685022069,0.3743583397,0.3841576436
C,0,-1.5296352042,-1.7861273988,1.4623007784
C,0,-2.5671232492,0.6235862913,0.4187014976
C,0,-2.9075652051,-1.5395550786,1.5018023309
H,0,-1.1078820894,-2.5930311555,2.0488726489
C,0,-3.4568804176,-0.303966462,0.9754335153
H,0,-3.5486334613,-2.1582858892,2.1176453478
C,0,-4.817332622,0.0546826804,0.9907089475
C,0,-4.2551620659,2.1358787932,-0.0955097671
C,0,-5.2086191505,1.2702223159,0.4562443544
H,0,-5.5497301184,-0.6202042804,1.4160379397
H,0,-4.5273385295,3.0911200464,-0.5246743198
H,0,-6.2474357238,1.5691944761,0.454044446
N,0,-0.412577264,1.3561417176,-0.1649167722
N,0,-2.9646222565,1.8089376732,-0.1070393478
Co,0,-1.4871204017,2.8346487749,-0.8037125348
Pd,0,-2.484112155,-2.8757143459,-0.2472297816
O,0,-2.7292099393,-4.1088873803,-1.8974228327
O,0,-2.6180657441,-3.4212826017,-2.9814468385

OER (Co@TBB-phen-Pd-H*)

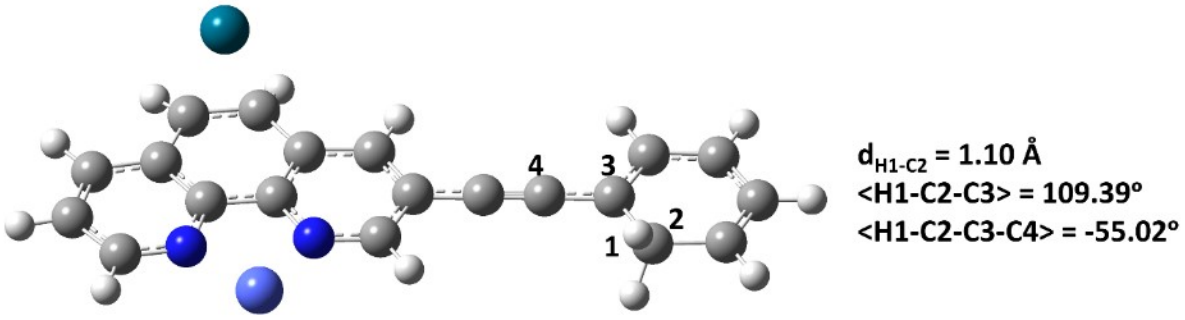

Fig S81. Optimized structure of the model system of **Co@TBB-phen-Pd-H*** obtained from DFT computation at B3LYP/6-311++G(d,p) level, LanL2DZ: ECP and basis set of Co and Pd, empirical dispersion = GD3BJ, solvent = water, PCM)

Charge = 2 Multiplicity = 1

C,0,6.3296090187,1.1125224474,-0.469395239
C,0,5.5524926377,-0.0664264569,0.0095456013
C,0,6.2266774153,-1.2388021019,0.3588518181
C,0,7.6086933329,-1.302537987,0.2534055211
C,0,8.3995583082,-0.2140190645,-0.2010599947
C,0,7.7928719366,0.9494995206,-0.5501444477
H,0,6.0970782314,1.9822844869,0.1656833884
H,0,5.6670976935,-2.0952966245,0.7091647446
H,0,8.1055081387,-2.2252139013,0.5301513004
H,0,9.4736047495,-0.3254533537,-0.2624517327
H,0,8.3678665181,1.7984986842,-0.8992661429
C,0,4.1720680622,0.0238361643,0.1000725876
C,0,2.9608861303,0.1129137228,0.1750964952
C,0,1.5634427914,0.214675371,0.2600033438
C,0,0.7879445573,-0.8575476465,0.7274961743
C,0,0.9308619623,1.4211602065,-0.1315446624
C,0,-0.6020825212,-0.7220663527,0.7886877766
H,0,1.2672563633,-1.7795377782,1.0300788544
H,0,1.510071661,2.2580878318,-0.4979108979
C,0,-1.1403014685,0.5206680546,0.3989375703
C,0,-1.5100981645,-1.761276659,1.2474238272
C,0,-2.5347675122,0.7659107649,0.4458950229
C,0,-2.9106776909,-1.5064681602,1.3077007423
H,0,-1.0806362587,-2.5631020157,1.8377467762
C,0,-3.4361421453,-0.2197705845,0.8914389176
H,0,-3.545289657,-2.1196380492,1.9379199356
C,0,-4.7984484059,0.1384467119,0.9238388244
C,0,-4.2144547885,2.314607664,0.0471105773
C,0,-5.1766836282,1.3990427404,0.4969545767

H,0,-5.5363117653,-0.5729753311,1.2736324069
H,0,-4.4897094675,3.304604567,-0.2929233235
H,0,-6.2164872033,1.6980434049,0.5053006577
N,0,-0.3869704171,1.5673498247,-0.0588860535
N,0,-2.9144445798,2.0091870123,0.0256088633
Co,0,-1.4476603754,3.0675832539,-0.5086574308
Pd,0,-2.4574198544,-2.622268083,-0.4406166873
H,0,5.9437697654,1.4309097359,-1.4505925919

References

1 H. Zhu, L. Gu, D. Yu, Y. Sun, M. Wan, M. Zhang, L. Wang, L. Wang, W. Wu, J. Yao, M. Du and S. Guo, *Energy Environ. Sci.*, 2017, **10**, 321–330.

2 Z. Yang, C. Zhao, Y. Qu, H. Zhou, F. Zhou, J. Wang, Y. Wu and Y. Li, *Adv. Mater.*, 2019, **31**, 1–8.

3 X. Wang, X. Zhou, C. Li, H. Yao, C. Zhang, J. Zhou, R. Xu, L. Chu, H. Wang, M. Gu, H. Jiang and M. Huang, *Adv. Mater.*, 2022, **34**, 1–13.

4 H. Guo, Q. Feng, J. Zhu, J. Xu, Q. Li, S. Liu, K. Xu, C. Zhang and T. Liu, *J. Mater. Chem. A*, 2019, **7**, 3664–3672.

5 S. Dilpazir, R. Liu, M. Yuan, M. Imran, Z. Liu, Y. Xie, H. Zhao and G. Zhang, *J. Mater. Chem. A*, 2020, **8**, 10865–10874.

6 S. Chen, F. Bi, K. Xiang, Y. Zhang, P. Hao, M. Li, B. Zhao and X. Guo, *ACS Sustain. Chem. Eng.*, 2019, **7**, 15278–15288.

7 L. Zhang, Y. Zhu, Z. Nie, Z. Li, Y. Ye, L. Li, J. Hong, Z. Bi, Y. Zhou and G. Hu, *ACS Nano*, 2021, **15**, 13399–13414.

8 J. Zhang, B. Cui, S. Jiang, H. Liu and M. Dou, *Nanoscale*, 2022, **14**, 9849–9859.

9 B. Wang, J. Liu, H. Ge, S. Fan, G. Zhang, L. Zhao and G. Li, *CrystEngComm*, 2022, **24**, 3894–3902.

10 W. Zou, J. Xiang and H. Tang, *New J. Chem.*, 2022, 8786–8793.

11 Y. Bai, Y. Wang, Z. Qiao, Y. Yang, L. Deng, C. Li, X. Chen, S. Wang, Y. Huang, X. Zhang and D. Cao, *J. Mater. Chem. A*, 2022, 16037–16045.

12 E. Vijayakumar, S. Ramakrishnan, C. Sathiskumar, D. J. Yoo, J. Balamurugan, H. S. Noh, D. Kwon, Y. H. Kim and H. Lee, *Chem. Eng. J.*, 2022, **428**, 131115.

13 Y.-F. Yaoa, Z.-Y. Huanga, W.-Y. Xiea, S.-J. Huangb, Z.-Y. Liua, G. Yanga, J.-S. Yea, H.-Y. Liua, X.-Y. Xiaoa and Incorporating, *Catal. Sci. Technol.*, ,

DOI:10.1039/D3CY00802A.

14 S. Halder, A. K. Pradhan, S. Khan and C. Chakraborty, *Energy Adv.*, , DOI:10.1039/d3ya00325f.

15 Z. Duan, M. Liu, X. Li, S. Yang, S. Liu, Q. Xu and G. Zeng, *Chem. Commun.*, 2022, **58**, 13214–13217.

16 M. Liu, Q. Xu, Q. Miao, S. Yang, P. Wu, G. Liu, J. He, C. Yu and G. Zeng, *J. Mater. Chem. A*, 2022, **10**, 228–233.

17 Q. Pan, X. Chen, H. Liu, W. Gan, N. Ding and Y. Zhao, *Mater. Chem. Front.*, 2021, **5**, 4596–4603.

18 S. Bhunia, A. Peña-Duarte, H. Li, H. Li, M. F. Sanad, P. Saha, M. A. Addicoat, K. Sasaki, T. A. Strom, M. J. Yacamán, C. R. Cabrera, R. Seshadri, S. Bhattacharya, J. L. Brédas and L. Echegoyen, *ACS Nano*, 2023, **17**, 3492–3505.

19 X. Wang, A. Guo, Y. Fu, M. Tan, W. Luo and W. Yang, *ACS Appl. Nano Mater.*, 2023, **6**, 3226–3235.

20 S. Halder and C. Chakraborty, *ACS Appl. Eng. Mater.*, 2023, **1**, 1799–1808.

21 R. Isci, T. Balkan, S. Tafazoli, B. Sütay, M. S. Eroglu and T. Ozturk, *ACS Appl. Energy Mater.*, 2022, **5**, 13284–13292.

22 J. J. Jarju, A. M. Díez, L. Frey, V. Sousa, E. Carbó-Argibay, L. P. L. Gonçalves, D. D. Medina, O. I. Lebedev, Y. V. Kolen'ko and L. M. Salonen, *Mater. Today Chem.*, , DOI:10.1016/j.mtchem.2022.101032.

23 Y. Tao, D. H. Yang, H. Y. Kong, T. X. Wang, Z. Li, X. Ding and B. H. Han, *Appl. Catal. B Environ.*, 2023, **339**, 123088.

24 Z. H. Zhu, B. Yu, W. Sun, S. Chen, Y. Wang, X. Li and L. P. Lv, *J. Power Sources*, , DOI:10.1016/j.jpowsour.2022.231583.

25 V. Rajagopal, M. Manivannan, M. Kathiresan, V. Suryanarayanan and L. A. Jones, *Mater. Chem. Phys.*, 2022, **285**, 126104.

26 W. Yan, S. Cao, Z. Xiao, F. Dai, T. Xing, Z. Li, Y. Chen, X. Lu and X. Li, *Electrochim. Acta*, 2021, **377**, 138107.

27 J. Li, P. Liu, J. Yan, H. Huang and W. Song, *Adv. Sci.*, 2023, **10**, 2206165–2206176.

28 L. Haitao, Q. Zhang, Z. Liang, H. Guo, Y. Wang, H. Lv, X. Li, W. Zhang, U.-P. Apfel and R. Cao, *Angew. Chemie*, 2022, **61**, e202201104–e202201110.

29 M. J. Frisch, G. W. Trucks, H. B. Schlegel, G. E. Scuseria, M. A. Robb, J. R. Cheeseman, G. Scalmani, V. Barone, G. A. Petersson, H. Nakatsuji, X. Li, M. Caricato, A. V. Marenich, J. Bloino, B. G. Janesko, R. Gomperts, B. Mennucci, H. P. Hratchian, J. V. Ortiz, A. F. Izmaylov, J. L. Sonnenberg, D. Williams-Young, F. Ding, F. Lipparini, F. Egidi, J. Goings, B. Peng, A. Petrone, T. Henderson, D. Ranasinghe, V. G. Zakrzewski, J. Gao, N. Rega, G. Zheng, W. Liang, M. Hada, M. Ehara, K. Toyota, R. Fukuda, J. Hasegawa, M. Ishida, T. Nakajima, Y. Honda, O. Kitao, H. Nakai, T. Vreven, K. Throssell, J. A. Montgomery, J. E. Peralta, F. Ogliaro, M. J. Bearpark, J. J. Heyd, E. N. Brothers, K. N. Kudin, V. N. Staroverov, T. A. Keith, R. Kobayashi, J. Normand, K. Raghavachari, A. P. Rendell, J. C. Burant, S. S. Iyengar, J. Tomasi, M. Cossi, J. M. Millam, M. Klene, C. Adamo, R. Cammi, J. W. Ochterski, R. L. Martin, K. Morokuma, O. Farkas, J. B. Foresman and D. J. Fox, *Wallingford CT*.

30 A. V. Krukau, O. A. Vydrov, A. F. Izmaylov and G. E. Scuseria, *J. Chem. Phys.*

31 L. S. Kassel, *J. Chem. Phys.*, 1936, **4**, 276–282.

32 Alex D. Beck, *J. Chem. Phys.*, 1993, **98**, 5648–5656.

33 P. J. Hay and W. R. Wadt, *J. Chem. Phys.*, 1985, **82**, 270–283.

34 W. R. Wadt and P. J. Hay, *J. Chem. Phys.*, 1985, **82**, 284–298.

35 S. Grimme, J. Antony, S. Ehrlich and H. Krieg, *J. Chem. Phys.*, , DOI:10.1063/1.3382344.

36 J. Tomasi, B. Mennucci and R. Cammi, *Chem. Rev.*, 2005, **105**, 2999–3093.

37 P. J. Stephen, F. J. Devlin, C. F. Chabalowski and M. J. Frisch, *J. Phys. Chem.*, 1994, **98**, 11623–11627.

38 J. K. Nørskov, J. Rossmeisl, A. Logadottir, L. Lindqvist, J. R. Kitchin, T. Bligaard and H. Jónsson, *J. Phys. Chem. B*, 2004, **108**, 17886–17892.

39 A. Valdes, Z. W. Qu, G. J. Kroes, J. Rossmeisl and J. K. Nørskov, *J. Phys. Chem. C.*, 2008, **112**, 9872–9879.

40 Y. Jia, L. Zhang, A. Du, G. Gao, J. Chen, X. Yan, C. L. Brown and X. Yao, *Adv. Mater.*, 2016, **28**, 9532–9538.

41 P. Wang, X. Zhang, J. Zhang, S. Wan, S. Guo, G. Lu, J. Yao and X. Huang, *Nat. Commun.*, 2017, **8**, 14580–14589.

42 E. Skúlason, G. S. Karlberg, J. Rossmeisl, T. Bligaard, J. Greeley, H. Jónsson and J. K. Nørskov, *Phys. Chem. Chem. Phys.*, 2007, **9**, 3241–3250.